

AN ABSTRACT OF THE THESIS OF

Jacqueline M. Sneed for the degree of Master of Science in
Geography presented on June 6, 1991.

Title: A Methodology to Directly Input Data from an Uncontrolled
Aerial Photograph into a Vector Based Geographic Information
System

Abstract approved: _____
A. Jon Kimerling

Historically the U.S. Forest Service has used uncorrected aerial photographs to delineate proposed and past management activities on the land base it manages. Transferring a boundary from an image not planimetrically correct to a planimetrically corrected image introduces errors. Positional accuracy of boundaries affects the number of acres the Forest is accountable for managing, and the annual sale quantity (ASQ) or annual board feet targets.

The purpose of this study was to develop a methodology that eliminated the need to transfer the boundary from an uncorrected to a corrected image. Raster and vector warping methods were evaluated with reference to positional accuracy and efficiency.

Due to the rugged topography of the Siuslaw National Forest, selection of ground control points (GCPs) was an important function in the accurate transformation of images. A Vector warping method, Rubber Sheeting the ARC/INFO projective transformation for all

digital GCPs, to all of the Global Position System (GPS) ground control points, provided the most accurate rectification of vector boundaries that had been digitized or scanned from an uncontrolled low elevation photograph.

A Methodology to Directly Input Data
from an Uncontrolled Aerial Photograph
into a Vector Based Geographic Information System

by

Jacqueline M. Sneed

A Thesis

submitted to

Oregon State University

in partial fulfillment of
the requirement for the
degree of

Master of Science

Completed June 6th, 1991

Commencement June 1992

APPROVED:

Professor of Geography in charge of major

Head of department of Geosciences

Dean of Graduate School

Date thesis is presented June 6, 1991

Author Jacqueline M Sneed

ACKNOWLEDGEMENTS

I would like to take this opportunity to thank all those who made this work possible.

I am indebted to the Siuslaw National Forest for awarding me the educational scholarship. This scholarship provided me with the funding and above all the time needed to complete my studies.

I would like to acknowledge my Committee members, Dr. A. Jon Kimerling, Dr. Gordon Matzke, Dennis White and Dr. Alan Niem for their guidance and editorial help. Thanks to the faculty and staff of the Geography Program at Oregon State University for their knowledge and support.

I appreciate the loving care friends gave to my children during the many nights I needed to study. This comfort of knowing my children were in good care allowed me to concentrate on my work.

I owe a special and humble thank you to the following: My dear friend Mary Walter for the many hours spent on editing all of my papers during graduate school and for always being there for me no matter what time of day.

To my husband who always believed in me and spent many a sleepless night doing whatever he could do to help. I especially thank him for his unlimited patience.

Finally, and above all this research and degree is dedicated to my three children, Miles, Nel, and Silas. They have sacrificed

more than any in this process. I thank them for their patience and understanding, the many nights at sitters and on the floor at work, the many hours of trying to be quiet and putting up with a crabby mom. These children have taught me more than anything else in life. Their encouragement gave me strength to continue. I thank you Miles for telling me at 2am as you lay on the floor beside me sick, as I was ready to quit "Mom you can't give up....you've got to keep going". That statement will always be a source of inspiration to me. Without the support of these special people this work would never have been completed.

TABLE OF CONTENTS

CHAPTER 1 - INTRODUCTION	Page
Problem.....	1
Current Practices in Siuslaw National Forest.....	2
Objectives.....	6
CHAPTER 2 - LITERATURE REVIEW	
Cartographic Accuracy and Rectified Satellite Imagery.....	8
Global Positioning Systems.....	12
CHAPTER 3 - STUDY AREA AND METHODS	
Study Area Descriptions.....	17
Ground Control Point Selection (GCP).....	22
Global Positioning System.....	22
Target Selection and Placement.....	23
Data Collection.....	24
Flight.....	25
Target Scale.....	26
Transformation and Warping of Raster and Vector Image Files	26
Raster Warping.....	28
Scanning the Photography.....	28
Geometric Rectification.....	29
Identification of Ground Control Points.....	29
Coordinate Transformations.....	30
Root Mean Square Error.....	31
Vector Warping.....	32
Coordinate Transformations.....	33
Transformation of the Study Area Boundaries (polygon).....	34
Root Mean Square Error (RMS error).....	35
Vector Warping "Rubber Sheeting".....	36
"Rubber Sheeting" the Vector File.....	37
Measurement Error.....	38
Systematic Error.....	38
Random Error.....	39
Mistakes or Blunders.....	39
Constant Errors.....	40
Determination of Study Area Boundaries.....	40
Identification of GCPs on Images.....	41
Instrument and Human Operator Error.....	42

	Page
CHAPTER 4 - RESULTS	
Transformation Comparisons.....	43
Rubber Sheeting Comparisons.....	45
Comparison of Rubber Sheeting with All Point Projective Transformation and the Rubber Sheeting with Inner GCPs Deleted.....	46
GPS, Rubber Sheeting Vector Warp, and Raster Warp Boundary Comparison.....	50
Rubber Sheeting Vector Warp and Raster Warp Comparisons....	51
Summary.....	52
 CHAPTER 5 - CONCLUSIONS	
Improvements to Study.....	53
Future Research Opportunities.....	54
Recommendations Based on Output.....	55
 BIBLIOGRAPHY.....	57
 APPENDIX 1 TABLES AND FIGURES.....	60
APPENDIX 2 CARTESIAN COORDINATE TRANSFORMATIONS.....	100
APPENDIX 3 HANDBOOK ON WARPING VECTOR BOUNDARY WITH ARC/INFO..	105

LIST OF FIGURES

	Page
Figure 1	Siuslaw National Forest Vicinity Map..... 18
Figure 2	Randall Study Area TIN..... 19
Figure 3	Gopher Study Area TIN..... 20
Figure 4	Peterson Study Area TIN..... 21
Figure 5	Rubber Sheeting Transformation..... 27
Figure 6	Raster Warping Procedure..... 28
Figure 7	Vector Warping Procedure..... 32
Figure 8	Cartesian Coordinate Transformation..... 35
Figure 9	Randall Study Area Four point transformation..... 66
Figure 10	Gopher Study Area Four point transformation..... 67
Figure 11	Peterson Study Area Four point transformation..... 68
Figure 12	Randall Study Area All point transformation..... 69
Figure 13	Gopher Study Area All points transformation..... 70
Figure 14	Peterson Study Area All points transformation..... 71
Figure 15	Randall Study Area Transformation comparison..... 72
Figure 16	Gopher Study Area Transformation comparison..... 73
Figure 17	Peterson Study Area Transformation comparison..... 74
Figure 18	Randall Study Area Rubber sheeting comparison..... 75
Figure 19	Gopher Study Area Rubber sheeting comparison..... 76
Figure 20	Peterson Study Area Rubber sheeting comparison..... 77

LIST OF FIGURES

	Page
Figure 21 Randall Study Area Four Point Method	78
Figure 22 Gopher Study Area Four Point Method	79
Figure 23 Peterson Study Area Four Point Method	80
Figure 24 Randall Study Area Boundary Method	81
Figure 25 Gopher Study Area Boundary Method	82
Figure 26 Peterson Study Area Boundary Method	83
Figure 27 Randall Study Area Rubber Sheeting Methods.....	84
Figure 28 Gopher Study Area Rubber Sheeting Methods.....	85
Figure 29 Peterson Study Area Rubber Sheeting Methods.....	86
Figure 30 Randall Study Area Four Point Method Comparison.....	87
Figure 31 Gopher Study Area Four Point Method Comparison.....	88
Figure 32 Peterson Study Area Four Point Method Comparison.....	89
Figure 33 Randall Study Area Buffered four point transformation.....	90
Figure 34 Gopher Study Area Buffered four point transformation	91
Figure 35 Randall Study Area Buffered all point transformation	92
Figure 36 Gopher Study Area Buffered all points transformation	93
Figure 37 Randall Study Area Buffered Vector-Raster comparison	94
Figure 38 Gopher Study Area Buffered Vector-Raster comparison	95
Figure 39 Peterson Study Area Buffered Vector-Raster comparison.....	96
Figure 40 Randall Study Area Vector-Raster comparison.....	97

LIST OF FIGURES

	Page
Figure 41 Gopher Study Area Vector-Raster comparison.....	98
Figure 42 Peterson Study Area Vector-Raster comparison.....	99

LIST OF TABLES

	Page
Table 1	Projective Transformation Comparisons.....43
Table 2	Rubber Sheeting Comparisons.....45
Table 3	Vector Warping Comparisons.....48
Table 4	GPS, Vector Warp, and Raster Warp Comparison.....50
Table 5	Randall Study Area Ground Control Point Coordinates....60
Table 6	Gopher Study Area Ground Control Point Coordinates....61
Table 7	Peterson Study Area Ground Control Point Coordinates...62
Table 8	RANDALL ROACH STUDY AREA RMS Error for Each GCP Vector Transformation.....63
Table 9	GOPHER FLYNN STUDY AREA RMS Error for Each GCP Vector Transformation.....64
Table 10	PETERSON STUDY AREA AREA RMS Error for Each GCP Vector Transformation.....65

A METHODOLOGY TO DIRECTLY INPUT DATA
FROM AN UNCONTROLLED AERIAL PHOTOGRAPH
INTO A VECTOR BASED GEOGRAPHIC INFORMATION SYSTEM

CHAPTER 1

INTRODUCTION

"The mission of the U.S. Department of Agriculture Forest Service focuses on natural resource management. The organization's vitality and ability to manage its lands depends on the rapid, accurate flow and exchange of information about these resources" (Raines 1987).

On-the-ground management decisions and information gathered on the managed resources are at the district level of the Forest Service. The amount of resource data gathered and the complexity of the resource relationships makes manual analysis formidable. Siuslaw National Forest has implemented a Geographic Information System (GIS) to automate the spatial analysis needed to manage these resources.

Problem:

Historically, the Forest Service has used uncorrected aerial photographs to delineate management activities on its land base. With these, photographic scales can be determined in area of flat terrain. Although the vertical aerial photograph presents a correct record of angles, constant changes in horizontal scale preclude accurate measurements of distance on simple overlays. An alternative is to transfer photographic detail to simple overlays

on planimetric maps. Planimetric maps are those that show the correct horizontal or plan position of natural and cultural features (Avery and Berlin 1985).

The Forest Service made its first attempt in 1974 to use orthophotography as a management tool to obtain accurate measurements of distance. An orthographic photo shows ground features in precise planimetric positions on a continuous tone image. An orthoprojection instrument that is connected to a stereoplotter removes geometric distortions optically. The plotter scans the stereo model in one continuous operation and removes the distortion. Once the aerial photograph is rectified into an orthophotograph, the 'corrected' imagery can be used as a planimetric map. An orthophotograph can be interpreted like a photo. The big advantages are that it has one scale despite the type of terrain, and has true distances, angles, and areas (subject only to constraints of the map projection employed) that can be measured directly, permitting features to be interpreted in their true, planimetric positions. Orthophotos are well suited as base maps for resource surveys since users often seem to read an orthophoto better than a conventional line and symbol base map. This increases understanding by resource personnel of various resource data (Lillesand and Kiefer 1987).

Current Practices in Siuslaw National Forest:

Photography for the orthophotography of the Siuslaw National Forest is flown at a scale of 1:40000. The final product is a 1:12000 scale, black and white orthophoto. The Siuslaw requests

the 1:12000 scale so the product is similar to the scale of the 9" x 9" low elevation color photography traditionally used for sale planning and 'timber' typing. Flights are on a ten year schedule to update the orthophotography. Flights for orthophotography for the Siuslaw were in 1975 and 1985 and the next is scheduled for 1995. The final product, is projected to be delivered in 1998. This results in 13 years between the time the present photography was taken (1985) and the time the updated photography will be delivered (1998).

Due to the cost of a cronapaque print of a half USGS quadrangle 1:12000 orthophoto (\$39.75 in 1989), and the 30" X 40" image dimensions, resource specialists on (interdisciplinary) sale planning teams mark spatial boundaries of stands of vegetation and proposed and actual timber sales on uncontrolled 9" x 9" color photography (scale ~ 1:12000). The boundaries of stands are then visually transferred by hand to the most recent black and white orthophoto. This process is done to achieve accurate measurements and to depict the spatial relationships between the vegetation resources of the forest.

The district silviculture departments on the Siuslaw National Forest designed a system in the late 1970's to manually record reforestation and stand improvement management activities, spatial boundaries, and their attributes. This system was designed to prepare the information for conversion into a GIS. Each Siuslaw National Forest district takes a low elevation (~1:6000) photograph taken of each stand harvested. These photos are used as 'base' maps of the harvested stands by silviculturists, contractors, and

resource managers. These base maps aid in planning, implementing, and recording management activities on the managed stands. Clear mylar overlays are used to record the physical location of each management activity, and data collection plot locations, for the stand. Attributes describing the type of activity, purpose, results, dates, materials used (e.g., type of trees planted), and costs of each are recorded. In the past, there were between 40 to 60 new managed stands each year per district. The photos are also utilized for approximately 15 to 18 years during reforestation and stand improvement phases of the managed stand.

Analysis of this historical spatial information shows trends in resource response to management activities over time, and helps to determine the costs and benefits for each type of silvicultural practice. Site specific data analysis enables resource managers to prescribe more effective silvicultural practices. Due to the variety and magnitude of information on managed stands, the work required for manual analysis is formidable.

Automation of the spatial analysis of these data requires moving all of the historical information into a GIS. At present, this conversion from analog to digital format is done by transferring all activities from mylar overlay, based on the low elevation photograph (uncontrolled, ~1:6000), onto a planimetrically corrected photograph (resource orthophotography, 1:12000). These data are then converted from analog to digital format by digitizing or scanning. This is the same process used by the sale planners as previously described, except that a different uncontrolled photo base is used. Each time a new activity takes

place, new positional boundaries must be determined before entry of these data into the GIS.

Error in positional accuracy of boundary lines when transferring from either the uncontrolled 9" x 9" color photography (~1:12000), or the uncontrolled color photography of harvested stands (1:6000), to the black and white orthophotography (~1:12000) can occur. This is a result of: 1) differences in scale, 2) variable clarity on the uncontrolled and orthographic photos, 3) relief displacement and distortion in the uncontrolled photography, 4) loss of ancillary data resulting from time differences in photography (e.g., roads cleared or timber felled), and 4) human error in transferring data.

Positional accuracy of boundaries can affect the number of acres the Forest is accountable for managing, and the annual sale quantity (ASQ) or annual board feet targets. Positional accuracy of the harvested area boundaries is also important since these boundaries are used as a template in the GIS for tracking the next 15 to 20 years of management activities on harvested stands.

Transferring a boundary from an image on one scale not planimetrically correct to another scale that is planimetrically correct introduces errors. Incorrect positional boundaries of the transferred data can cause topological problems such as nearly coincidental lines and sliver polygons which are very time consuming to correct.

Objectives:

The objective of this research is to eliminate the step of transferring the boundary from an image which is not planimetrically corrected and of different internal scales, to that of a corrected image. A handbook for resource managers describing the techniques of warping (or correcting) low elevation photographs was a product of this effort.

In the fall of 1989 two methods were proposed to the Siuslaw National Forest that would: 1) lead to direct input of the new managed stands into the GIS vegetation layer without having to manually transfer the boundary of an activity from a uncontrolled base to a controlled base, and 2) facilitate automation of spatial analysis of historical management activities.

The first method converts the uncontrolled low elevation photograph of a harvested stand of vegetation into a planimetrically corrected image. The second method rectifies the vector activity boundaries that have been digitized or scanned from an uncontrolled low elevation photograph.

The elimination of the step from a uncontrolled base to a controlled base will result in reduction of positional boundary error, save time at each data entry and greatly simplify the updating process of the vegetation and management activity layers in GIS.

The following chapters will: 1) review the literature pertaining to cartographic accuracy and rectification of remotely sensed imagery, and advances in global positioning systems (GPS),

2) discuss the techniques used in the methodology of raster and vector warping, 3) discuss the results of testing each warping method , 4) propose future research needed in the area of rectification of low elevation photography, and 5) recommend a warping method that would best meet the needs of the U.S. Forest Service.

CHAPTER 2

LITERATURE REVIEW

An understanding of the theory of cartographic accuracy of remote sensing products, and present technology in rectification of aerial photography and satellite imagery was needed before methodologies could be determined in this study. A literature search was performed in two major fields: 1) cartographic accuracy and rectification of satellite imagery; and 2) advancements in the technology of global positioning system (GPS).

Cartographic Accuracy and Rectified Satellite Imagery:

The cartographic accuracy of the first Landsat systems was of relatively low quality due to the procedures employed in rectification of the imagery. Studies conducted on the (second generation) Landsat-4 Multi Spectral Scanner (MSS) and Thematic Mapper (TM) satellite image data revealed inaccuracies in rectification (Welch 1984). Positional errors of approximately \pm 55m (meters) existed based on rectification procedures involving the use of 20-30 well distributed Ground Control Points (GCP) and second or third degree polynomial equations. A subset of Thematic Mapper data rectified with 10 ground control points indicated a much higher order of geometric quality. Higher order polynomials did appear to improve the rectification accuracy. The greatest practical cartographic accuracies of both MSS and TM data sets were assessed at about 2/3 to 1 pixel. Three major sources that

contributed to these errors were 1) data resolution limiting the determination of the location of ground control points, 2) mapping errors of ground control points on quads and subsequent digitizing errors that averaged about ± 10 -15m, and 3) terrain relief that produced displacements between ± 10 and ± 30 m (Welch 1984).

A U.S. Geological Survey (USGS) study of Landsat-4 concluded that TM data met 1:100000 scale planimetric requirements from the geometric standpoint where suitable control was available (Colvocoresses 1984). University College London conducted studies using Satellite Probatoire d'Observation de la Terre (SPOT) stereo images to provide data for topographic mapping. The accuracy needed for mapping at 1:50000 scale with 20m contours was possible with the use of analytical stereoplotters, (Dowman 1987). Dowman reported that the 10m data, obtained from SPOT and other satellites, were adequate for 1:50000 scale image mapping although location of GCPs and digitizing errors increased inaccuracies.

Other studies into the combination of image processing techniques with photogrammetric instruments were conducted in Canada (Kratky 1988). The geometric model developed in Kratky's study was designed to model the physical reality of imaging, satellite orbits and the earth's geoidal shape, rather than being based upon indirect empirical image fitting and warping, as frequently adopted in non-photogrammetric approaches. The results in the study were sufficient to support topographic mapping at 1:50000 and smaller scales. Discrete points had root mean square (RMS) errors of 5 to 6m in planimetry and 4 to 8m in elevation.

The Flathead National Forest in Montana used remote sensing and image processing techniques to map stands of vegetation to support GIS activities (Bain 1988). Field methods and standards for cover type mapping were developed, and a system to aggregate vegetation classifications for various applications was designed. Image accuracy improved as personnel gained more experience in locating GCPs, although these data were limited to 1/2 to 1 pixel accuracy (Bain 1988).

Other Flathead National Forest satellite experience included use of SPOT to update the Timber Stand Map Record System (TSMRS), and to map the spatial locations of logging operations. The use of SPOT images produced at 1:24000 scale in place of orthophotos was investigated for TSMRS. Orthophoto maps were overlaid onto the 1:24000 SPOT images to visually check the spatial quality. This process uncovered cartographic errors on the quads due to the photogrammetric process used in producing orthophotographs.

The U.S. Forest Service recently completed a report (Bain 1991) on use of the global positioning system to provide control for Remote Sensing Satellite Imagery used in GIS. A comparison of a GPS controlled image and a conventional map controlled image with 36 GPS points did not show any improvement in the image transformation accuracy. GPS points on controlled images which had large positional errors (2-4 pixels) also had large positional errors on the GPS controlled image. Bain (1988) believed this was not due to GPS technology but to the present image processing transformation methods.

In further experiments in the Bain study GIS vector (x, y coordinate) files were overlaid on five SPOT images to determine if GIS digital features such as roads could be maintained and updated using SPOT imagery. Transformation of SPOT data using a polynomial equation worked well when good ground control was established and where little terrain relief existed. Considerable distortion was retained in areas of large terrain relief. The project evaluation team concluded that a fully operational GPS cannot meet user requirements for satellite data. The team concluded that due to terrain relief problems, a modeling technique, such as a digital elevation model or a photogrammetric model, during image processing would be required to give satellite imagery the positional accuracies required to support GIS (Bain 1988). Polynomial equations do not model the topography as they would in a digital elevation model (DEM) or a photogrammetric model.

Use of polynomial equations in image processing systems has been a common method of rectifying satellite images. Only recently is the problem of terrain relief being addressed by designers of image processing software. In the near future, terrain modeling rectifying software will be available on some image processing systems. Irish (1990) described four proposed correction levels for satellite imagery.

"Geometrically uncorrected image data represents the first correction level and is denoted as A data for TM and 1A for SPOT. The second correction level consists of imagery without distortions from the sensor, platform motion and earth (i.e. revolution and curvature), and is referred to as P-systematic for TM and 1V 1B 2A for SPOT. Orbit errors, however, was not accounted for and this 'corrected' imagery is shifted from its true location by unacceptable margins. At the third

correction level, ground control was used to generate geodetically accurate products. The TM georeferenced P-products at this level are not GIS compatible because of a satellite heading orientation; however the geocoded P is a north-oriented GIS product" (Irish 1990). "The fourth correction level represents products of the highest quality. Products at this level have all distortions removed, including those caused by terrain relief, and are called orthoimages" (Irish 1990).

STX Remote Sensing Services, a company developing terrain modeling rectifying software, is employing an earth-sensor modeling approach for the Landsat and SPOT satellites (Irish 1990). A GIS image data layer that exceeds National Map Accuracy standards at 1:24000 scale results from this earth-sensor modeling approach. The STX earth-modeling uses geometrically raw TM A or SPOT 1A data. Mapping relationships are established between the raw images and the GIS reference area with sensor, platform, orbit and earth models. Updating and refinement of the satellite's orbit are accomplished through the use of ground control points in geocoding (Irish 1990).

Terrain-relief distortions are modeled differently in STX's highest correction level imagery than geocoded TM P and SPOT 2B. Geocoded TM P and SPOT 2B products have the mean elevation removed but the high-order terrain effects remain. Terrain-relief distortions are measured and adjusted pixel by pixel with elevation models in the STX's highest correction level imagery (Irish 1990).

Global Positioning Systems:

Senus (1981) envisioned the great benefits of GPS equipment to the Mapping, Charting and Geodesy community. Developments of this technology included the first GPS receivers of satellite data for

geodetic survey applications. Accuracy of absolute positioning was limited in 1981 by the expected uncertainties in the orbit and the clocks of the NAVSTAR satellites.

At present GPS uses a constellation of 21 satellites orbiting the earth at a 10,900 mile altitude. In 1993, a 24 satellite constellation is planned so as to provide 24 hour, world wide coverage for civilian use. This constellation will eliminate areas of degraded navigation capability that are present in the 18 + 3 constellation (Hurn 1989).

The Global Positioning System (GPS) will be used in the 1990's for cm-level measurements of crustal motion and for sub-decimeter earth orbiter positioning and navigation. GPS orbits for these applications will be required to be accurate to 10-20 cm. Lichten (1990) of the Jet Propulsion Laboratory discussed factors that are expected to play a role in improvement to the decimeter level. These include the use of worldwide ground tracking networks and improved orbit modeling. Refinements in orbit modeling, combined with the availability of a worldwide tracking network and the dense distribution of tracking sites in North and South America, have improved orbit determination precision to about 60 cm for four of the seven GPS satellites tracked in a specific orbit. These orbit results are consistent with the precision of other measurements. Lichten states that as more satellites are launched and GPS technology matures, GPS orbit accuracy should improve to the level of tens of centimeters by the mid-1990's.

Lichten and Border (1987) reported repeatability of 2-5 parts in 10^{**8} (10 to the eighth power) in all three components. 1 part

in 10**8 corresponds to 1mm in 100 km. Solutions of this kind are presently only available to researchers. Such highly accurate solutions require satellite positions ≤ 1 m. Because such accurate orbits are generally not yet available, researchers are forced to estimate GPS orbital improvement simultaneously with estimating baselines. Precise observation of GPS signal delay and/or delay rate between receiving points on the earth enables precise measurement of the baseline vectors between those points (Lichten and Border 1987). Accurate knowledge of the GPS satellite orbits is essential for an accurate baseline solution.

The Siuslaw National Forest tested the accuracy of the Trimble Navigation Pathfinder two way receivers (Schlaich 1990). The following position levels (number of satellites visible and or method of occupation) were tested:

(1) Remote Unit observing a maximum of 3 satellites with no correction back to the Base Unit (2D PT mode).

(2) Remote Unit observing 4 satellites with no correction back to the Base Unit (3D PT mode).

(3) Remote Unit observing 4 satellites with a correction back to the Base Unit (3D DIF mode).

(4) Remote Unit observing 4 satellites at an Eccentric point and then using a bearing and distance tie for computations to the benchmark position. This is corrected back to the Base Unit (3D DIF ECC mode).

(5) The same type of observation as the 3D DIF ECC with no correction to the Base Unit (3D PT EDD mode).

The Trimble specifications call for ± 25 meters for the Point (PT) positions (2D or 3D). Observations on the Siuslaw National Forest were found in practice to give values within 5 - 10 meters.

The Trimble specification for the 3D differential mode call for accuracy of 3 - 5 meters. The Siuslaw's observations gave values within 2 - 3 meters.

Variability was found in the 2D and 3D observations when the elevation of a point was questionable. A 300 foot difference was found in the (x, y) coordinate of a point when the elevation was off by 100 ft. Accuracy of the elevation needed to be ± 50 ft for 2D coverage to give consistent values (Schlaich 1990).

Remondi (1985) pioneered kinematic GPS surveying and conducted the first experiments. Kinematic differential GPS surveying is the latest development in GPS. This technique makes use of carrier phase observations, allowing data to be collected from a moving object. Kinematic differential GPS yields centimeter relative accuracy in seconds for slow-moving land vehicles. While one antenna remains stationary at some initial point, the other antenna is moved from one station to another. The only constraint on the path of the moving antenna is visibility of the satellites. Both receivers record the carrier phase observations continuously. The theory and software originally developed by Remondi has been refined at the University of Maine (Quirion 1987).

Kinematic differential GPS has been used for decimeter positioning of airplanes (Mader 1986, Krabill 1987). High-precision airplane positions from this technique can replace

expensive ground control in photogrammetry. Densification for photo control is a frequent and major use of GPS surveying today.

GPS has the potential to revolutionize the practice of surveying, to provide new meaning to the numerical records of surveyors, and to make high quality measurement and rectification techniques available to surveyors, photogrammetists, geographers and related disciplines that were formerly only available to a limited audience.

GPS technology provides a feasible method to obtain the ground control points (GCPs) necessary to rectify the low elevation photography used in this study. Kinematic differential GPS will enable a resource manager to establish GCP's in five year and older stands of vegetation on the Siuslaw National Forest without the intensive labor required to clear the ground for target placement.

CHAPTER 3

STUDY AREA AND METHODS

Study Area Descriptions:

On the Siuslaw National Forest (Figure 1) three recently harvested units were selected as study areas, Randall Roach unit 2, Gopher Flynn unit 2, and Peterson unit 2. The study areas represent the varied topography in the Coast Range.

Randall Roach unit 2 on the Alsea Ranger District, is a 51 acre clearcut located in Township 12 south, Range 9 west, Section 10 (latitude 44 31' north and longitude 123 47' west). Elevations in the area range from 250' to 850'; aspect is predominately north with two minor slopes facing northeast and two facing northwest. Topography is gentle to moderate with general north/south ridges and a broad bench dominating the center of the area. The average slope is 25%, with 20% of the area gentle (<15% slope), 80% of the area moderate (15-50% slope), and 0% of the area steep (>50%) in slope (Figure 2) (Carr 1987).

Gopher Flynn unit 2 on the Alsea Ranger District, is a 29 acre clearcut located in Township 12 south, Range 9 west, Section 18, (latitude 44 33' north and longitude 123 17' west. Elevation ranges from 700' to 900'. Topography includes a series of small benches broken by the headwaters of Traxtel Creek with a south and east aspect. The average slope is 50%, 10% of the area is gentle (<15% slope), 50% of the area is moderate (15-50% slope), and 40% of the area is steep (>50%) (Figure 3) (McCall 1987).

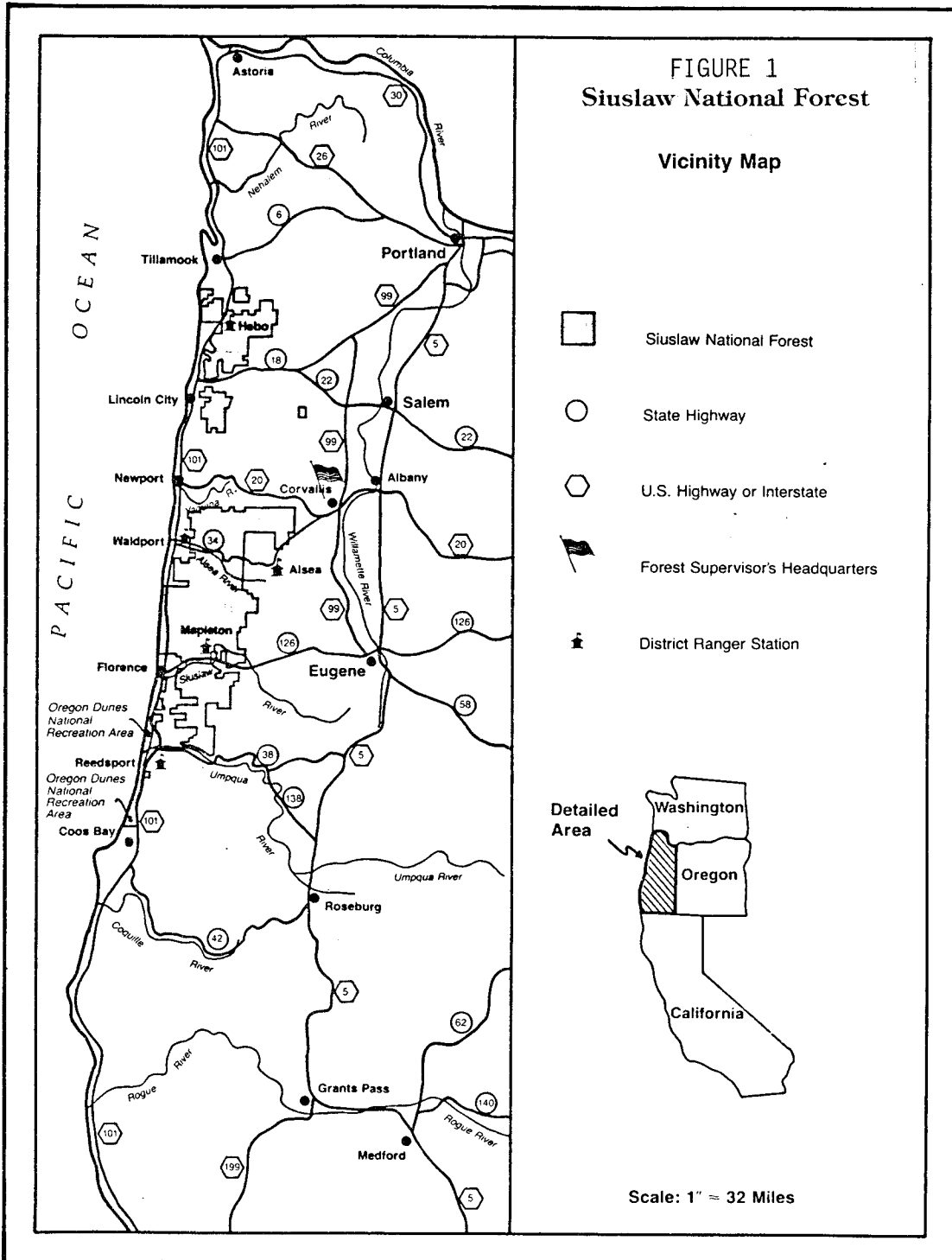
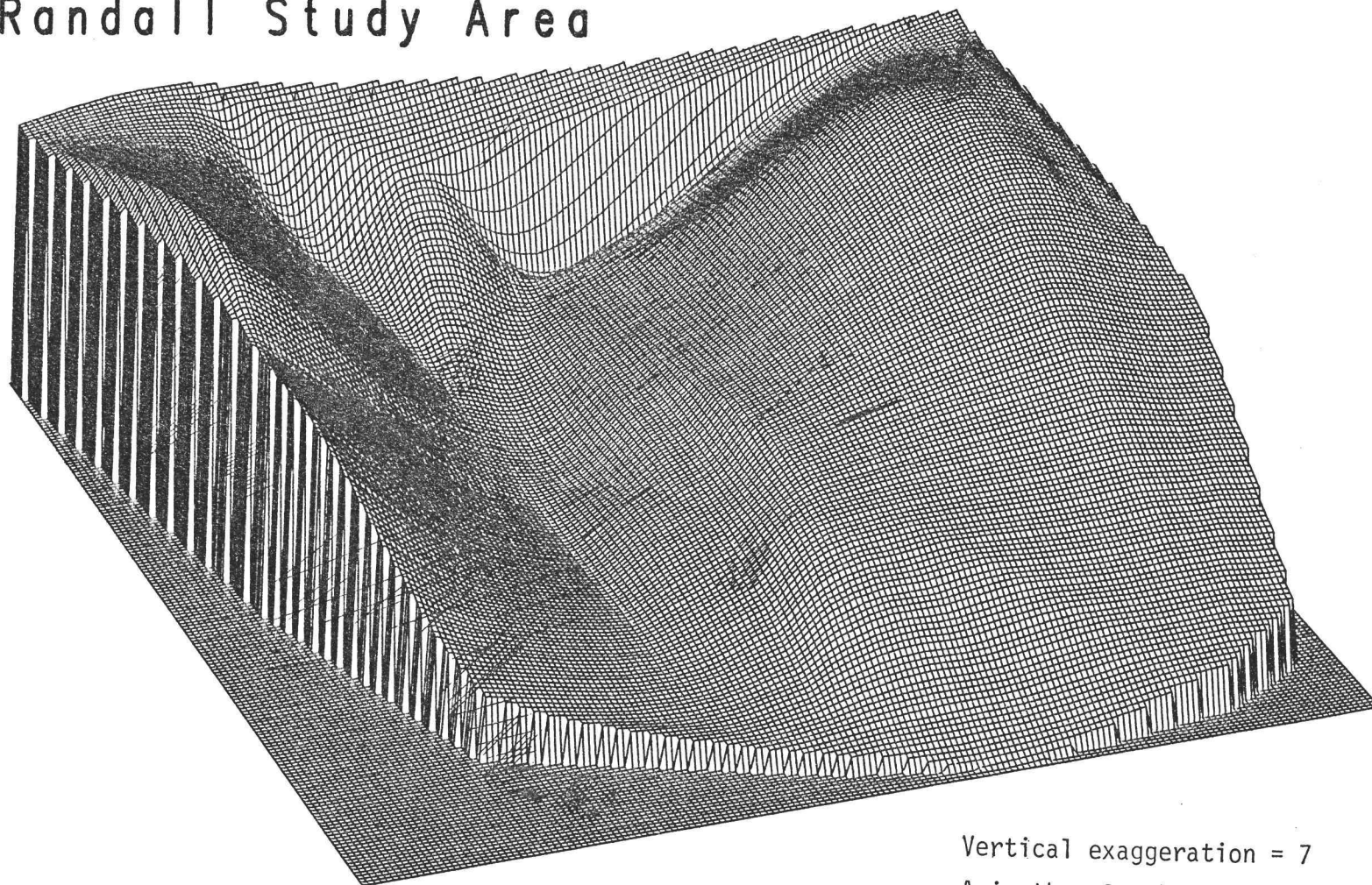


FIGURE 2

Randall Study Area



Vertical exaggeration = 7
Azimuth = Southeast

FIGURE 3
Gopher Flynn Study Area

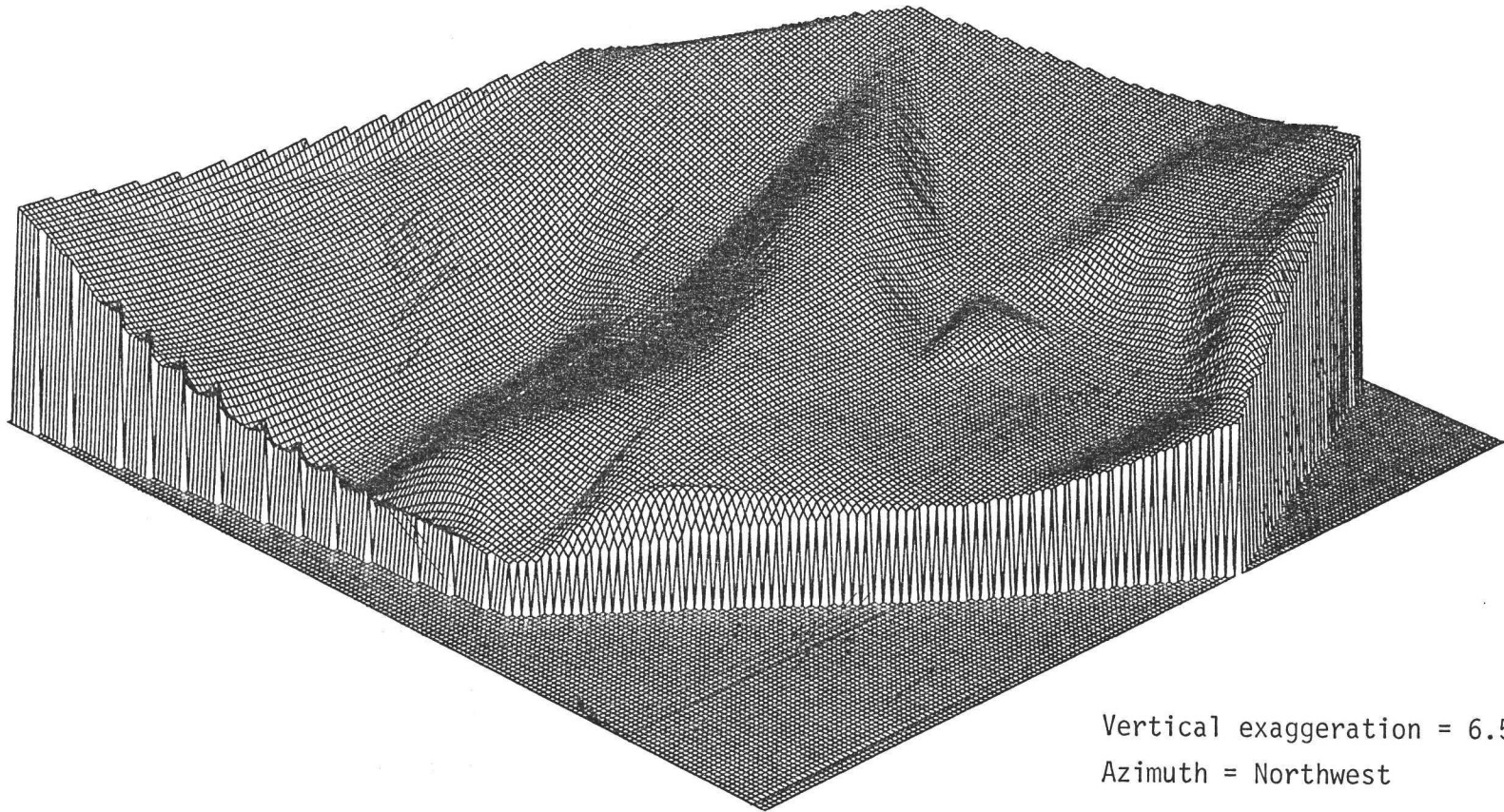
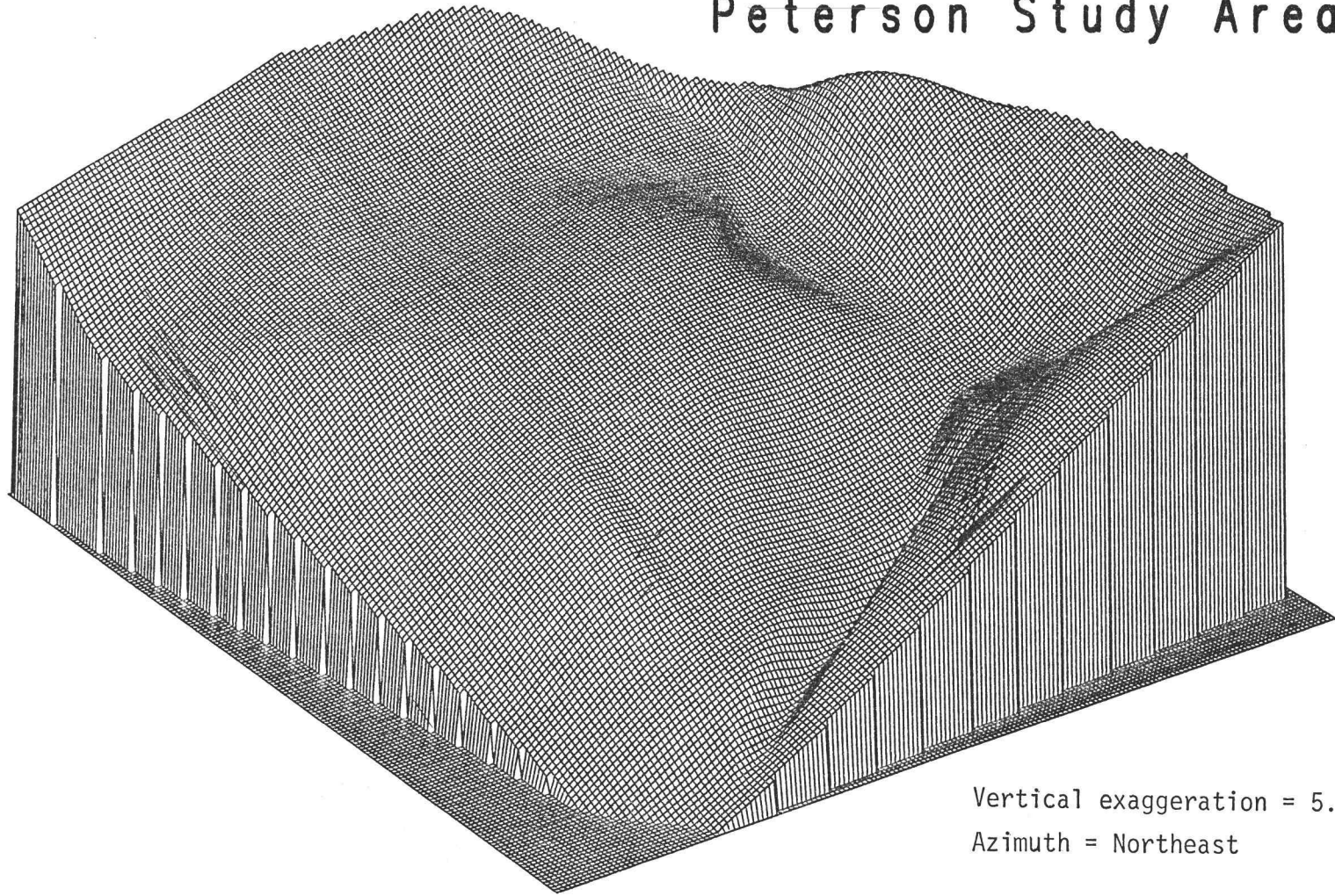


FIGURE 4

Peterson Study Area



Vertical exaggeration = 5.75
Azimuth = Northeast

Peterson unit 2 on the Waldport Ranger District, is a 65 acre clearcut located Township 12 south, Range 11 west, Section 11, (latitude 44 32' north and longitude 123 59' west). Elevation of the area ranges from 400' to 980'; the general aspect of the area is south to southwest with two minor slopes facing southeast. Slopes over most of the area are moderate, generally ranging from 20 to 50%. Areas immediately along Peterson Creek and tributary draws are quite steep (Figure 4) (Roab 1976).

Ground Control Point Selection (GCP):

Selection of GCP's is very important for accurate transformation of images. Initial field reconnaissance of each potential study area included: 1) determination of location and number of adequate ground control points, and 2) estimation of time required to establish these points. GCPs were chosen to establish a control network that captured all major elevation changes.

Global Positioning System:

A GPS receiver unit was used to establish the latitude, longitude and elevation of each control point. All units were GPS Pathfinders manufactured by Trimble Navigation, of Sunnyvale, California. The system is based on the Trimble Advanced Navigation Sensor with dual channel sequencing. The receivers were L1 frequency, C/A code (SPS) preamplifier antenna, and have a 4 line 16 character alphanumeric display with up to 448k RAM. Three Trimble Pathfinder Units, each weighing approximately 15 lbs, were used. One unit was placed on a known control (base) station with

the other two used as remote units for locating the selected ground control sites. The distance from the control stations to the study areas were two miles from Peterson, five miles from Gopher, and two miles from Randall.

The geographic location of each study area, and the estimated time required to establish the control points, was used to determine the time windows of the satellites needed to obtain 3D differential mode. Given the geometric positions of the satellites, four pseudo ranges are sufficient to compute the position of the receiver and its clock error. Pseudo range equals the distance between the satellite and the receiver plus a small corrective term for receiver clock errors. Differential correction is a process of removing slight errors from GPS readings from the mobile units. A mathematical correction of coordinates is performed and adjusted to a known reference. This is done by having a GPS unit on a base station of known coordinates, continually collecting data used in the differential correction of data from the mobile GPS units. In July, 1990, there was an average window of 6 hour each day when 3D differential mode was possible.

Target Selection And Placement:

Once the satellite windows were established for each study area, a schedule was set up to install the GCPs. The contracted scale of the photography was 1:6000. To determine the appropriate target characteristics, the Geometronics and Photogrammetry Group, USFS Regional Office was consulted along with the ASPRS Manual of

Photogrammetry (Henriken 1980). An officially accepted formula for target size was not found. According to the ASPRS Manual of Photogrammetry, "The size and shape of the targets will be influenced by such factors as the type of photogrammetric equipment to be used, the altitude at which the photography will be taken, the nature of the terrain, and the requirements of the specific project." The photogrammetry group determined that for a scale of 1:6000 the target should have a leg width of 3.3" and a length (from tip to tip) of 4'. The formula that the Group developed follows. Target leg length L (from tip to tip) is $L = \text{PSR}/6000 \times 4$, where PSR is the Photo Scale Reciprocal (e.g., the 6000 in 1:6000 scale) and the width $W = L/15$ (Dawson 1991). Due to the inconsistency in leg lengths the USFS requested that each Forest determine target size based upon the above formula. Thereafter the target size was standardized to ready made 4' square targets, made of non-reflective vinyl, with a diagonal, 4" wide, white cross on a black background. These are used successfully for photo scales as small as 1:6000.

For this project each control point was marked with a black and white 4' X 4' bullseye target. The targets were generally nailed onto a 2-3' diameter and a 2-3' high stump. When stumps were not available the targets were secured to the ground with nails, with rocks used as additional anchors.

Data Collection:

Each remote station required 4-6 minutes to record information. To make the correction back to the base, data must be

recorded from common satellites by both units. It was determined that anything less than 100 common records would not provide valid latitude and longitude data (Schlaich 1990). Field work for all three units was completed in five days, July 21-25, 1989, and the field crew consisted of five to six people.

Flight:

The flight needed to occur soon after the targets were placed to insure correct positioning. Within one week of target placement, the contractor, Environmental Aeroscientific of Corvallis, Oregon, shot low elevation photos of each study area at a scale of 1:6000. Each area was centered on one photo. A 70mm Hasselblad camera with 2445 Kodak aerial negative film was flown at 4000 ft mean sea level on the Peterson and Gopher areas and at 4300 ft mean sea level for the Randall area. To produce 1:24000 scale photography, the camera was set at an aperture of f/11, with a shutter speed of 1/500, and a focal length of 2 inches. The representative fraction (RF) is determined by the following formula:

$$RF = \frac{F}{H}$$

where F = focal length and H = altitude of the aircraft above ground datum (Avery and Berlin 1985). After the film was developed it was apparent that the photography was taken at the incorrect altitude. Because it was not possible to rephotograph the study areas, and remark ground control locations, Environmental Aeroscientific had the negatives enlarged four times to

approximately 1:6000 scale. Even then it was difficult to locate the GCP's on the photograph with a 3.0 power stereoscope. Some GCPs were hidden by shadows from adjacent stands of timber along the borders of the study areas.

Target Scale:

The appropriate target size for 1:24000 photography is $L = 23.2'$ and $W = 2.4'$ (USFS method).

Transformation and Warping of Raster and Vector Image Files:

Both raster warping and vector warping methods were developed to eliminate the step of transferring the boundary from an image which is not planimetrically correct and varying in scale, to that of a corrected image .

The Raster Warping method converts a raster image of the uncontrolled photograph into a planimetrically corrected image (Figure 5). The boundary lines of the management activity can be drawn on and digitized or scanned directly off the corrected image. The vector warping method "rubber sheets" the vector file of the uncorrected image. In this method, the boundary of the management activity is drawn onto the uncorrected image. It is digitized directly from this image. The vector file of the boundary is next transformed to geographic coordinates and "rubber sheeted" to fit the surface of the area. The process of rubber sheeting involves stretching the map surface causing digitized features to move. The ARC/INFO "rubber sheeting" process is accomplished by the Delauney Triangulation technique. Changes in x

and y for both the digitizer coordinates and the geographic coordinates is called the Z factor for each point. A Triangular Irregular Network is generated from the Z factors of the points using linear interpolation based on the three nearest points (Moreland 1991). A piecewise linear transformation was used. A set of deformation vectors or links are defined and indicate where coordinates are to be moved. After a set of links has been established, ARCEDIT in ARC/INFO first constructs a rubber sheeting transformation and then relocates map features (Figure 5) (ESRI 1987).

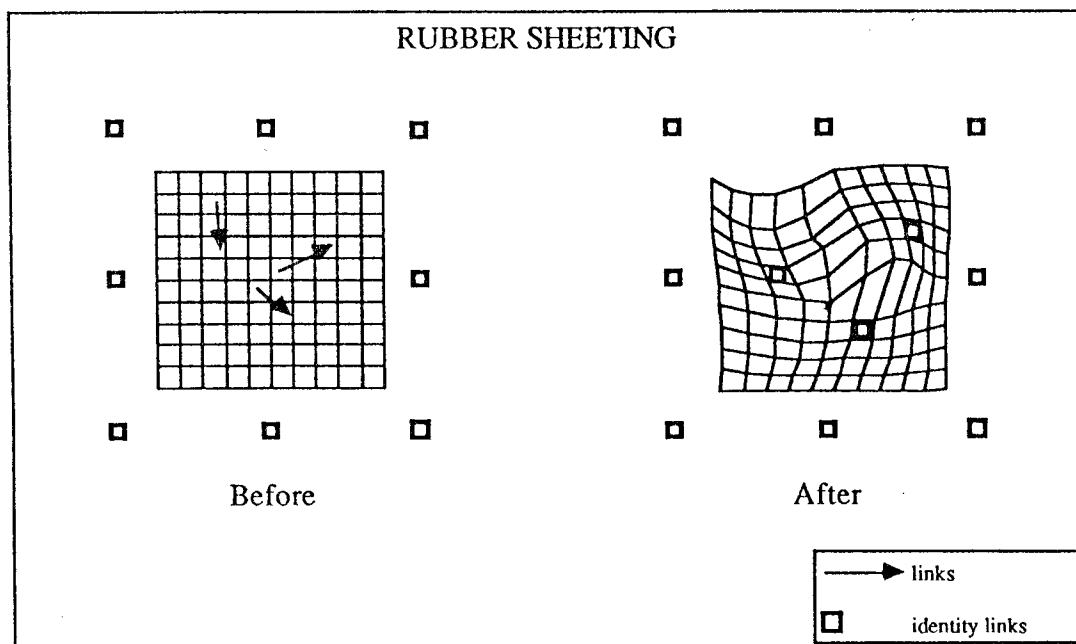


Figure 5. Rubber Sheeting Transformation (ESRI 1987).

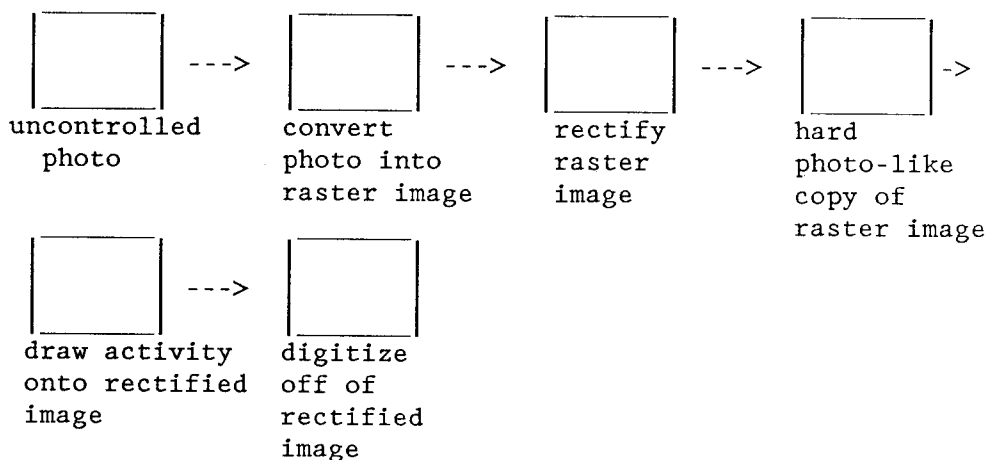
Raster Warping:

Figure 6. Raster Warping Procedure

Scanning the Photography:

The uncontrolled photography was initially converted from analog to digital format by using a video "frame grabber". The digital image was 512 columns X 480 rows. The resolution was too coarse to identify the GCP's on the cathode-ray tube (CRT) screen.

The Cartographic Services in the Geosciences Department at Oregon State University scanned the photographs using an EIKONIX scanning camera and a high intensity light table containing four 150 watt quartz halogen bulbs. The EIKONIX scanner used a 2048 element linear array of charge coupled devices (CCD's) to convert the quantity of light striking each element into an electrical current. The current from each was assigned a digital value based on its strength, creating a machine readable image file. Driven by an extremely fine stepping motor, the array of CCD's swept over the transparency. The scanning camera was capable of a resolution up to 2048 pixels by 2048 pixels. Each image or part of an image

scanned could be divided into over 4 million individual picture elements (i.e., 2048 X 2048). For this project, study areas were scanned at a resolution of 800 by 800 pixels with a ground resolution of 1.8 meters. This was sufficient resolution to allow identification of the approximate location of the GCPs on the digital image. The areas were scanned in band sequential format for the red, green, and blue bands using filters of these colors placed in the optical path.

Geometric Rectification:

Spatial interpolation or "resampling", must be performed in order to geometrically rectify a remotely sensed image to a raster format map coordinate system. In spatial interpolation the geometric relationship between the input pixel location (row, column) and the associated map coordinate of the same point (x, y) are identified. This relationship establishes the geometric coordinate transformation used to relocate every pixel in the original input image to its proper position in the rectified output image (x, y) (Green, as cited in Jensen 1986, pp 104).

Identification of Ground Control Points:

The contractor reformatted the band sequential files to a format where the row-and-column location of the GCPs could be identified on the digital image (See Tables 5, 6, and 7 in Appendix 1). Identification of GCPs on the digital image was difficult because of the original quality of the photography. The quality of GCPs could be identified on Randall and Gopher and located to

within 1 to 3 pixels. Peterson was scanned twice to enhance its resolution, but was too washed out to identify the GCPs. GCP identification on Peterson was approximate with ancillary data, known location on the ground, and by the pattern of the pixels.

Coordinate Transformations:

Non-systematic errors in the identification of GCPs on the digital image were removed by identifying the UTM location of the GPS's on the ground and the row-and-column location on the digital image, and mathematically modeling the geometric distortion present. Least-squares criteria can be used to model the correction without explicitly identifying the source of distortion. Jensen (1986 pp 104) states that for

"moderate distortions in a relatively small area of an image (e.g., a quarter of a Landsat or TM scene), a six-parameter affine transformation is sufficient to rectify the imagery to a geographic frame of reference."

Transforming (x, y) coordinates from a digitizing tablet to UTM (E, N) grid coordinates is a Cartesian coordinate transformation. The coordinate transformation must account for translational shifts, scaling differences and a rotation angle. Translation and scale changes in x and y, skew, and rotation are distortions in digital data that are modeled in a coordinate transformation (Kimerling 1989) (Appendix 2).

Jensen (1986, p. 104) states that

"when all six operations are combined into a single expression, it becomes

$$x' = a_0 + a_1 x + a_2 y$$

$$y' = b_0 + b_1 x + b_2 y$$

where x and y (column, row) are positions in the output-rectified digital image and (x',y') represent the corresponding positions in the original input image".

Root Mean Square Error:

How well the six coefficients derived from the least-squares regression of the initial GCPs account for the distortion in the input image should be determined before rectifying the complete set of data. Root mean square error (RMS error) is computed for each GCP to measure distortion not corrected for by the six-coefficient affine coordinate transformation. The equation is:

$$\text{RMS error} = \sqrt{(x' - x)^2 + (y' - y)^2}$$

(Jensen 1986 pp 105). The formula for the total RMS for a study area is:

$$\text{Total RMS error} = \sqrt{\frac{e_1^2 + e_2^2 + e_3^2 + \dots + e_n^2}{n}}$$

where e = the positional difference between the UTM location and the digitizer location of each GCP. Jensen (1986, p. 105) describes this process.

"The square root of the squared deviations represents a measure of the accuracy of this GCP in the image. By computing RMS error for all GCPs, it is possible to see which GCPs exhibit the greatest error, and to sum all the RMS error. If an evaluation of the total RMS error

reveals that a given set of control points exceeds this threshold, it is common practice to 1) delete from the analysis the GCP that has the greatest amount of individual error, 2) recompute the six coefficients, and 3) recompute the RMS error for all points. This process continues until one of the following occurs: the total RMS error is less than the threshold specified, or until too few points remain to perform a least-squares regression to compute the coefficients".

The Environmental Aeroscientific raster warp program is limited to using four GCPs. The program would automatically select the four GCPs with the lowest error. The method employed in this prototype selected the four GCPs based on spatial location rather than RMS error.

Although a raster warp program was to be developed by the contractor using all control points, the program was never produced, so the image was warped using a maximum of four control points. The four outer most points were selected and the study area boundaries of the raster warped images were digitized from the CRT screen. These files were converted to a MOSS export file, then converted to ARC/INFO format on the Data General system used by the Siuslaw National Forest.

Vector Warping:

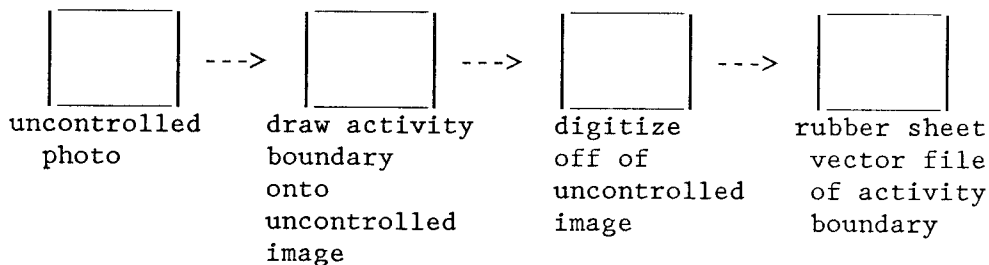


Figure 7. Vector Warping Procedure.

The boundary of each study area and the control points were converted from analog to digital format by digitizing directly off the uncontrolled photograph (Figure 7). The ARCEDIT program was used with the ARC/INFO software to do the digitizing.

ARC/INFO is a vector based Geographic Information System (GIS). Digitizing in ARC/INFO resulted in a file of x,y digitizer coordinates of the GCPs and arcs (vectors) of the boundaries of the study area. The following procedure was developed to 1) transform the digitizer coordinates into UTM coordinates, and 2) rubber sheet the arcs and points into a planimetrically corrected image. Appendix 3 contains the detailed procedures to warp the vector boundaries using ARC/INFO software.

Coordinate Transformations:

The non-systematic error in the identification of GCPs on the low elevation unrectified photograph was reduced by identifying the UTM location of the GCPs in the study area and the (x, y) coordinate locations in the ARC/INFO vector file of the digitized study area, allowing mathematical modeling of the geometric distortion present. This is the same method described in the raster modeling of geometric distortion.

The vector warping transformation was done in two phases: 1) along the boundary of the study area (polygon coverage), and 2) for the GCPs (point coverage).

Transformation of the Study Area Boundaries (polygon):

The TRANSFORM command in ARC/INFO changes coverage coordinates using an affine or a projective transformation function based on GCPs called "tics" in ARC/INFO. "The affine transformation scales, rotates and translates all coordinates in the coverage using the same equation" (ESRI 1989 transform p. 2). As previously described, the x coordinates are scaled differently than the y coordinates and the transformation is based on a minimum of three GCPs. The transformation function is based on comparing the coordinates of the input coverage GCPs with the coordinates for corresponding GCPs in the output coverage. The Tic-IDs are used to identify the GCPs to be compared. The ARC/INFO version of the six parameter affine transformation function is:

$$\begin{aligned}x' &= Ax + By + C \\y' &= Dx + Ey + F\end{aligned}$$

where x and y are coordinates of the input coverage, and x' and y' are coordinates of the output coverage. The units of measurement are normally meters (in ARC/INFO) for both sets of coordinates. Coefficients A,B,C,D,E, and F are determined by comparing the location of GCPs in the input coverage and their locations in the output coverage. As before, a minimum of three GCPs are required to calculate an affine transformation that scales, translates, and rotates the GCP coordinates.

Alternatively, the projective transformation in ARC/INFO is recommended if the input coverage was digitized directly off of aerial photography (ESRI 1989).

"The accuracy of the transformation depends on the surface terrain photographed, the angle between the camera and the ground, and the altitude from which the photograph was taken. The best results are obtained when photographing from higher altitudes, when located directly above and pointing directly down toward a portion of the surface which is relatively flat" (ESRI 1989 transform command description pp 2).
Based upon a more complex formula than the affine transformation a minimum of four GCPs are required for the projective transformation.

$$x' = (Ax + By + C)/(Gx + Hy + 1)$$

$$y' = (Dx + Ey + F)/(Gx + Hy + 1)$$

Root Mean Square Error (RMS error):

RMS error can be calculated for each transformation performed, and indicates how accurate the derived transformation is. The following hypothetical example (Figure 8) illustrates the relative location of four control points (tics) before and after they were transformed.

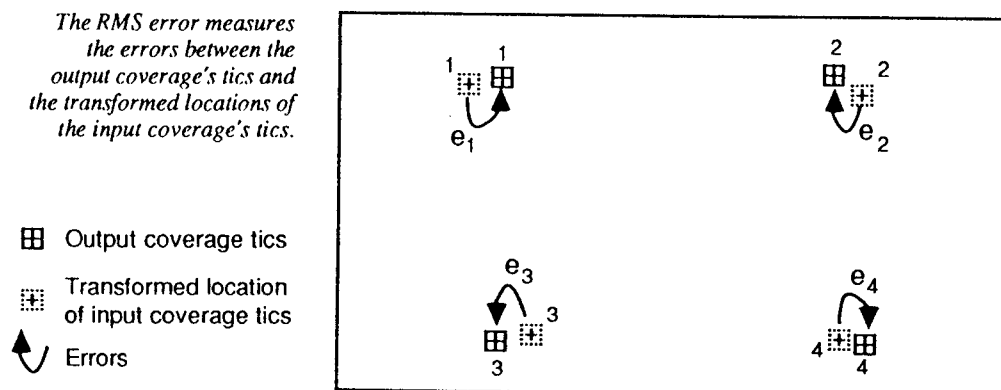


Figure 8. Cartesian Coordinate Transformation (ESRI 1989)

Because the transformation is derived using the least squares method, more GCPs than the minimum necessary must be used. Nineteen GCPs were used for Randall, 27 for Gopher, and 26 for Peterson.

The projective transformation was used because the input coverage was taken from an aerial photograph. However, due to the high relief in the Siuslaw National Forest the projective transformation used alone would not correct the vector file. See Appendix 2 for the transformation procedure.

Tables 8, 9, and 10 in Appendix 1 show the GCPs error squared for each point in the study area. These tables show the error between the input digitizer (x, y) coordinates of a GCP, and the output, UTM (x1, y1) coordinates of the same GCP. The order of the error squared represents the GCP lowest to highest numeric value of error squared. The unit of measure for the error is meters.

Vector Warping "Rubber Sheeting":

Point and polygon coverages were created in UTM coordinates for: a) the polygon coverage of the digitized boundary of the study areas, b) the digitized point coverage of the GCPs of the study areas, and c) the original GPS point coverage that was generated from the UTM GPS coordinates. A "coverage" is defined by ESRI as "the basic unit of storage in ARC/INFO. It is a digital version of a single map sheet layer and generally only describes one type of map feature. A coverage contains both the locational data and thematic attributes for map features in a given area" (ESRI 1990).

Transformed coverages were then created for the area boundary and the GPS points.

Transformed coverages were also created using only the four outer most GCPs for the area boundary and GCPs.

"Rubber Sheeting" the Vector File:

Due to the high topographic relief of the study areas, "rubber sheeting" was performed on each area after GCPs were transformed from digitizer to UTM coordinates.

The TRANSFORM command shifted, rotated and scaled all coordinates in the study areas but did not perform "rubber sheeting".

For comparisons, each study area had boundary versions derived from: 1) walking the area boundary with a Trimble pathfinder collecting the GCPs in real world coordinates, resulting in <area>.GPS, 2) digitizing the area boundary from an unrectified aerial photograph, resulting in <area>.DIG, 3) the ARC/INFO projective transformation of the digitized area boundary <area>.DIG, using all GCPs, resulting in <area>.Trans, 4) the ARC/INFO Projective transformation of digitized area boundary <area>.DIG, using the four outer most GCPs resulting in <area>.Trans4, 5) the ARC/INFO process of rubber sheeting <area>.Trans with all GPS ground control points resulting in <area>.RS, 6) the ARC/INFO process of rubber sheeting <area>.Trans4 with all GPS ground control points resulting in <area>.RS4, 7) the ARC/IVNFO process of rubber sheeting <area>.Trans with the boundary GPS ground control points resulting in <area>.RSlink, 8) the

ARC/INFO process of rubber sheeting <area>.Trans4 with the boundary GPS ground control points resulting in <area>.RS4link, 9) the ARC/INFO process of rubber sheeting <area>.Trans4 with the four outer most GPS ground control points resulting in <area>.RS4link4, 10) the digitizing the area boundary from the raster warped image using the four outer most GCPs in Environmental Aeroscientific's transformation resulting in <area>.RAS.

The resulting boundaries and GCP positional locations from the various vector and raster warping methods shifted in a non-systematic direction and distance.

Measurement Error:

Photogrammetry is a science that frequently requires measurements. In the process of measuring any quantity, factors such as human limitations, instrumental imperfections, and instabilities in nature produce inexact measurements. No matter how carefully a measurement is performed, there will always be some error. Errors in quantitative measurements can be classified into the four types: 1) systematic, 2) random 3) constant errors, and 4) blunders or mistakes (Wong 1980).

Systematic Error:

A systematic error in measurement follows a mathematical or physical law. Corrections can be calculated and systematic error eliminated if the conditions producing the error are determinable. Systematic errors remain constant in size and algebraic sign if the conditions affecting them are constant. Systematic errors are

often called cumulative errors because their algebraic signs tend to remain the same and therefore are additive. Shrinkage or enlargement of photographs are examples of systematic errors in photogrammetry. Aerial cameras with lens distortions are an example of systematic error (Wong 1980).

Random Error:

Once systematic errors have been corrected the remaining errors are classified as random or accidental. Random errors are produced by the limitations of the instrument and people taking the measurements, as well as by variations in the environment. Although usually small in magnitude, random errors can never be completely eliminated (Wolf 1974). Unlike systematic errors, random errors are modeled by laws of probability. They are also called compensating errors because the 50 percent probability of being either positive or negative tends to produce a compensating effect. A digitizer produces a random error each time it is used. For example the ALTEX digitizing table is accurate to .003 of an inch with a resolution of .001 of an inch. Measurements should be taken under wide a range of operating conditions as possible to minimize the effect of random errors (Wong 1980).

Mistakes or Blunders:

Blunders are mistakes caused by carelessness or confusion and are not classified as errors. They can be of any sign and magnitude. Blunders are detected by repeated measurements (Wong 1980)

Constant Errors:

The measuring instrument is a common source of constant error and always have the same sign and magnitude. Errors can be detected and corrected by accurate calibration of the instruments. Personal bias of the observer is also classified as a constant error (Wong 1980).

Error entered into the boundary determination process in different ways, as will be described below.

Determination of Study Area Boundaries:

Independent determinations of the study area boundaries were made by surveyors, silviculturists, and Environmental Aeroscientific personnel. This independent determination of area boundaries added confusion (noise) in determining which error caused positional shift of boundary lines and GCPs within and between each warping method tested.

Boundary lines for the <area>.GPS, <area>.DIG, and <area>.RAS data sets were independently determined at different times and by different methods.

Boundaries of Rand.GPS and Goph.GPS were walked by surveyors in 1989. Geographic coordinates of the boundaries were recorded with a Trimble Pathfinder as they walked the boundaries that were not delineated on a photo or flagged on the ground. Surveyors followed 'fire trails' and used their own judgment as to the location of the clear cut boundary. Boundaries were unclear in dense brush and riparian areas.

Boundaries of Rand.DIG, Goph.DIG, and Pete.DIG, were determined by photo interpretation by silviculturists who manage young stands of vegetation. Actual boundaries on the ground are known and drawn on uncontrolled photographs.

Boundaries of Rand.RAS, Goph.RAS, and Pete.RAS were determined by photo interpretation by Environmental Aeroscientific and digitized from the CRT screen. Actual boundaries on the ground were not known, but were interpreted by using visual cues to activities on photos.

Identification of GCPs on Images:

Another source of error was placement of the GCPs onto aerial photographs and digital images. It was very difficult to locate the GCPs on the photograph using a 3.0 power stereoscope due to a small target size for 1:24000 scale photography. GCPs that were hidden by shadows from adjacent stands of timber along the borders of the study areas were identified by knowing the locations on the ground. GCP identification on the digital image was more difficult than on the aerial photo due to loss of resolution in the digital image on the CRT. The degree of difficulty in locating the GCPs depended on the original quality of the photograph. Randall was of high quality, Gopher moderate and Peterson, poor. GCPs could be identified on Randall and Gopher and located to within 1 to 3 pixels. GCPs in the Peterson study area could only be identified by known location on the ground and the pattern of the pixels on the CRT.

Instrument and Human Operator Error:

The random errors caused by the instruments limitations: 1) \pm 5 meters for the study area boundaries and GCPs measured by the Trimble pathfinder, and 2) .003 of an inch accuracy and repeatability, and .001 of an inch resolution for the ALTEX digitizing tablet. This tablet was used to digitize study area boundaries into vector and raster format.

Human caused errors of boundary and GCPs placement on the ground and imagery, and inherent instrument error added 'noise' to the comparison and evaluation of methods used in this prototype. These errors will be reflected in the results reported in the next chapter.

CHAPTER 4RESULTS

Size, shape, and location of the boundaries and GCP's of each study area were compared by the methods employed to obtain the rectified products. Figures 9 through 42 illustrate the direction and magnitude of shifts by the positional locations of the boundaries and GCPs for each study area (Appendix 1).

Transformation Comparisons:

Use of the four outer most GCPs in the projective transformation resulted in a smaller acreage in all study areas relative to acreage resulting from projective transformations performed using all of the GCPs (Table 1).

Table 1. Projective Transformation Comparisons

	Randall		Gopher		Peterson	
	<u>acres</u>	<u>RMS/GCP</u>	<u>acres</u>	<u>RMS/GCP</u>	<u>acres</u>	<u>RMS/GCP</u>
4 GCPs	49.56	0.0/04	28.94	0.0/04	60.81	0.0/04
All GCPs	50.09	9.9/19	29.59	9.1/27	63.00	11.1/26

Difference	.53		.65		2.19	

The four outer most point projective transformation uses the four GCPs as anchors and moves them to the exact location of the GPS ground control points as evidenced by the RMS of 0.0. The remainder of the GCPs are not adjusted and the boundary is moved by the adjustment of the four chosen GCPs (Figures 9, 10, and 11 in Appendix 1).

The all point projective transformation uses all of the GCPs in a least squares solution and moves them as close as possible to the GPS ground control points as evidenced by the RMS of 9.9 for Randall, 9.1 for Gopher, and 11.1 for Peterson. The boundary is moved by the adjustment of all of the GCPs (Figures 12, 13 and 14 in Appendix 1). Spatial comparisons between the all point and the four point projective transformations are made in Figures 16, 17, and 18 in Appendix 1.

The increase in computed acreage for all study units from the four point transformation to the all point transformation is dependent not solely on the transformation function but also on the original error in locating the digital GCPs and their topographic location within the unit (e.g. ridge, draw, middle of area, boundary of area). There was a seemingly random shift in direction and distance of the GCPs in relation to the GPS ground control locations for all study areas between the four point and all point projective transformation. This shift reflected the error in the placement of the GCPs onto the aerial photograph and the pointing error in digitizing.

The all point projective transformation partially adjusted for these errors at all the GCPs, whereas the four point projective transformation adjusted for only the four selected GCPs.

This variable shift in direction and distance in GCPs due to their positional error results in either an increase or decrease in acreage between methods and areas. Consequently a more meaningful assessment of change may be the positional shift in boundaries between methods.

Rubber Sheeting Comparisons:

The rubber sheeting process using the four point projective transformation and the all point projective transformation resulted in approximately the same acreage (Table 2) and shape for all four study areas (Figures 18, 19 and 20 in Appendix 1).

Table 2. Rubber Sheeting Comparisons.

	Randall		Gopher		Peterson	
	acres	GCP	acres	GCP	acres	GCP
4pt Trans	50.08	04	29.20	04	62.39	04
All Trans	50.11	19	29.42	27	61.79	26

This method used all the GCPs in both the four point and all point projective transformations. The original differences in four point and all point were minimized by the rubber sheeting process.

There are slight differences in each study area boundary between the four point and all point rubber sheeting. The difference between the two rubber sheeting processes is approximately nine meters in the southwest corner of the Peterson area boundary. GCP #55 was used as an anchor point in the four point projective transformation, which moved point 55 to the actual GPS location. In the all point projective transformation this point was not moved to to the GCP location. Therefore there is approximately 18 meters difference in the southwest corner between the two projective transformation processes. There is approximately a nine meter difference in this same corner of the Peterson study area between the all point projective transformation and the rubber sheeting process using the all point projective transformation. Figure 20 shows the boundary line shifting halfway between the two projective transformation processes. Boundary lines in the northeast corner (GCP # 8) of the Gopher study area (Figures 10, 13, and 16 in Appendix 1) and in the northwest corner (GCP #58) of the Randall study area (Figures 11, 14, and 17 in Appendix 1) illustrate this process. In all three areas (Peterson # 55, Gopher # 8, and Randall # 58) the GCPs were placed near but not close enough to the outer most boundaries. Placement of these GCPs contributed to inaccurate boundary determination.

Comparison of Rubber Sheeting with All Point Projective

Transformation and the Rubber Sheeting with Inner GCPs Deleted:

The placement of GCP's on the boundaries of the study area in turn determines the placement of the area's boundary. To determine

the role the inner GCP's played in the placement of area boundaries, or future interior boundaries, links in the rubber sheeting process were dropped for the interior points. Variations in the links used were compared to determine the resulting exterior and interior boundary placement by the number and placement of GCPs used. The descriptions of the methods used are as follows:

method 1 - rubber sheeting the resulting point and polygon coverages of the projective transformation with all of the GCPs to all the points in the point coverage of the GPS ground control.

method 2 - rubber sheeting the resulting point and polygon coverages of the projective transformation with all of the GCPs to only the boundary points in the point coverage of the GPS ground control.

method 3 - rubber sheeting the resulting point and polygon coverages of the projective transformation with the four outer most points to all the points in the point coverage of the GPS ground control.

method 4 - rubber sheeting the resulting point and polygon coverages of the projective transformation with the four outer most points to only the boundary points in the point coverage of the GPS ground control.

method 5 - projective transformation using all GCPs

method 6 - projective transformation using four outer most points.

method 7 - rubber sheeting the resulting point and polygon coverages of the projective transformation with the four outer most

points to only the four outer most points in the point coverage of the GPS ground control.

Table 3 shows the area calculation for each area for each method.

Table 3. Vector Warping Comparisons

	Randall	Gopher	Peterson
	acres	acres	acres
method 1	50.11	29.42	61.79
method 2	50.66	29.51	61.58
method 3	50.08	29.20	62.39
method 4	50.26	29.59	62.43
method 5	50.09	29.59	62.99
method 6	49.56	28.94	60.81
method 7	49.95	28.94	60.96

Figures 21 - 26 in Appendix 1 show the links used in the rubber sheeting process. The resulting vector warps (Figures 27 - 32 in Appendix 1) show the directional and distance shifts in the study area boundaries and GCPs. The direction and magnitude of shift in the GCPs toward the GPS ground locations when performing the various projective transformations indicates the importance of the inner GCP's on the placement of exterior and interior boundaries.

Method 1 shifted the GCPs to the same location as the GPS ground control points. Method 2 utilized all of the GCPs in the projective transformation and the boundary points in the Rubber Sheetting process. Method 3 utilized the four outer most points in the projective transformation and all of the GCPs in the transformation. The acreage for Randall and Gopher is larger using method 2 than method 3 but smaller for Peterson (Figure 17 in Appendix 1). This difference is caused by the error in locating the digital GCPs and their topographical location within the area. Method 1 and #2 boundaries are the same for Randall and Gopher except where the closest boundary GCP was not used as a link (Figures 24, 25 in Appendix 1). In these areas there is approximately between 5-10 meters difference in positional shift. The boundaries for these two methods were approximately the same for the Peterson area (Figure 26 in Appendix 1). Method 1 and #3 boundaries had slight positional differences for all study areas except in locations where a GPS ground control point was not near the boundary of the unit. In these locations there is approximately between 5-10 meters difference in positional shift.

Method 4 used fewer links than methods 1,2, and 3. There were greater positional shifts in method 4 boundary relative to method 1 than the boundaries resulting from methods 2 and 3 (Figures 24, 25, and 26 in Appendix 1).

Approximately 80%, 70%, and 60% of the perimeter of the boundaries of the Gopher, Peterson, and Randall areas had 5-10 meter positional differences in boundaries between methods 1 and 5 (Figure 13, 14, and 12 in Appendix 1).

The positional locations of the boundaries for all three study areas for methods 6 and 7 were essentially the same (Figures 30, 31, and 32 in Appendix 1). The positional shifts in boundaries were less for these methods than for method 5 (Figure 12, 13, and 14 in Appendix 1). The computed acreage for all study areas was the smallest for these methods.

GPS, Rubber Sheeting Vector Warp, and Raster Warp Boundary

Comparison:

Errors introduced by the independent determination of the study area boundaries by surveyors, silviculturists, and Environmental Aeroscientific personnel, and by the different instruments used are difficult to compare accurately; therefore an error buffer approach was used for another method of assessment.

Table 4. GPS, Vector Warp, and Raster Warp Comparison

	Randall	Gopher	Peterson
	<u>acres</u>	<u>acres</u>	<u>acres</u>
GPS	49.68	30.08	not done
Method 1	50.11	29.42	61.79
Raster Warping	51.63	34.72	60.65

Study area boundaries from the GPS, rubber sheeted vector warp and the raster warp methods were buffered five meters due to the \pm five meter accuracy of the GPS (Figures 33 through 39 in Appendix 1). There was overlap in most areas between methods when the boundaries were buffered, except where there was an obvious

boundary placement error. The three instances of obvious error were 1) the GPS boundary of the Randall study area in the northwest corner going into the timber following the fireline, whereas the rubber sheeted boundary followed the cutting boundary (Figure 37 in Appendix 1), 2) the straight line of Randall's southern boundary following a landline, whereas the rubber sheeted boundary followed the fireline (Figure 37 in Appendix 1), and 3) the buffer in the southeast section of Gopher being excluded in the GPS and rubber sheeted boundary but being included in the raster warp (Figure 38 in Appendix 1). Peterson did not have boundaries delineated by the GPS, there were no obvious boundary delineation deviations between the rubber sheeting and raster warp methods (Figure 39 in Appendix 1).

Not including the boundary delineation errors, there was approximately a 30% overlap in boundaries of the GPS and method 3 in Gopher and 60% in Randall (Figures 34, 33 in Appendix 1). The overlap between the GPS and method 1 boundaries were 45% in Gopher and 30% in Randall (Figures 36, 35 in Appendix 1).

Rubber Sheeting Vector Warp and Raster Warp Comparisons:

(Figures 33 - 42 in Appendix 1). The raster warp method used the same four GCPs that were employed in the four point projective transformation (Randall #58, 51, 10 and 3 (Figure 21 in Appendix 1); Gopher #15, 61, 12, and 8 (Figure 22 in Appendix 1); and Peterson #66, 1, 9, and 55 (Figure 23 in Appendix 1). The technique used to warp the raster image was not revealed by the developer to Environmental Aeroscientific or to the author. Generally the digital image was warped to the selected four GCPs.

The vector and raster warped boundaries match in the areas of these GCPs. Where buffered boundaries do not overlap, it is assumed to be due to a difference in boundary delineation or the lack of a GCP in the raster warp. Not including the boundary delineation errors there were approximately 50% overlaps in buffered boundaries in the Peterson study area between the raster and vector warp methods, 60% in Gopher, and 60% in Randall (Figures 37 - 39 in Appendix 1).

Summary:

GCPs were installed on three study areas in the Siuslaw National Forest to establish the ground control needed to rectify a low elevation (1:6000) aerial photograph. raster and vector warping methods were evaluated in terms of their accuracy and efficiency.

Due to the rugged topography of the Siuslaw National Forest, selection of GCPs was an important function in the accurate transformation of images. GCPs should be positioned to establish a control network that captures all major elevation changes. Vector warping methods resulting from using the four outer most points and the outer boundary points (methods 2 - 7) do not provide as accurate a spatial fit of the interior and exterior boundaries as that of the vector warping method (method 1) using all of the originally selected GCPs.

Before adequate comparisons of positional accuracy can be made of the vector and raster warping methods the boundaries of the raster image need to be adjusted to the vector image.

CHAPTER 5

CONCLUSIONS

Improvements to Study:

Independent determination of the study area boundaries added confusion in determining which error caused positional shift of boundary lines and GCPs within and between each warping method tested. Confusion resulting from this error prevented comparisons of the GPS boundary (which should have served as "ground truth"), to the boundaries of the vector and raster warp methods.

Higher confidence in the positional accuracy of area boundaries, resulting from the various warping methods, would be gained if delineation of these boundaries would be made by someone who has been to the area and knows where the actual activity boundary is located. This boundary should be used as a the source for each warping method used.

Error in placement of the GCPs onto aerial photographs and digital images would have been reduced if the adequate target size for the scale of the photography (1:24000) had been used. Due to this error, the confidence in identification of GCPs on the raster image was too low for comparison of the vector and raster warp methods.

When procuring aerial photography for this type of rectification, care must be taken to use the appropriate target

size for the scale of the resulting photography. A 4' X 4' target size is recommended for 1:6000 scale photography.

Future Research Opportunities:

Elimination of GCP identification error due to the photography being flown at the 1:24000, and boundary identification error resulting from independent delineation would allow comparison of the positional shifts in the GPS boundary with that of the resulting boundaries from the various vector and raster warp methods tested.

The use of polynomial equations in image processing systems has been a common method of rectifying remotely sensed images. Higher order polynomial equations in terrain relief modeling are being developed by designers of image processing software to address the problem of terrain relief in rectification of remotely sensed imagery. ERDAS is developing terrain modeling rectifying software for image processing system. Field data collected in this study will be used to develop the software. The results of this rectification and the implementation of its procedure can be evaluated against the vector warp methods tested in this research.

Kinematic differential GPS has been used for decimeter positioning of airplanes. High-precision airplane positions can replace traditional and expensive ground control in photogrammetry. Expanding this technology to establish a ground control network that captures all major elevation changes for a 10 to 60 acre area from kinematic differential GPS in an airplane would make this rectification technology more feasible and probable

for natural resource management agencies to implement into their day-to-day management.

Recommendations Based on Output:

To facilitate automation of spatial analysis of historical and present management activities, and to minimize duplication of input when adding new managed stands into the GIS vegetation layer it is recommended that the Siuslaw National Forest do the following:

1) Establish a ground control network that captures all major elevation changes for each managed stand of vegetation. This research has shown the placement of the exterior and interior GCPs of an area determines the placement of the areas boundaries within a GIS. It is helpful and important to locate GCPs close to the boundary of the study area and at major points of elevation change in the interior.

2) Establishment of these GCPs should be done with a GPS unit in 3D differential mode to achieve an accuracy of 3-5 meters. Black and white 4' X 4' bullseye targets should be used to identify the GCP on a 1:6000 aerial photograph.

3) Procure a 1:6000 color aerial photograph for each managed stand. Each stand should be centered on one photograph. Photography should be taken soon after the targets are in place to insure correct positioning.

4) Delineation of the area boundary should be done by a person who visited the site and knows the location of the boundary.

5) Digitize the area boundary into a GIS.

6) Rubber sheet (using the ARC/EDIT link method) the resulting point and polygon coverages, with all of the GCP's, to all of the GPS ground control points in the GPS coverage (method 1).

Of the tested methods, this method provides the most accurate rectification of vector boundaries that have been digitized or scanned from an uncontrolled low elevation photograph.

Once this managed area boundary is rectified in the GIS, additional interior lines of future activities can be digitized directly off of the 1:6000 photograph. The digital lines of past activities can be used as a template when boundaries of new activities are coincidental to the boundaries of the past activities. The manual overlay system of recording activities should be maintained as well as the digital records. This manual overlay system will provide quick and efficient identification of these coincidental lines. Upkeep of this manual overlay system will provide the tool for manuscripting the activities of the management area for input in GIS and reduce a duplication of data input. Using such methods, only one controlled aerial photograph is needed to track activities for the managed stand of vegetation for every 25 to 30 years.

BIBLIOGRAPHY

- Avery, T.A., and G.A. Berlin. 1985. Interpretation of Aerial Photographs. Macmillian Publishing Company, New York, pp. 115, 137-8.
- Bain, S. 1988. Landsat classification/field correlation methods for vegetation classification. Proceedings of the Second Forest Service Remote Sensing Applications Conference, Slidell Louisiana and NSTL Mississippi, April, 1988.
- Bain, S., Reid, J. E. McMullen, H. Lachowski, V. Landrum. 1991. Integrating Remote Sensing Into Resource Data Collection. Unpublished Report Project 615, USDA Forest Service, Washington D.C. 1991.
- Carr, D.A. 1987. Silvicultural Prescription for Proposed Timber Sale, Randall Roach 88 u-2. Unpublished Manuscript. Alsea Ranger District, Siuslaw National Forest, Alsea, Oregon.
- Colvocoresses, A.P. 1984. Mapping with the Landsat-4 thematic mapper. Proceedings of the 50th Annual Meeting, ASP 1984.
- Dawson, R., 1991. Unpublished Interview. Photogrammetry Group Leader, USFS, Regional Office, Portland, Oregon.
- Dowman, I.J. 1987. The Prospects for Topographic Mapping using SPOT Data. Proceedings of SPOT 1 Image Utilization Assessment, Results, Paris, France 1987.
- ESRI. 1987. ARCEDIT Users Guide. Rubber Sheeting. ESRI, Redlands, California. chapter 14.
- ESRI. 1989. ARC/INFO Volume 2. Command References Transform. ESRI, Redlands, California.
- ESRI. 1990 ARC/INFO Volume 1. The ARC/INFO data model. ESRI, Redlands, California. chapter 5 pp 1.
- Henriken, S. W., and S.H. Schroeder, and R.K. Brewer, 1980. Field Surveys for Photogrammetry. The Manual of Photogrammetry - Fourth Edition. ASPRS, Falls Church, Va. pp. 441-5.
- Hurn, J., 1989. GPS, A Guide to the Next Utility. Trimble Navigation LTD. Sunnyvale Ca. 76 pp.
- Irish, R. 1990. Geocoding Satellite Imagery for GIS Use. GIS World, Inc. August/September 1990. pp. 59-62.
- Jensen, J.R., 1986. Introductory Digital Image Processing, A Remote Sensing Perspective. Prentice-Hall, Englewood Cliffs, New Jersey. pp. 102-115.

- Kimerling, A.J., 1989. Unpublished Interview. Professor of Cartography, Oregon State University, Corvallis, Oregon.
- _____. Cartesian Coordinate Transformations. Unpublished Paper. Oregon State University, Corvallis, Oregon.
- Krabill, W.B., and C.F. Martin, 1987. Aircraft Positioning Using Global Positioning System Carrier Phase Data. Journal of Navigation, 34(1), pp. 1-21.
- Kratky V. 1988. Rigorous Photogrammetric Processing of SPOT Images at CCM Canada. Proceedings of the International Symposium on Topographic Applications of SPOT data, Sherbrooke, Quebec, Canada.
- Lichten, S.M., J.S. Border, 1987. Strategies for High-precision Global Positioning System Orbit Determination. Journal of Geophysical Research, Vol. 92, No. B12, November 1987, pp. 12,751-12-762.
- Lichten, S.M. 1990. Towards GPS Orbit Accuracy of Tens of Centimeters. Geophysical Research Letters Vol. 17 No. 3 pp. 215-218.
- Lillesand, T.M., R.W. Kiefer, 1987. Remote Sensing and Image Interpretation. John Wiley and Sons, New York. pp. 337.
- Mader, G.L. 1986. Dynamic positioning Using GPS Carrier Phase Measurements. Manuscripta Geodetica, II(4) pp. 272-7.
- McCall, K., and R.A. Alexander, 1987. Silvicultural Prescription for Proposed Timber Sale, Gopher Flynn u-2. Unpublished Manuscript. Alsea Ranger District, Siuslaw National Forest, Alsea, Oregon.
- Moreland, W. 1991. Delauney Triangulation Technique, Unpublished Interview, Programmer, ESRI, Redlands, Ca.
- Naraghi, M., W. Stromberg, and M. Daily, 1983. Geometric Rectification of Radar Imagery Using Digital Elevation Models. Photogrammetric Engineering and Remote Sensing, Vol. 49. pp. 195-9.
- Quirion, C. 1987. Centimeter-Level GPS Surveys in Seconds: Formulation and Analysis. Proceedings: ASPRS/ACSM Annual Meeting, Baltimore, March 29-April 3.
- Raines, M., 1987. The Role of GIS in Spatial Resource Information Management - A Forest Service Perspective. GIS '87 San Fransico - Second Annual International Conference. pp. 111-121.
- Remondi, B. W. 1985. Global Positioning System Carrier Phase: Description and Use. NOAA Technical Memorandum NOS NGS-42.

Roab, P., 1976. USDA Environmental Analysis Report, Commerical Timber Sale, Peterson 820. Unpublished Manuscript. Waldport Ranger District, Siuslaw National Forest, Waldport, Oregon.

Schlaich, D., and M. Schwartz, 1990. Test Project Evaluation of BLM Coordinates Using Trimble Pathfinders. Unpublished Report. pp. 1-3.

Seidel, K., F. Ade, and J. Lichtenegger, 1983. Augmenting LANDSAT MSS Data with Topographic Information for Enhanced Registration and Classification. IEEE Transactions on Geoscience and Remote Sensing, Vol. GE-21. pp. 252-8.

Senus, W. J., R. W. Hill. 1981. GPS Application to Mapping, Charting and Geodesy. Journal of The Institue of Navigation, Vol. 28, No. 2, Summer 1981.

Welch, R., and E.L. Usery. 1984. Cartographic assuracy of Landsat-4 MSS and TM image data. Transactions on Geoscience and Remote Sensing, Vol. GE-22, No. 3, May 1984.

Wolf, P.R., 1974. Elements of Photogrammetry. McGraw-Hill, Inc., USA. pp. 230.

Wong, K.W., 1980. Basic Mathematics of Photogrammetry. ASPRS Manual of Photogrammetry, Fourth Edition, ASPRS Falls Church, Va. pp. 69.

APPENDICIES

APPENDIX 1
TABLES AND FIGURES

TABLE 5. Randall Study Area Ground Control Point Coordinates

file location on screen Row/Column - (enlargement area A) R:64 C:4
(enlargement area B) R:264 C:4

POINT	Screen		File		ENLARGEMENT	UTM COORDINATE	LATITUDE	LONGITUDE	ELEVATION
	row	column	row	column					
1	- 494	377	558	381	- A	438544.7097E - 4932041.4430N	- 44-32-27.724	- 123-46-24.831	- 265.560
2	- 216	427	580	431	- B	438498.5844E - 4932004.2646N	- 44-32-26.505	- 123-46-26.905	- 276.427
3	- 208	487	572	491	- B	438475.1704E - 4931943.9747N	- 44-32-24.544	- 123-46-27.940	- 276.255
4	- 295	349	359	353	- A	438750.4709E - 4931950.6585N	- 44-32-24.845	- 123-46-15.469	- 175.25
5	- 225	338	289	342	- A	438832.5047E - 4931924.7975N	- 44-32-24.032	- 123-46-11.741	- 226.055
6	- 176	312	240	316	- A	438882.6945E - 4931943.7649N	- 44-32-24.662	- 123-46-09.475	- 181.925
7	- 268	251	332	255	- A	438840.2463E - 4932029.6404N	- 44-32-27.432	- 123-46-11.435	- 153.41
8	- 102	314	166	318	- A	438960.3142E - 4931882.6460N	- 44-32-22.705	- 123-46-05.932	- 255.555
9	- 128	194	192	198	- A	438996.7781E - 4932012.1519N	- 44-32-26.913	- 123-46-04.335	- 255.295
10	- 30	267	94	271	- A	439059.7800E - 4931884.4267N	- 44-32-22.793	- 123-46-01.426	- 244.425
50	- 154	128	218	132	- A	439009.1481E - 4932079.0583N	- 44-32-29.085	- 123-46-03.803	- 234.55
51	- 262	78	326	82	- A	438948.2017E - 4932202.1053N	- 44-32-33.054	- 123-46-06.617	- 149.825
52	- 342	121	406	125	- A	438828.7966E - 4932208.0437N	- 44-32-33.210	- 123-46-12.030	- 135.94
53	- 357	215	421	219	- A	438764.4083E - 4932124.9034N	- 44-32-30.496	- 123-46-14-912	- 166.925
54	- 416	210	480	214	- A	438703.9459E - 4932163.1515N	- 44-32-31.717	- 123-46-17.668	- 185.68
55	- 416	124	480	128	- A	438759.5360E - 4932251.7125N	- 44-32-34.604	- 123-46-15.187	- 128.69
56	- 503	157	567	161	- A	438656.4195E - 4932269.3806N	- 44-32-35.145	- 123-46-19.867	- 119.26
57	- 296	223	660	227	- B	438512.0712E - 4932253.6826N	- 44-32-34.592	- 123-46-26.401	- 140.945
58	- 336	272	700	276	- B	438452.0281E - 4932233.4846N	- 44-32-33.919	- 123-46-29.113	- 150.915
59	- 332	357	696	361	- B	438423.8035E - 4932105.7857N	- 44-32-29.772	- 123-46-30.337	- 219.64

TABLE 6. Gopher Study Area Ground Control Point Coordinates

file location on screen Row/Column - (enlargement area A) R:164 C:0
(enlargement area B) R:164 C:200

POINT	Screen		File		ENLARGEMENT AREA	UTM COORDINATE ZONE 10 (meters)		LATITUDE - LONGITUDE		ELEVATION (meters)			
	row	column	row	column									
1	-	347	392	511	392	-	A	-	433729.9865E - 4930954.6086N	-	44-31-50.968 - 123-50-02.484	-	252.40
2	-	265	400	429	400	-	A	-	433729.0219E - 4931028.7703N	-	44-31-53.371 - 123-50-02.562	-	250.55
3	-	198	361	312	361	-	A	-	433688.8150E - 4931094.7234N	-	44-31-55.495 - 123-50-04.414	-	256.47
4	-	221	390	385	390	-	A	-	433725.9066E - 4931076.0458N	-	44-31-54.902 - 123-50-02.725	-	254.51
5	-	197	422	361	422	-	A	-	433762.9649E - 4931099.5208N	-	44-31-55.675 - 123-50-01.057	-	250.96
6	-	211	503	375	503	-	A	-	433840.0878E - 4931092.8095N	-	44-31-55.483 - 123-49-57.560	-	253.125
7	-	314	300	478	500	-	B	-	433837.1156E - 4930989.6197N	-	44-31-52.138 - 123-49-57.647	-	243.52
8	-	240	388	404	588	-	B	-	433916.0616E - 4931072.9653N	-	44-31-54.865 - 123-49-54.109	-	260.355
9	-	174	338	338	538	-	B	-	433858.5716E - 4931121.7820N	-	44-31-56.428 - 123-49-56.736	-	277.14
10	-	135	441	299	441	-	A	-	433762.2257E - 4931159.0226N	-	44-31-57.603 - 123-50-01.118	-	276.20
11	-	226	299	390	299	-	A	-	433633.5568E - 4931061.5603N	-	44-31-54.402 - 123-50-06.902	-	270.29
12	-	65	395	299	395	-	A	-	433715.1593E - 4931223.2867N	-	44-31-59.670 - 123-50-03.280	-	282.153
13	-	79	500	243	500	-	A	-	433819.3351E - 4931218.0270N	-	44-31-59.534 - 123-49-58.558	-	292.19
14	-	178	112	342	112	-	A	-	433440.3817E - 4931090.9094N	-	44-31-55.289 - 123-50-15.667	-	276.835
15	-	426	1	590	1	-	A	-	433346.0384E - 4930832.8856N	-	44-31-46.896 - 123-50-19.821	-	279.095
50	-	381	371	545	371	-	A	-	433715.3618E - 4930910.2297N	-	44-31-49.525 - 123-50-03.126	-	248.45
51	-	419	338	583	338	-	A	-	433683.6645E - 4930862.8161N	-	44-31-47.978 - 123-50-04.540	-	232.785
52	-	383	265	547	265	-	A	-	433605.9872E - 4930901.9049N	-	44-31-49.219 - 123-50-08.077	-	245.45
53	-	396	195	560	195	-	A	-	433525.3452E - 4930871.2550N	-	44-31-48.199 - 123-50-11.716	-	219.57
54	-	423	113	587	113	-	A	-	433444.9702E - 4930845.2012N	-	44-31-47.328 - 123-50-15.345	-	251.64
55	-	346	56	510	56	-	A	-	433399.4332E - 4930925.0661N	-	44-31-49.901 - 123-50-17.445	-	258.17
56	-	270	67	434	67	-	A	-	433403.2575E - 4931000.9068N	-	44-31-52.360 - 123-50-17.307	-	261.10
57	-	182	60	346	60	-	A	-	433391.6942E - 4931089.4339N	-	44-31-55.225 - 123-50-17.872	-	276.025
58	-	277	228	441	228	-	A	-	433562.5740E - 4931003.9338N	-	44-31-52.511 - 123-50-10.091	-	243.97
59	-	292	161	456	161	-	A	-	433488.0062E - 4930977.8818N	-	44-31-51.642 - 123-50-13.457	-	232.94
60	-	326	329	490	329	-	A	-	433671.9728E - 4930956.4663N	-	44-31-51.009 - 123-50-05.113	-	257.67
61	-	86	185	250	185	-	A	-	433510.5077E - 4931187.7022N	-	44-31-58.449 - 123-50-12.535	-	286.95

TABLE 7. Peterson Study Area Ground Control Point Coordinates

file location on screen Row/Column - (enlargement area A) R:40 C:2
 (enlargement area B) R:240 C:2
 (enlargement area C) R:174 C:250

POINT	Screen		File		ENLARGEMENT AREA	UTM COORDINATE ZONE 10 (meters)		LATITUDE - LONGITUDE		ELEVATION (meters)
	row	column	row	column						
1	124	420	16	422	A	423430.5168E	4931295.2063N	44-31-58.333	123-57-49.241	296.36
2	192	332	232	334	A	423343.8549E	4931231.7336N	44-31-56.243	123-57-53/133	247.88
3	227	191	267	193	A	423202.1408E	4931192.7981N	44-31-54.927	123-57-59.532	221.64
4	350	404	390	406	A	423434.7523E	4931085.3759N	44-31-51.535	123-57-48.937	236.46
5	129	262	303	512	C	423535.8498E	4931180.5264N	44-31-54.657	123-57-44.408	251.92
7	364	462	538	712	C	423750.0610E	4930960.7275N	44-31-47.616	123-57-34.587	279.90
8	289	429	463	679	C	423712.5894E	4931035.0136N	44-31-50.009	123-57-36.324	282.30
9	457	439	631	689	C	423741.1610E	4930864.5825N	44-31-44.497	123-57-34.939	278.41
10	121	311	295	561	C	423581.1819E	4931194.7740N	44-31-55.136	123-57-42.362	269.12
11	192	250	366	500	C	423535.6478E	4931110.9106N	44-31-52.401	123-57-44.380	236.00
50	348	337	522	587	C	423636.5114E	4930949.9038N	44-31-47.222	123-57-39.725	227.39
51	325	268	499	518	C	423565.5295E	4930980.9194N	44-31-48.200	123-57-42.957	210.89
52	313	475	553	477	B	423531.4028E	4930919.2019N	44-31-46.187	123-57-44.470	210.73
53	283	411	523	413	B	423458.8215E	4930930.6420N	44-31-46.530	123-57-47.764	175.47
54	300	244	540	246	B	423283.6095E	4930904.4742N	44-31-45.615	123-57-55.687	157.94
55	359	183	599	185	B	423219.6482E	4930829.0700N	44-31-43.147	123-57-58.544	116.46
56	301	137	541	139	B	423157.7929E	4930886.9531N	44-31-44.999	123.58-01.377	114.26
57	423	206	463	208	A	423235.2063E	4930989.1685N	44-31-48.341	123-57-57.925	176.50
58	330	286	370	288	A	423303.6539E	4931098.7735N	44-31-51.919	123-57-54.883	219.36
59	251	144	291	146	A	423175.3785E	4931171.6059N	44-31-54.230	123-58-00.733	210.04
60	349	120	389	122	A	423139.9791E	4931069.7577N	44-31-50.916	123-58-02.282	160.67
61	240	108	280	110	A	423105.7817E	4931179.4042N	44-31-54.456	123-58-03.890	177.15
62	173	89	213	91	A	423092.4072E	4931254.1493N	44-31-56.873	123-58-04.536	192.22
63	202	341	376	591	C	423610.0436E	4931109.3866N	44-31-52.380	123-57-41.009	281.75
65	70	3	110	302	A	423300.6258E	4931245.0345N	44-31-59.898	123-57-55.152	278.25
66	58	86	98	88	A	423083.8992E	4931350.2222N	44-31-59.983	123-58-04.973	238.94

TABLE 8

RANDALL ROACH STUDY AREA
RMS error for each GCP
Vector Transformation

Pt #	vector file		UTM COORDINATE - ZONE 10		Error	
	X in	Y in	X output	Y output	squared	order
1	-21.89	14.37	438544.7097E	- 4932041.4430N	- 47.16	- 8
2	-21.65	13.85	438498.5844E	- 4932004.2646N	- .63	- 1
3	-21.74	13.24	438475.1704E	- 4931943.9747N	- 82.20	-10
4	-23.99	14.77	438750.4709E	- 4931950.6585N	-144.20	-15
5	-24.73	14.86	438832.5047E	- 4931924.7975N	-166.77	-17
6	-25.26	15.08	438882.6945E	- 4931943.7649N	-383.42	-20
7	-24.32	15.79	438840.2463E	- 4932029.6404N	- 40.86	- 7
8	-26.09	15.07	438960.3142E	- 4931882.6460N	- 14.41	- 5
9	-25.82	16.33	438996.7781E	- 4932012.1519N	-181.09	-18
10	-26.88	15.57	439059.7800E	- 4931884.4267N	- 5.92	- 2
50	-25.53	17.05	439009.1481E	- 4932079.0583N	-245.27	-19
51	-24.39	17.63	438948.2017E	- 4932202.1053N	- 10.57	- 3
52	-23.46	17.23	438828.7966E	- 4932208.0437N	-110.17	-13
53	-23.31	16.21	438764.4083E	- 4932124.9034N	- 12.11	- 4
4	-22.63	16.18	438703.9459E	- 4932163.1515N	- 91.81	-12
55	-22.71	17.18	438759.5360E	- 4932251.7125N	- 21.54	- 6
56	-21.83	16.82	438656.4195E	- 4932269.3806N	- 58.35	- 9
57	-20.86	16.05	438512.0712E	- 4932253.6826N	-114.74	-14
58	-20.39	15.58	438452.0281E	- 4932233.4846N	- 84.17	-11
59	-20.62	14.54	438423.8035E	- 4932105.7857N	-145.85	-16

TABLE 9

GOPHER FLYNN STUDY AREA
RMS error for each GCP
Vector Transformation

Pt #	vector file		UTM COORDINATE - ZONE 10		Error	
	X in	Y in	X output	Y output	squared	order
1	-26.74	16.89	433729.9865E	4930954.6086N	-192.15	-24
2	-26.80	17.80	433729.0219E	4931028.7703N	3.16	-1
3	-26.43	18.54	433688.8150E	4931094.7234N	4.96	-2
4	-26.72	18.23	433725.9066E	4931076.0458N	-140.98	-20
5	-27.07	18.60	433762.9649E	4931099.5208N	-204.64	-26
6	-27.95	18.36	433840.0878E	4931092.8095N	15.74	-5
7	-27.88	17.25	433837.1156E	4930989.6197N	35.65	-11
8	-28.85	18.01	433916.0616E	4931072.9653N	-179.99	-23
9	-28.33	18.73	433858.5716E	4931121.7820N	-268.51	-27
10	-27.29	19.19	433762.2257E	4931159.0226N	52.74	-12
11	-25.74	18.20	433633.5568E	4931061.5603N	-105.66	-18
12	-26.79	19.96	433715.1593E	4931223.2867N	69.62	-13
13	-27.94	19.79	433819.3351E	4931218.0270N	-192.67	-25
14	-23.74	18.77	433440.3817E	4931090.9094N	5.67	-3
15	-22.53	16.11	433346.0384E	4930832.8856N	-103.54	-17
50	-26.50	16.53	433715.3618E	4930910.2297N	99.18	-16
51	-26.19	16.11	433683.6645E	4930862.8161N	27.82	-9
52	-25.42	16.60	433605.9872E	4930901.9049N	7.96	-4
53	-24.60	16.41	433525.3452E	4930871.2550N	-166.59	-22
54	-23.73	16.13	433444.9702E	4930845.2012N	-164.75	-21
55	-23.11	16.97	433399.4332E	4930925.0661N	22.68	-6
56	-23.24	17.79	433403.2575E	4931000.9068N	32.87	-10
57	-23.18	18.73	433391.6942E	4931089.4339N	84.05	-14
58	-24.97	17.71	433562.5740E	4931003.9338N	26.42	-8
59	-24.31	17.54	433488.0062E	4930977.8818N	-132.11	-19
60	-26.08	17.15	433671.9728E	4930956.4663N	96.61	-15
61	-24.54	19.74	433510.5077E	4931187.7022N	26.51	-7

TABLE 10

PETERSON STUDY AREA
RMS error for each GCP
Vector Transformation

Pt #	vector file		UTM COORDINATE - ZONE 10		Error squared	order
	X in	Y in	X output	Y output		
1	-21.91	16.82	423430.5168E	- 4931295.2063N	-480.41	-26
2	-20.92	16.06	423343.8549E	- 4931231.7336N	- 4.40	- 3
3	-19.33	15.72	423202.1408E	- 4931192.7981N	- 95.61	-14
4	-21.70	14.40	423434.7523E	- 4931085.3759N	- 13.06	- 6
5	-22.84	15.31	423535.8498E	- 4931180.5264N	- 2.05	- 2
7	-24.99	12.75	423750.0610E	- 4930960.7275N	-125.28	-18
8	-24.64	13.58	423712.5894E	- 4931035.0136N	- 88.88	-13
9	-24.73	11.72	423741.1610E	- 4930864.5825N	- 76.76	-10
10	-23.32	15.42	423581.1819E	- 4931194.7740N	- .28	- 1
11	-22.76	14.59	423535.6478E	- 4931110.9106N	- 11.05	- 5
50	-23.63	12.87	423636.5114E	- 4930949.9038N	- 78.82	-12
51	-22.88	13.19	423565.5295E	- 4930980.9194N	-123.40	-17
52	-22.44	12.60	423531.4028E	- 4930919.2019N	-180.56	-21
53	-21.72	12.86	423458.8215E	- 4930930.6420N	-161.29	-20
54	-19.94	12.76	423283.6095E	- 4930904.4742N	- 60.09	- 9
55	-19.28	12.11	423219.6482E	- 4930829.0700N	-274.88	-23
56	-18.77	12.73	423157.7929E	- 4930886.9531N	-290.64	-24
57	-19.54	13.60	423235.2063E	- 4930989.1685N	- 5.31	- 4
58	-20.38	14.62	423303.6539E	- 4931098.7735N	- 78.76	-11
59	-19.10	15.56	423175.3785E	- 4931171.6059N	- 15.87	- 7
60	-18.69	14.49	423139.9791E	- 4931069.7577N	- 99.13	-15
61	-18.46	15.64	423105.7817E	- 4931179.4042N	-120.74	-16
62	-18.28	16.33	423092.4072E	- 4931254.1493N	-384.72	-25
63	-23.68	14.50	423610.0436E	- 4931109.3866N	-149.11	-19
65	-20.56	17.41	423300.6258E	- 4931245.0345N	-266.32	-22
66	-18.26	17.55	423083.8992E	- 4931350.2222N	- 57.64	- 8

FIGURE 9
Randall Study Area
Four point transformation

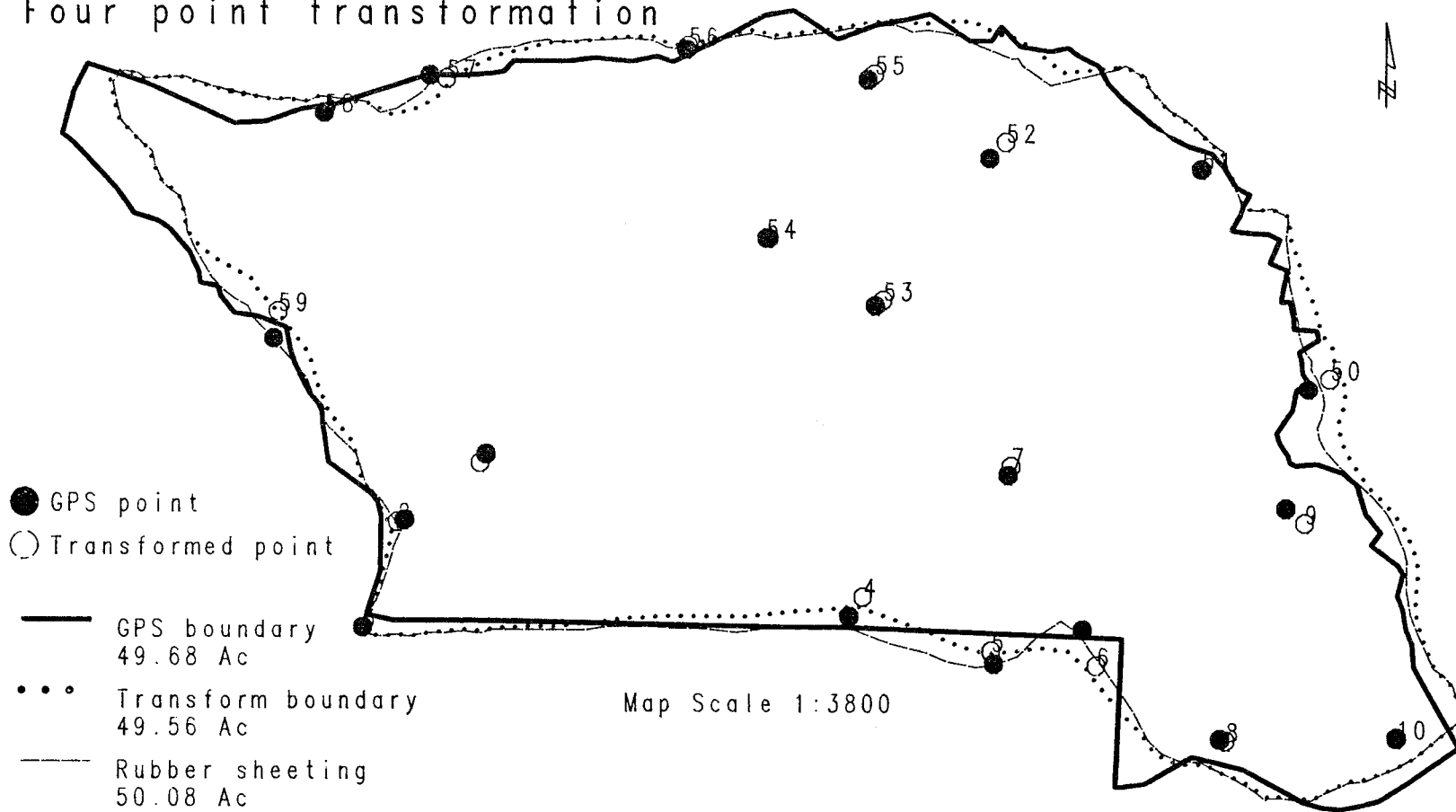


FIGURE 10

Gopher Flynn Study Area

Four point transformation

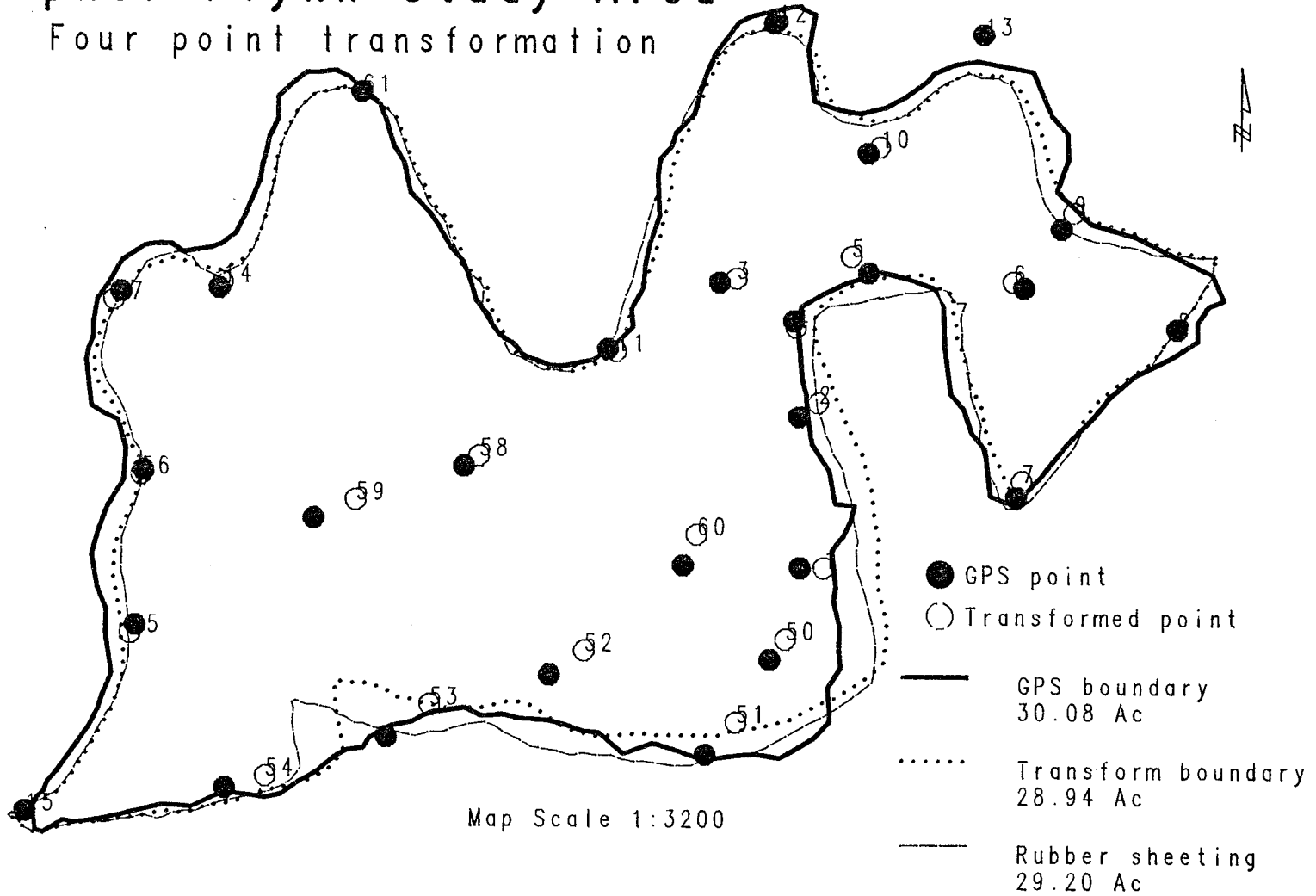


FIGURE 11

Peterson Study Area

Four point transformation

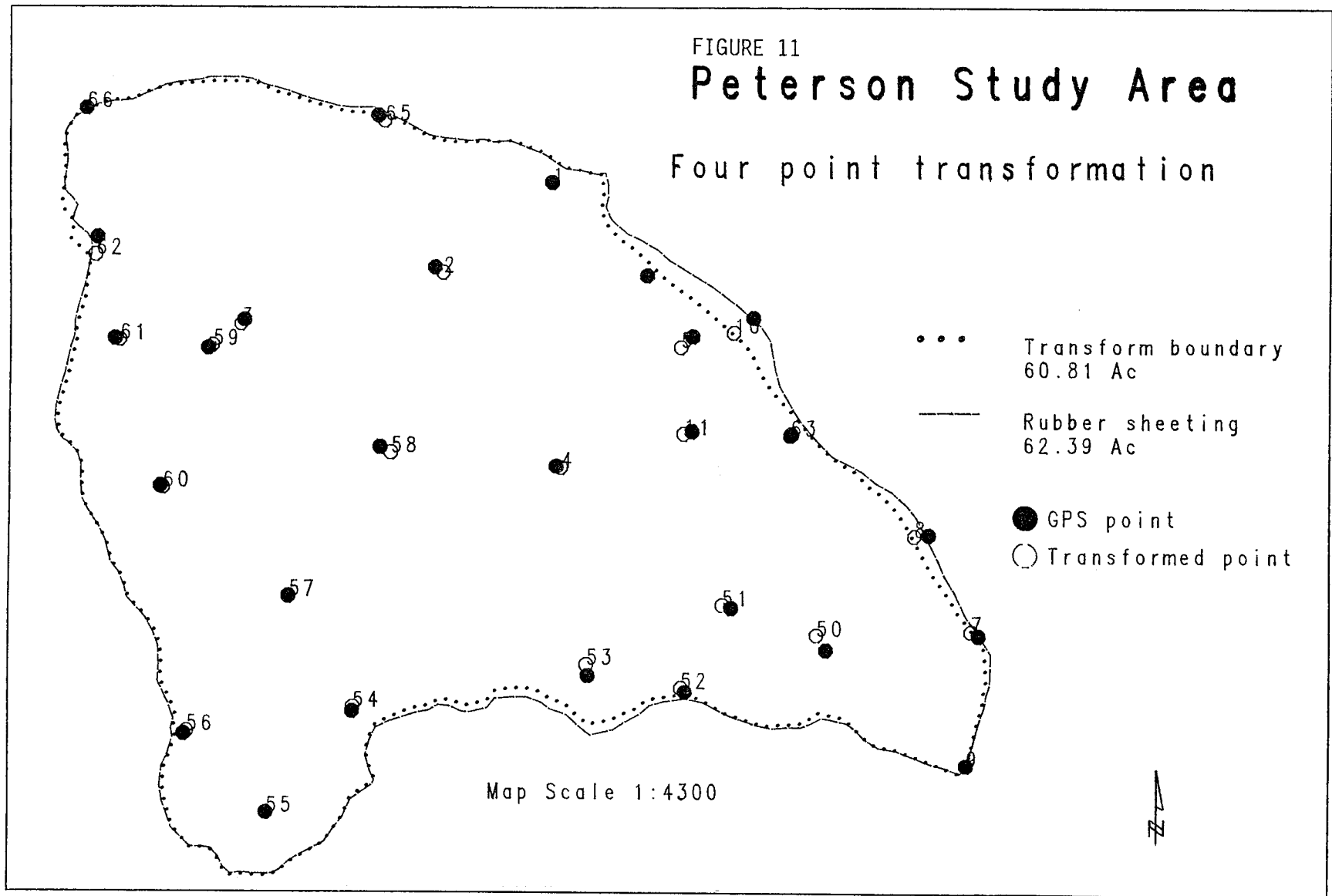


FIGURE 12

Randall Study Area

All point transformation

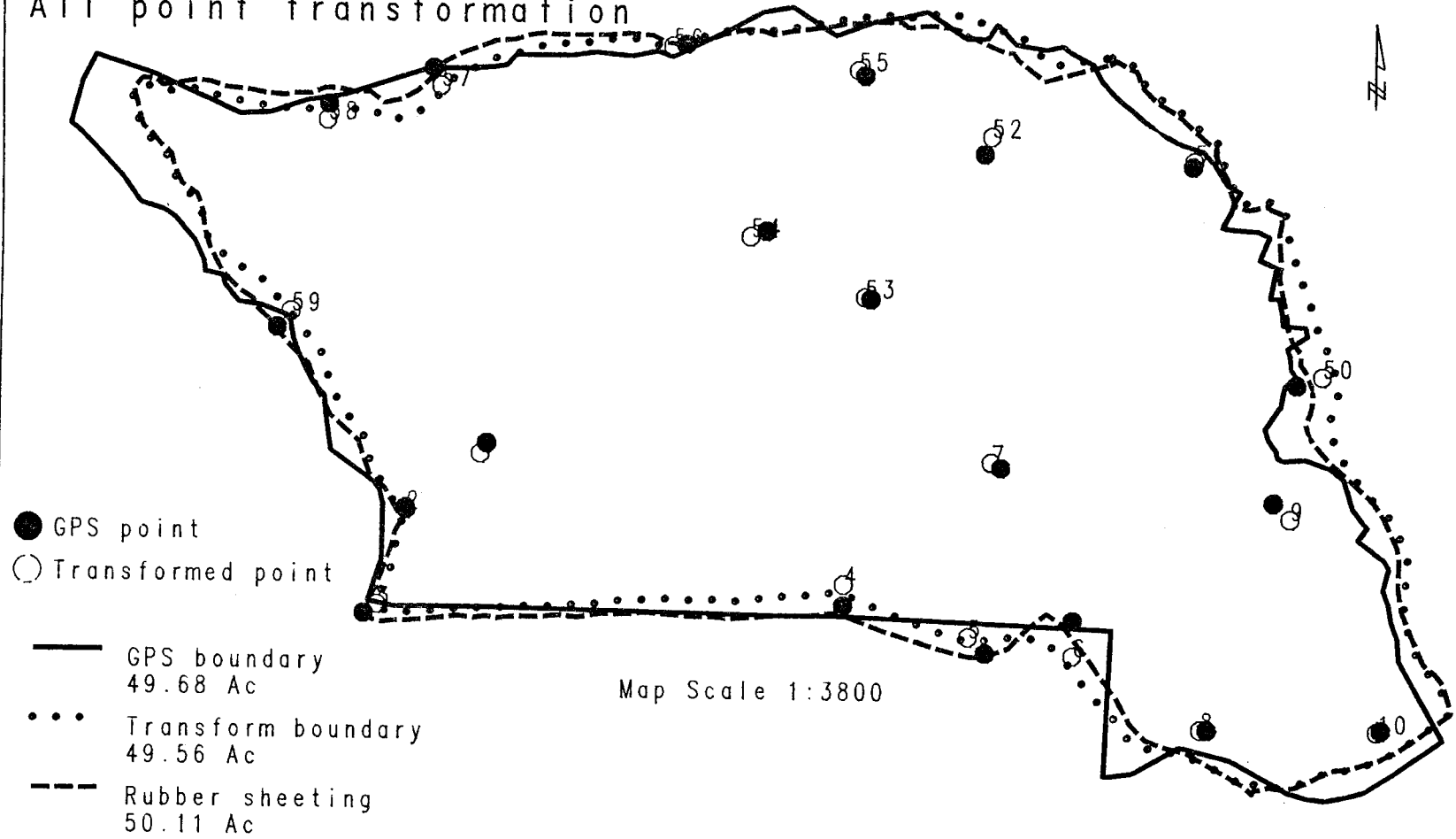
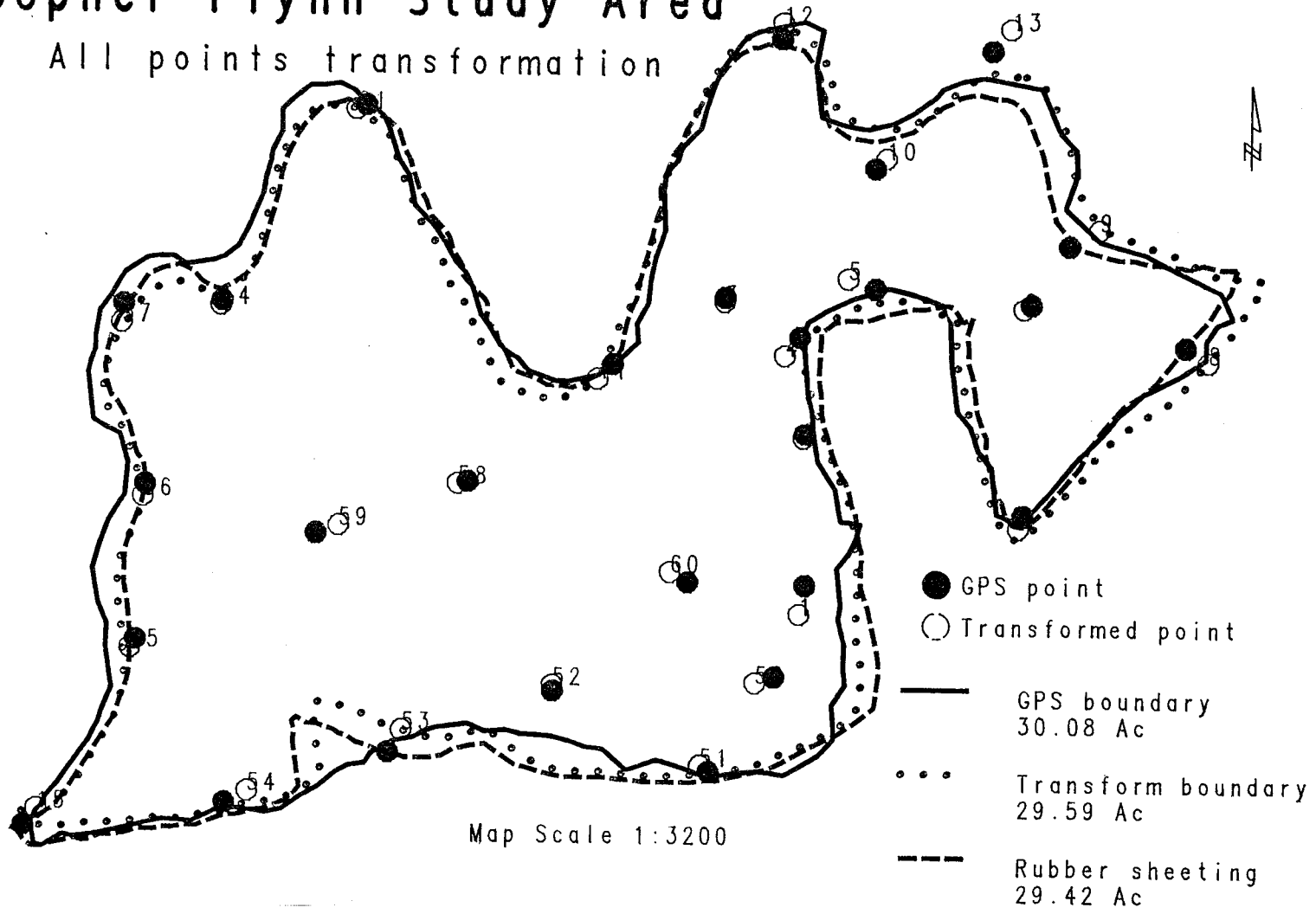


FIGURE 13
Gopher Flynn Study Area
All points transformation



Map Scale 1:3200

FIGURE 14

Peterson Study Area

All points transformation

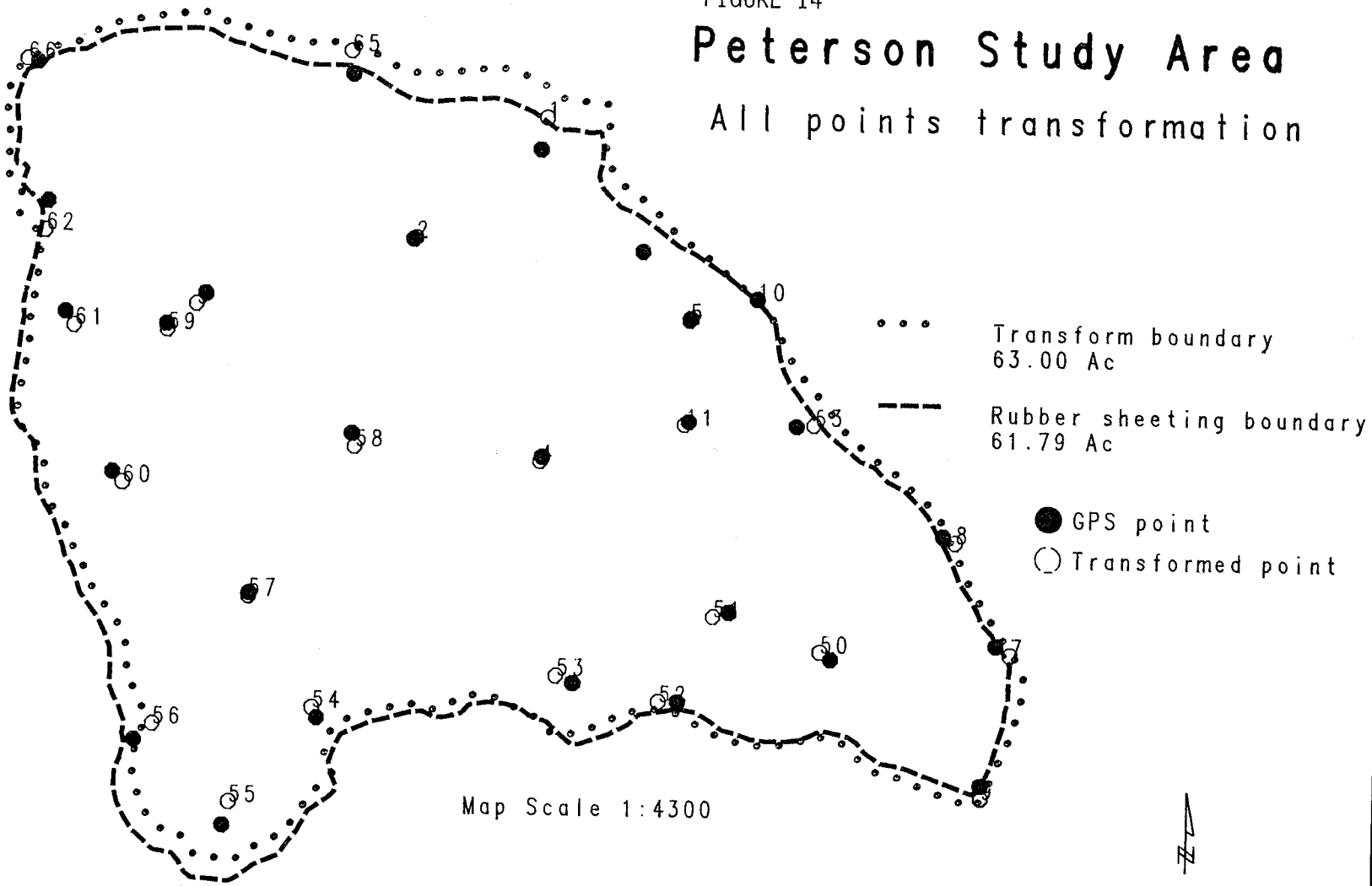
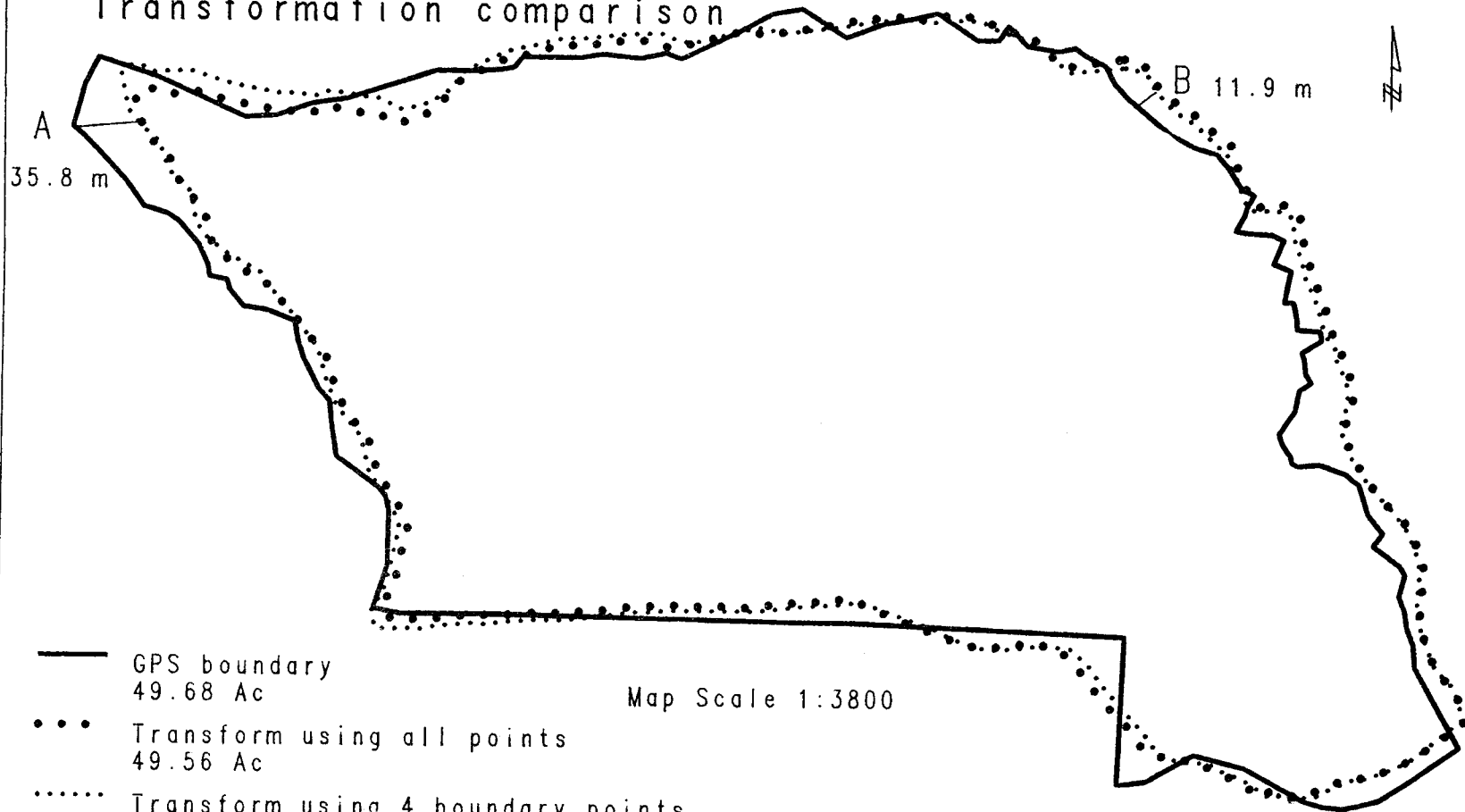


FIGURE 15
Randall Study Area
Transformation comparison



- GPS boundary
49.68 Ac
- Transform using all points
49.56 Ac
- Transform using 4 boundary points
50.09 Ac

Map Scale 1:3800

FIGURE 16
Gopher Flynn Study Area
Transformation comparison

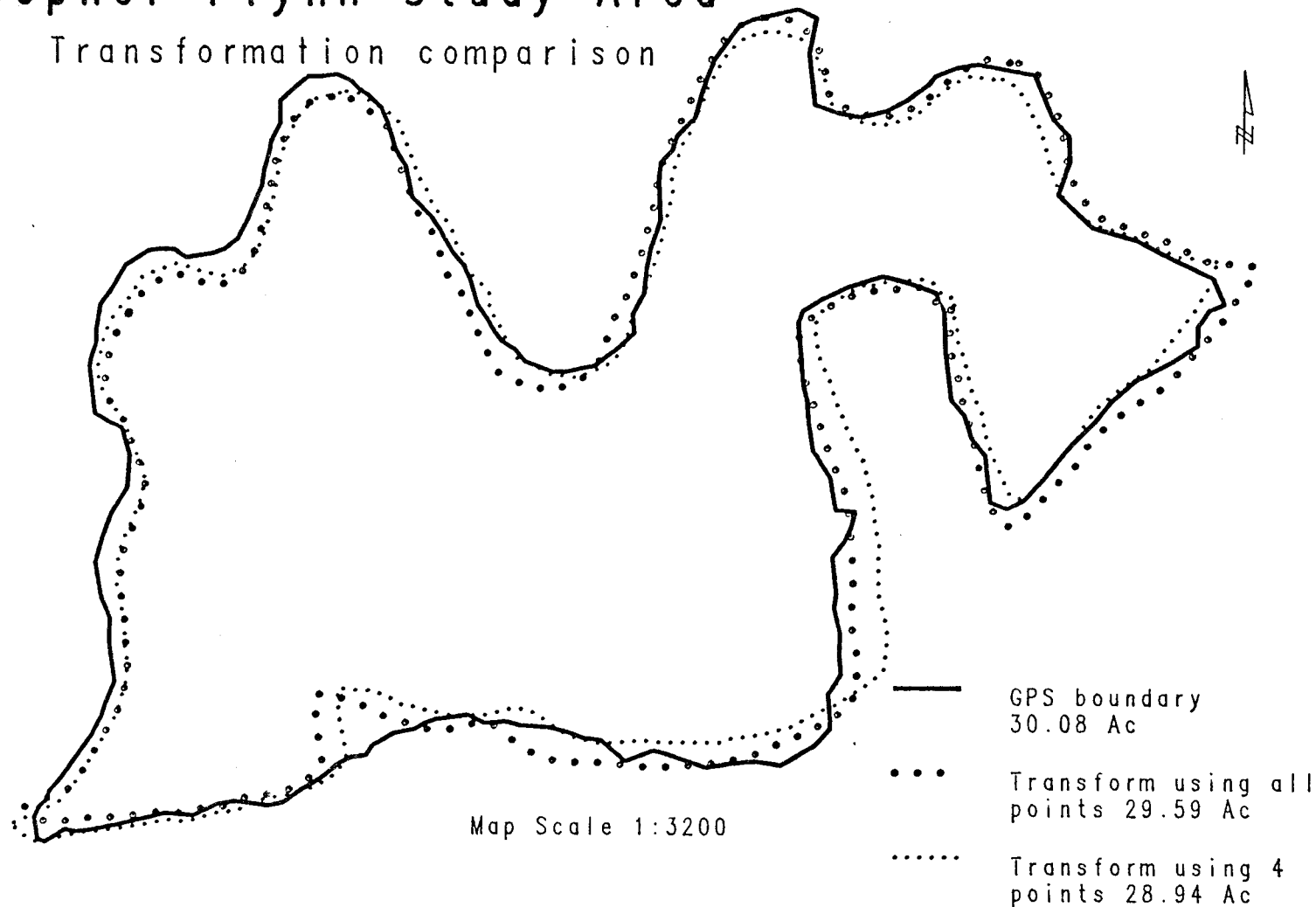
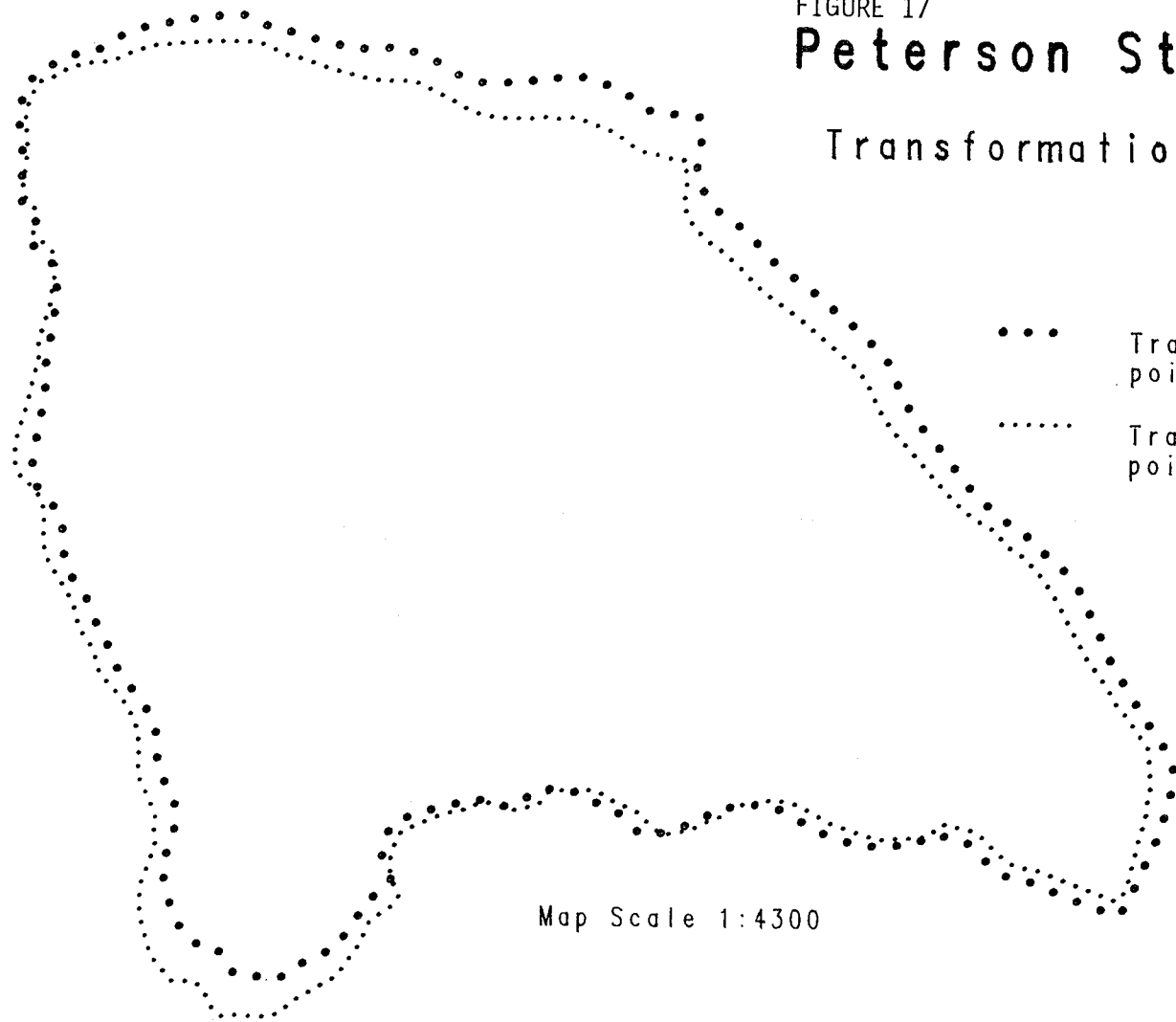


FIGURE 17

Peterson Study Area

Transformation comparison



- Transform using all points 63.00 Ac
- Transform using 4 points 60.81 Ac

Map Scale 1:4300



FIGURE 18

Randall Study Area

Rubber sheeting comparison

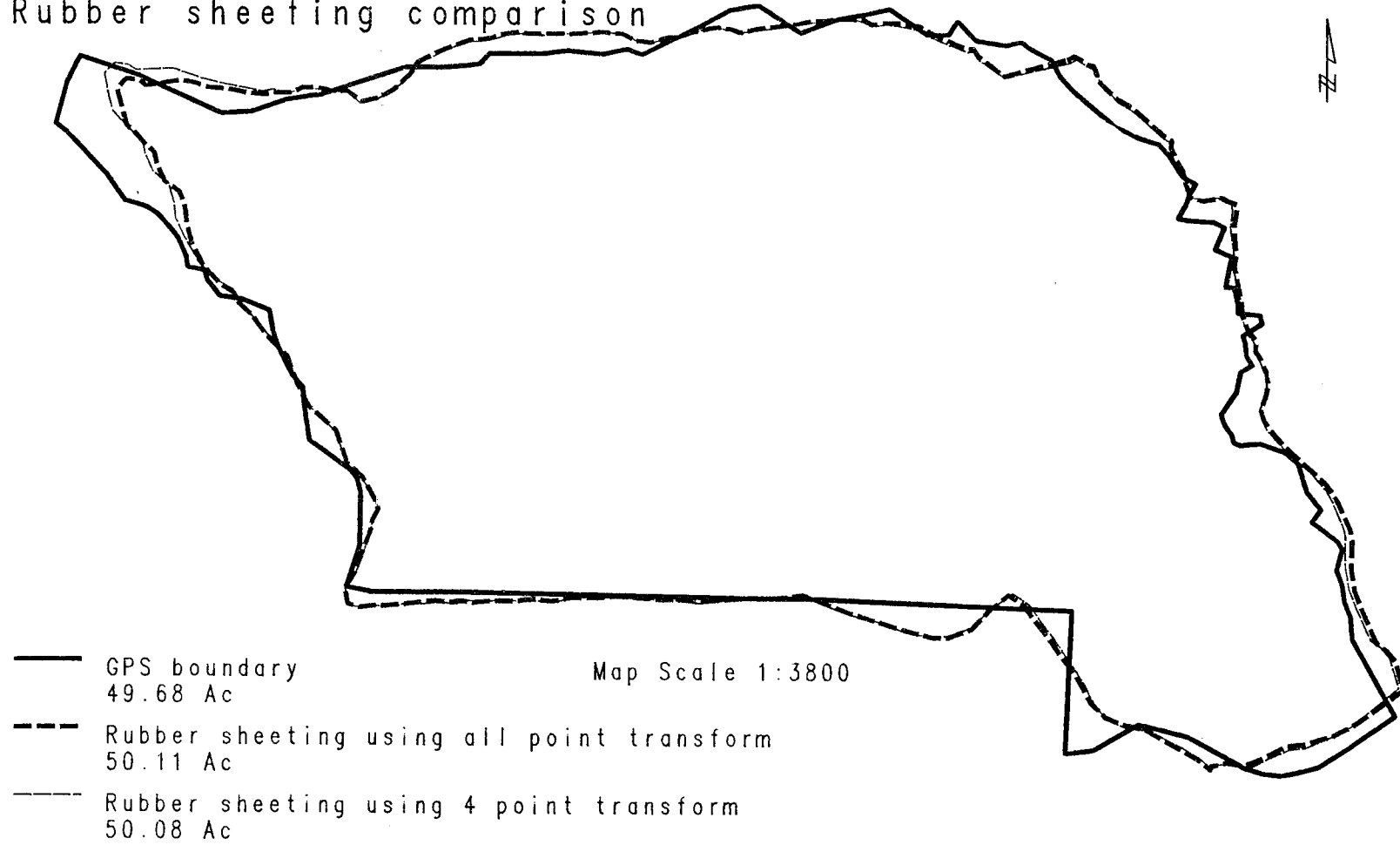
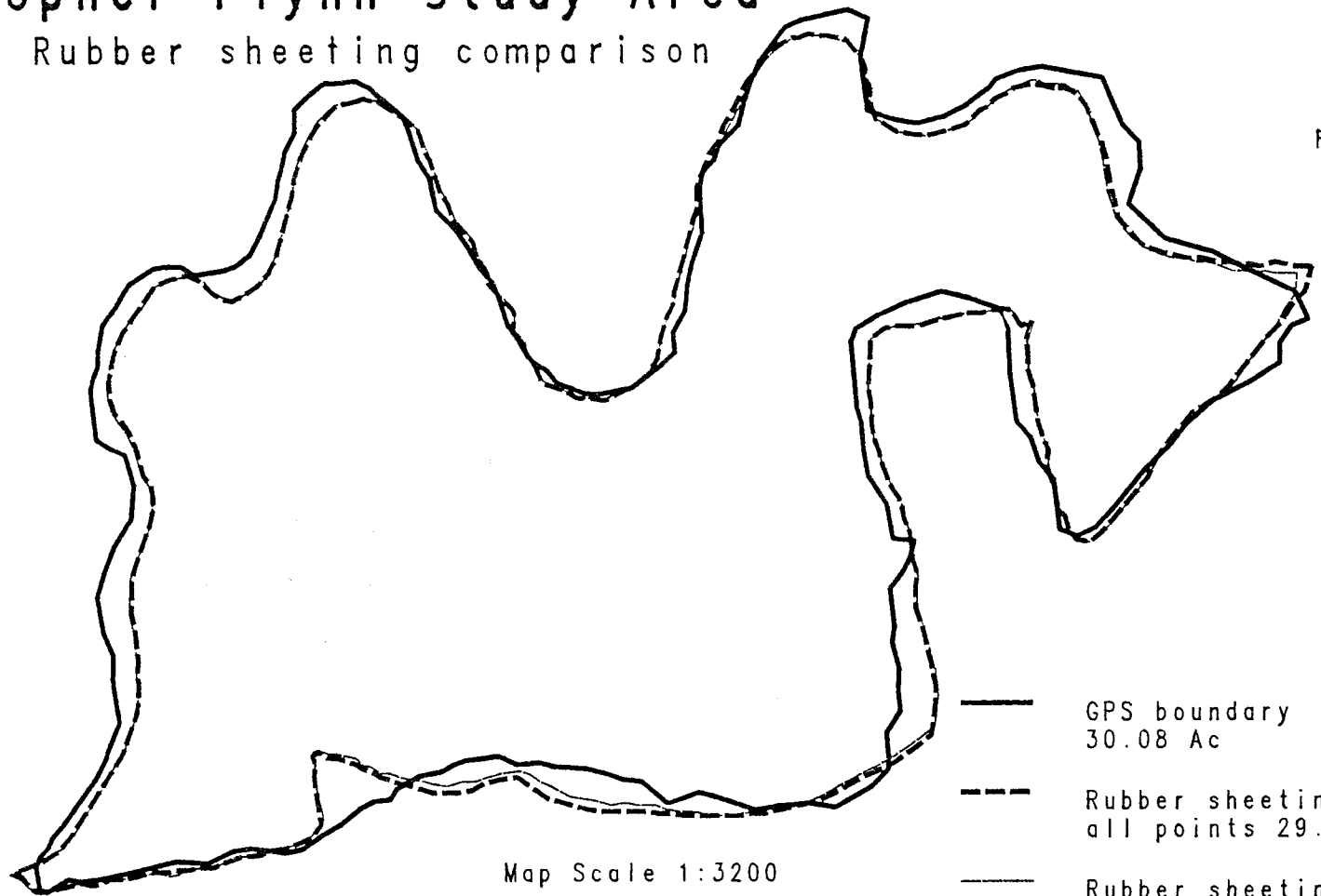


FIGURE 19
Gopher Flynn Study Area
Rubber sheeting comparison



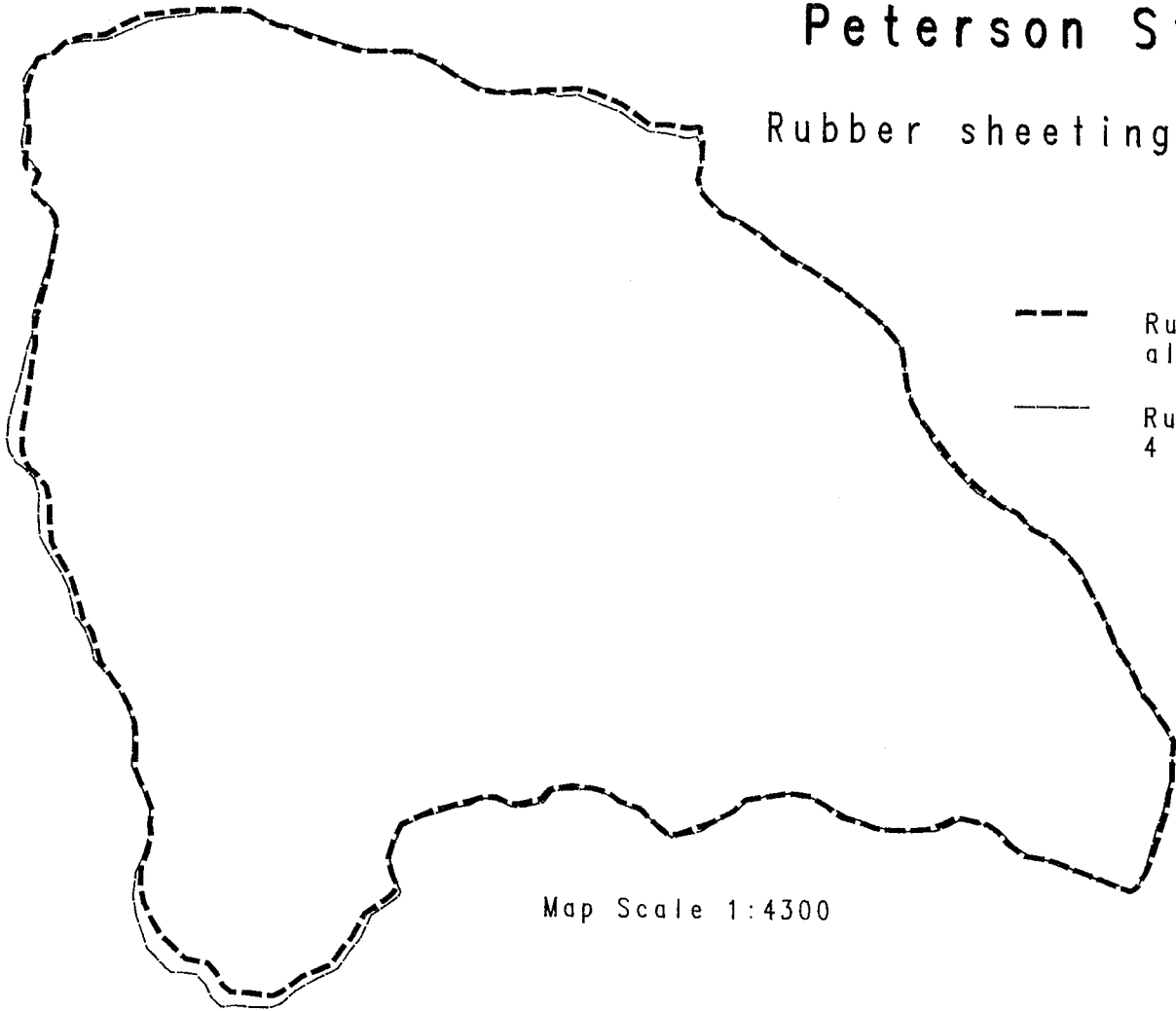
Map Scale 1:3200

- GPS boundary
30.08 Ac
- - - Rubber sheeting using
all points 29.42 Ac
- · - Rubber sheeting using
4 points 29.20 Ac

FIGURE 20

Peterson Study Area

Rubber sheeting comparison



--- Rubber sheeting using
all points 61.79 Ac

— Rubber sheeting using
4 points 62.39 Ac

Map Scale 1:4300



FIGURE 21

Randall Study Area

Four Point Method

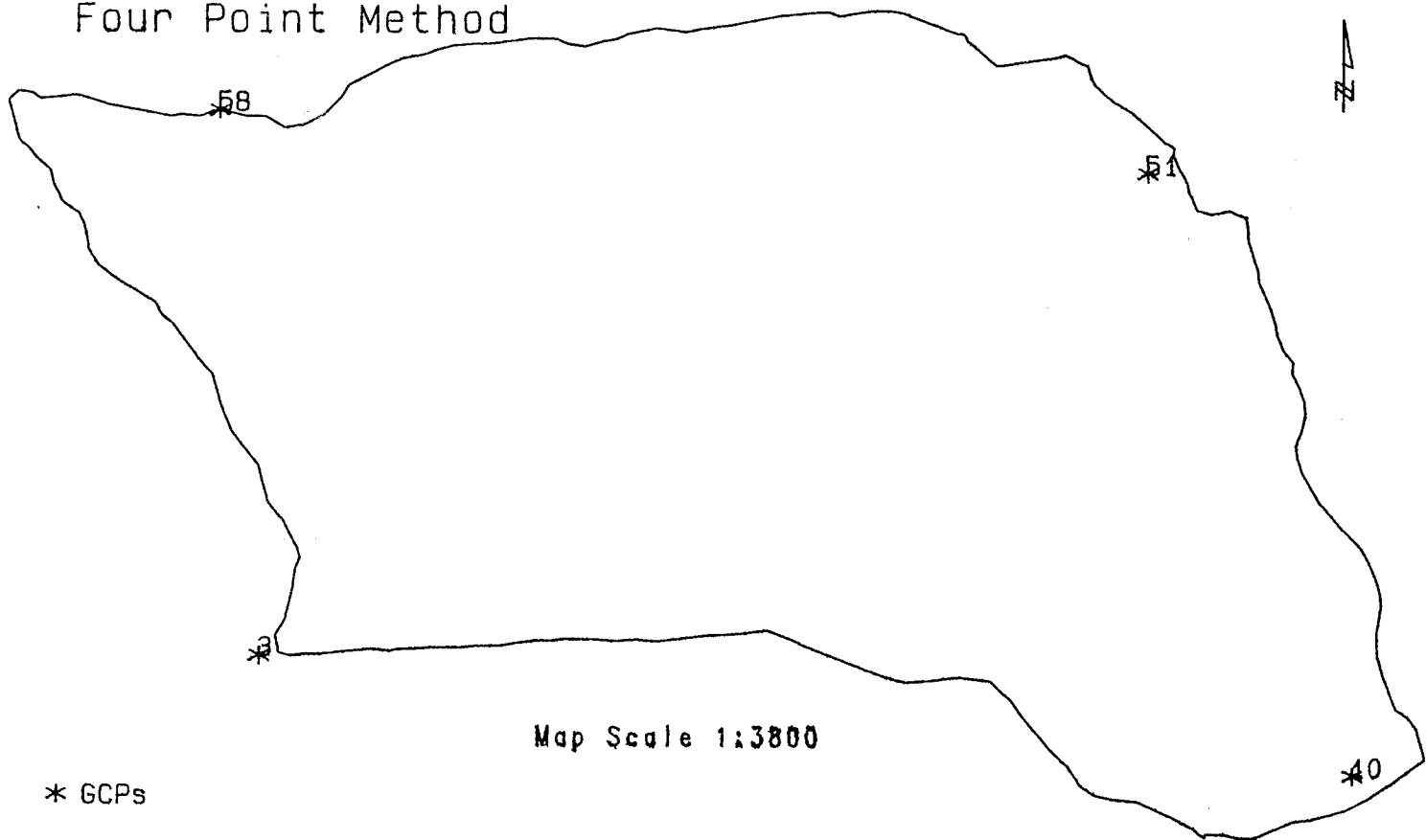
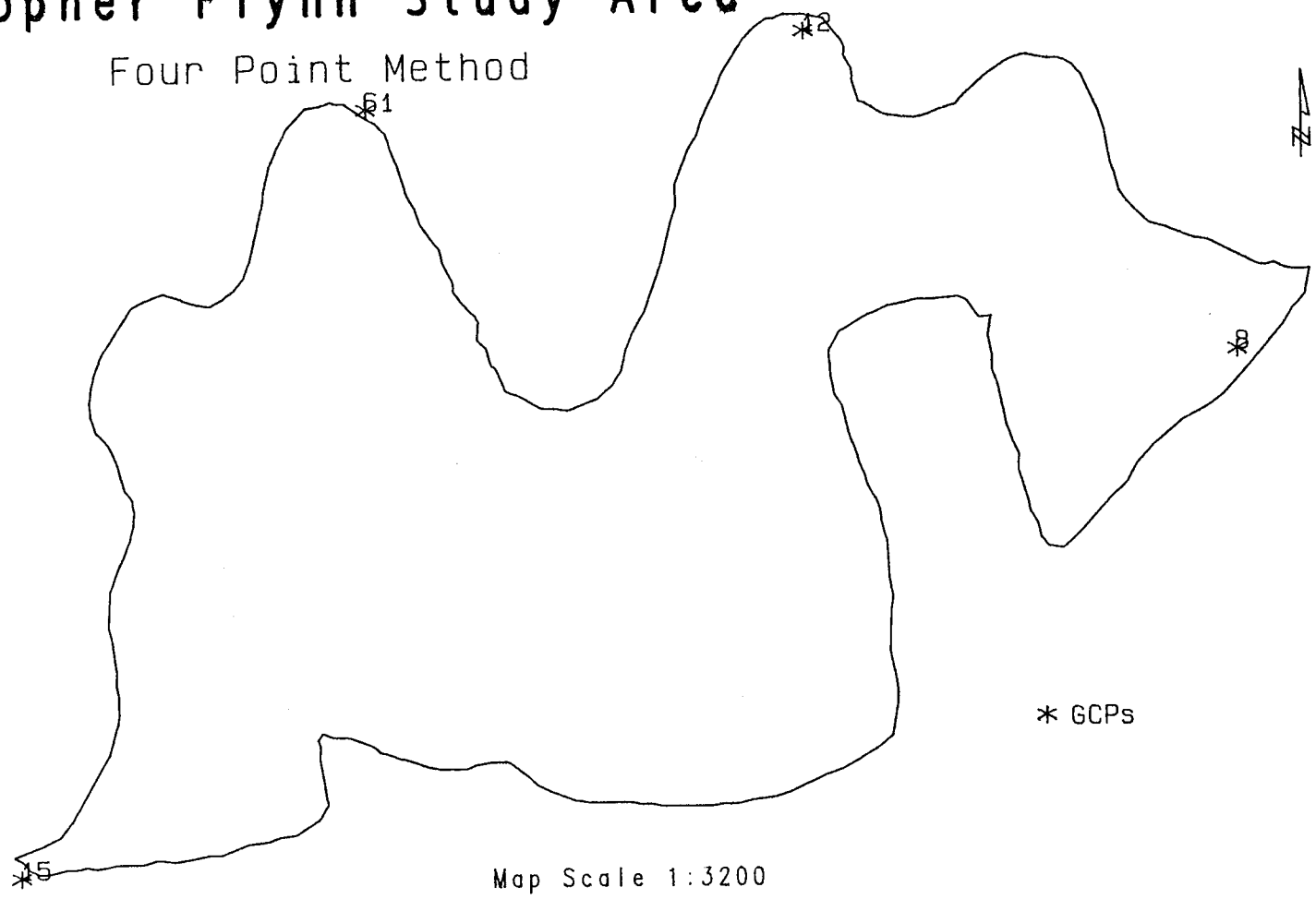


FIGURE 22
Gopher Flynn Study Area

Four Point Method



Map Scale 1:3200

FIGURE 23

Peterson Study Area

Four Point Method

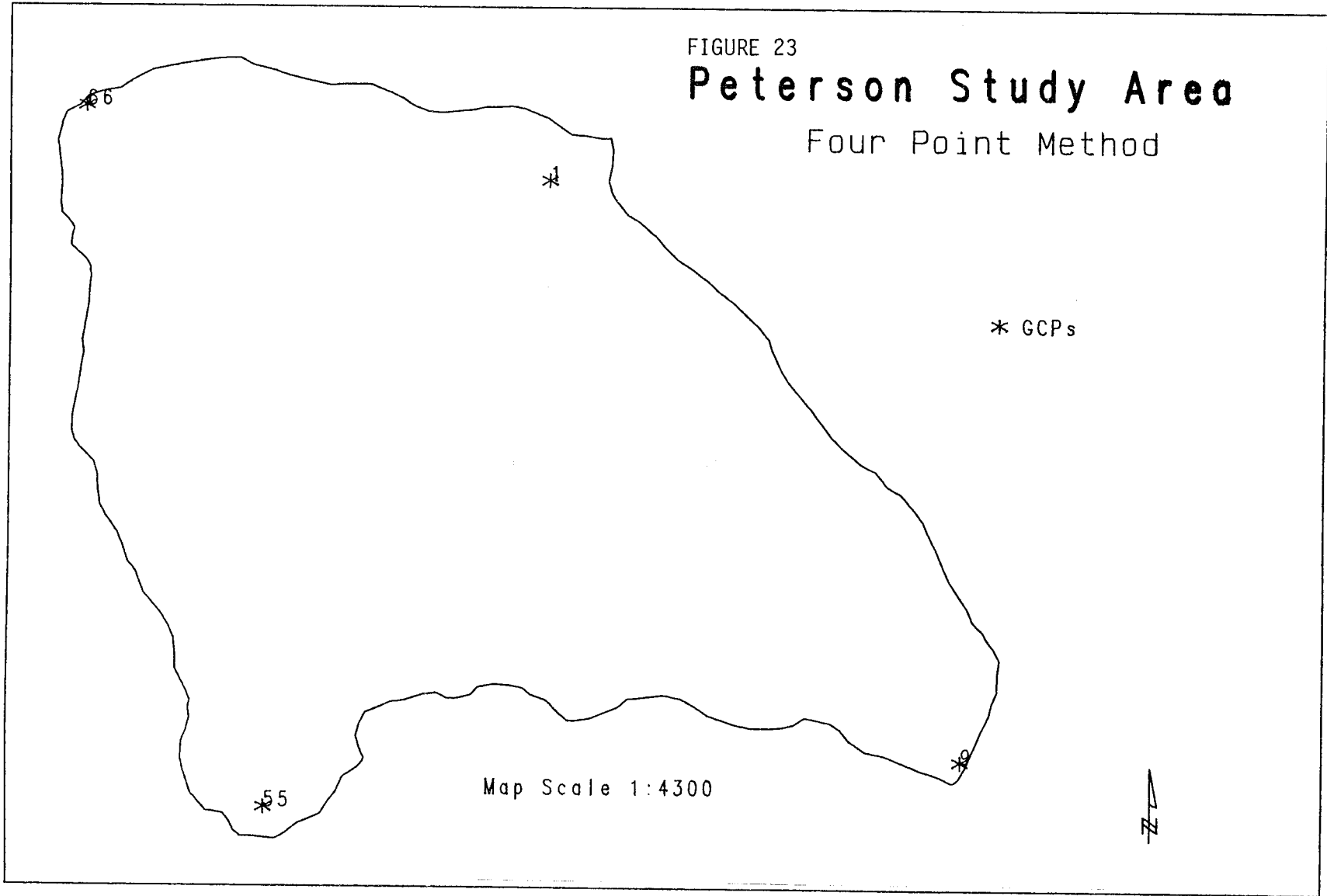


FIGURE 24

Randall Study Area

Boundary Method

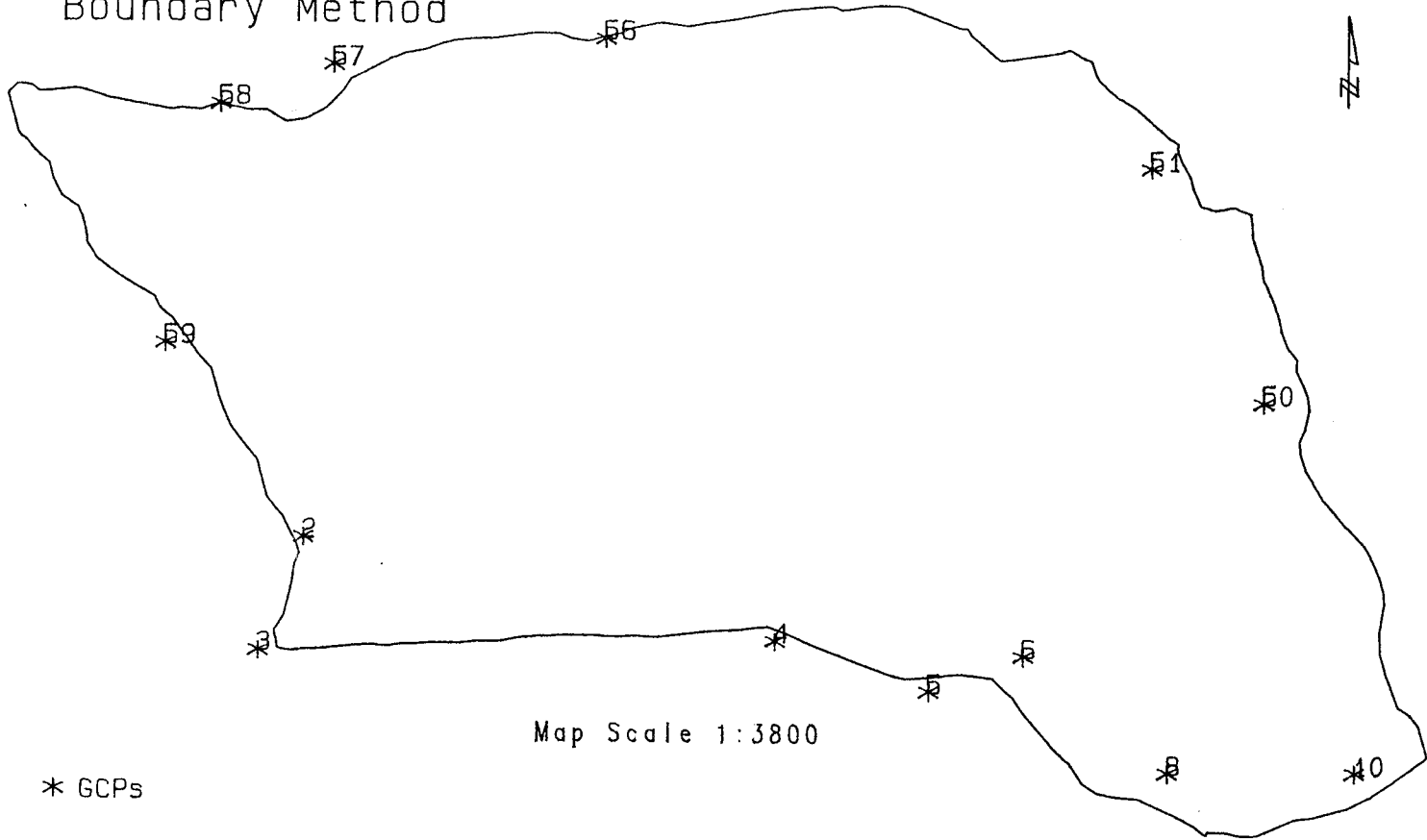


FIGURE 25

Gopher Flynn Study Area

Boundary Method

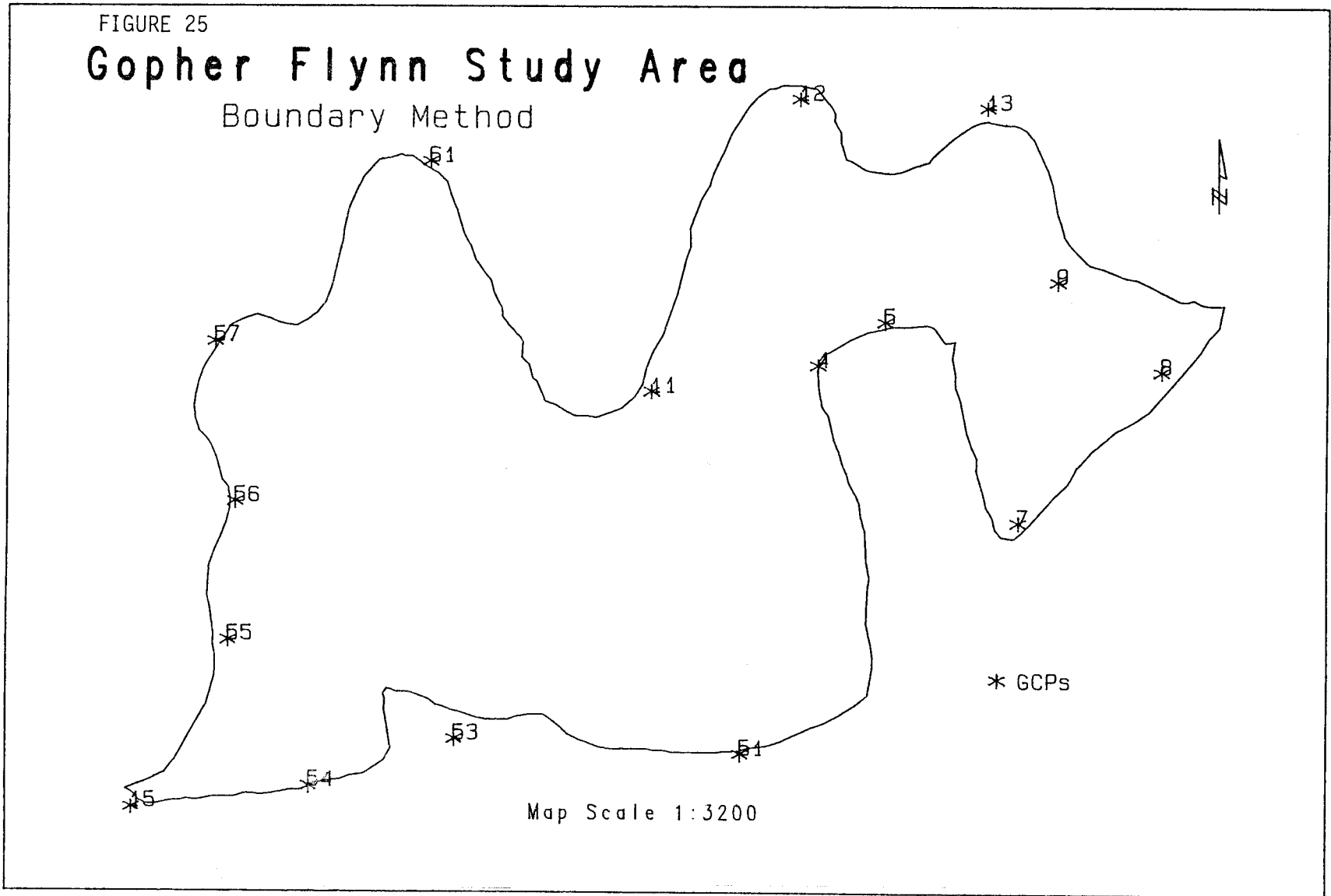


FIGURE 26

Peterson Study Area

Boundary Method

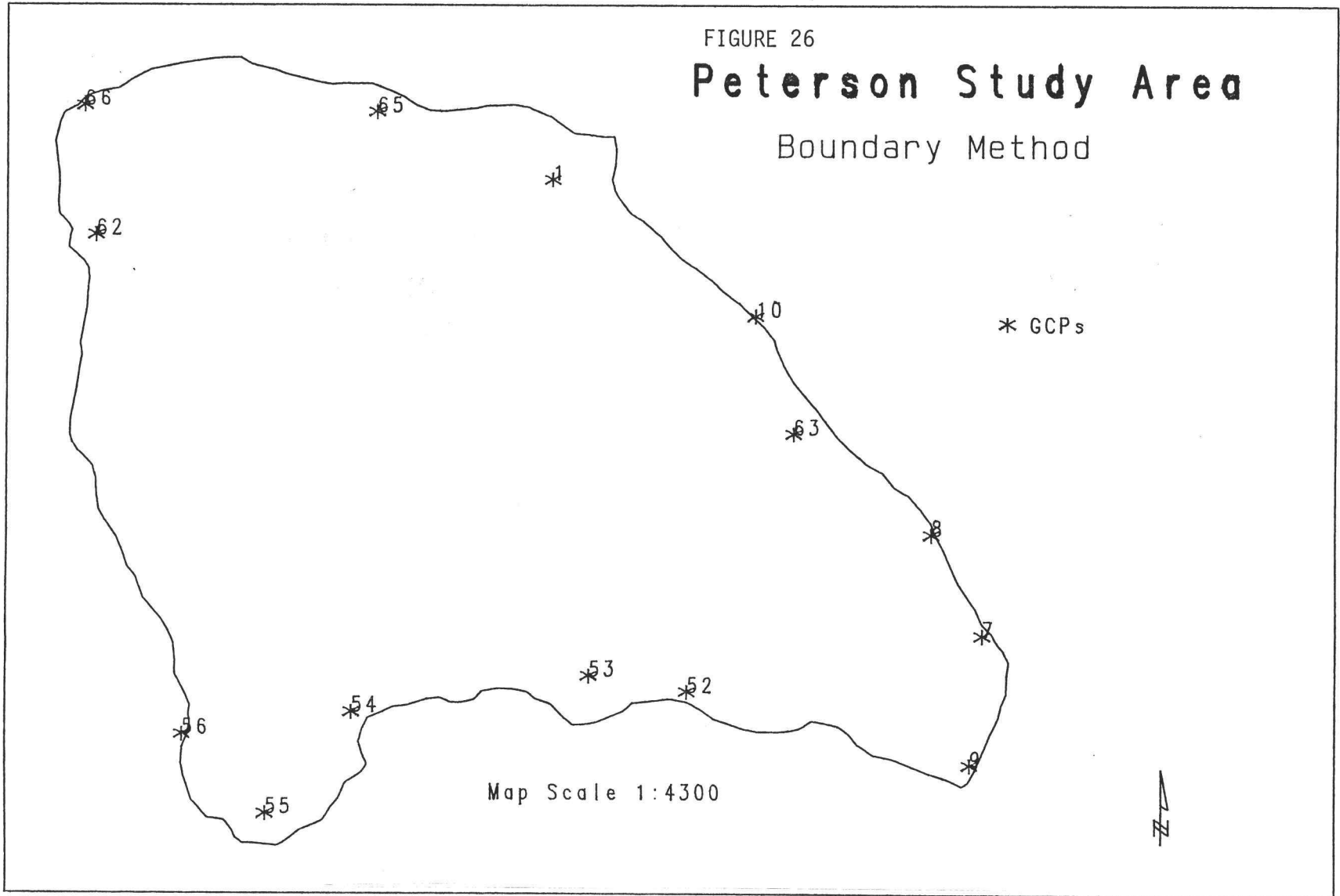


FIGURE 27
Randall Study Area

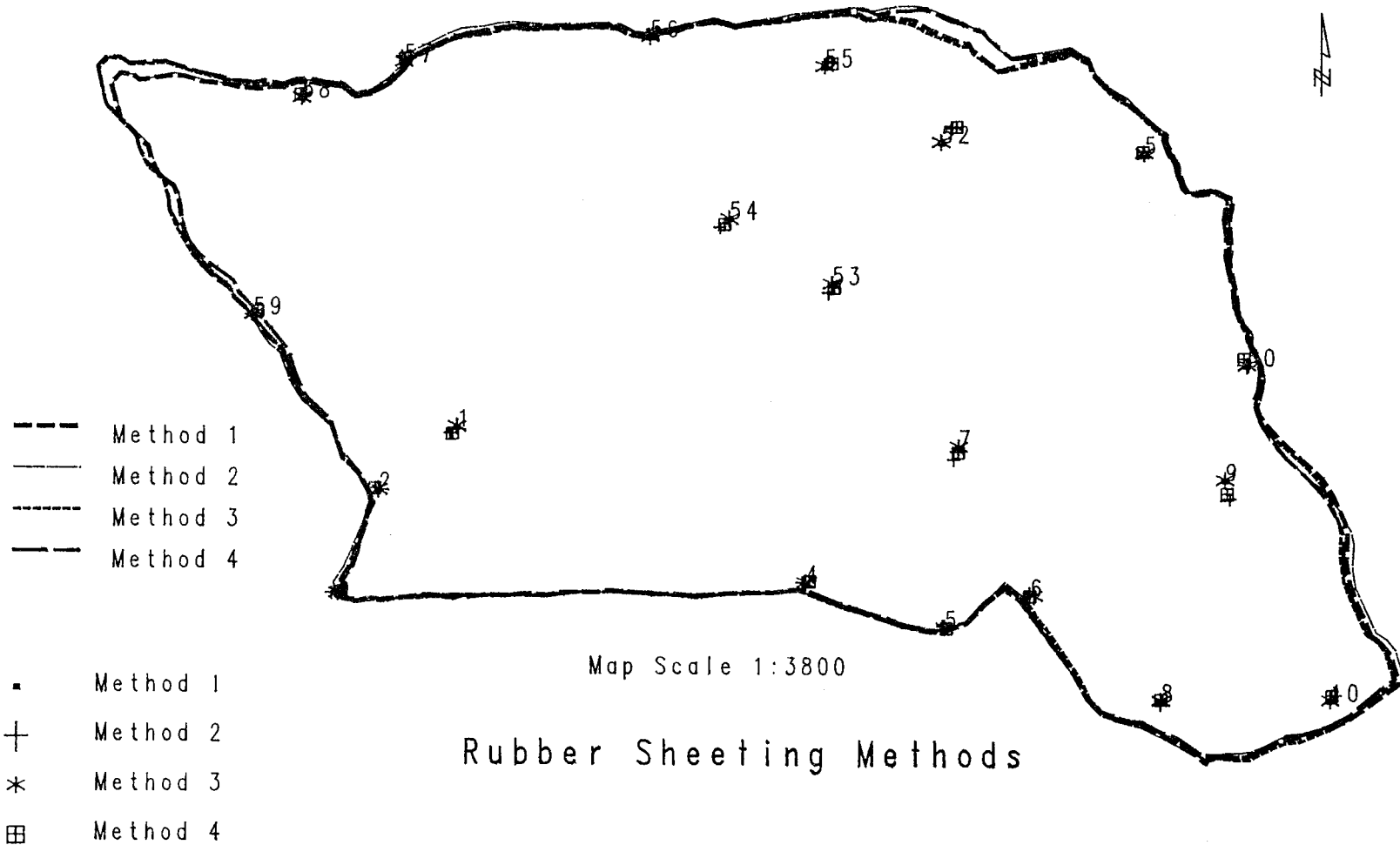


FIGURE 28

Gopher Flynn Study Area

Rubber Sheeting Methods

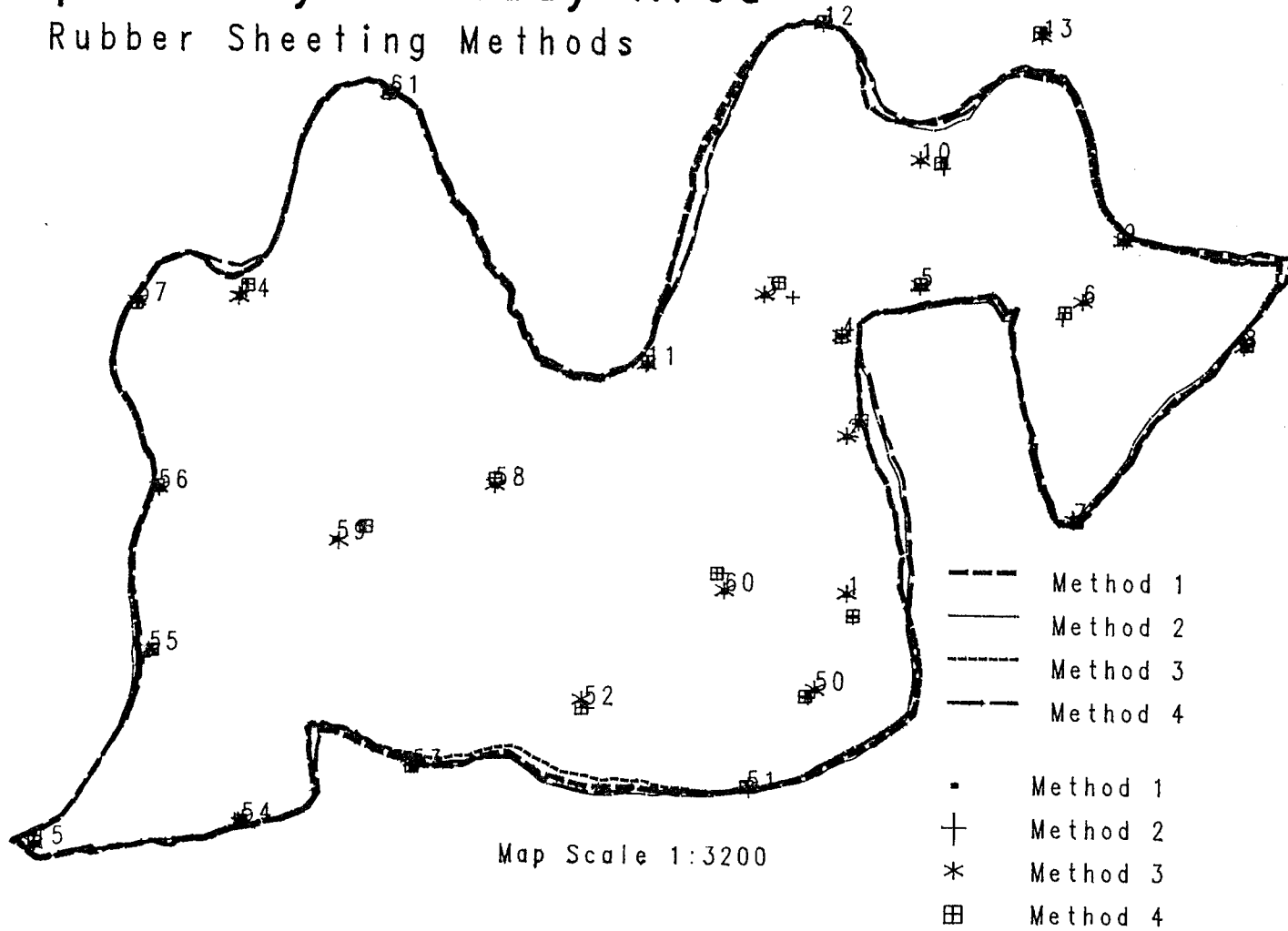
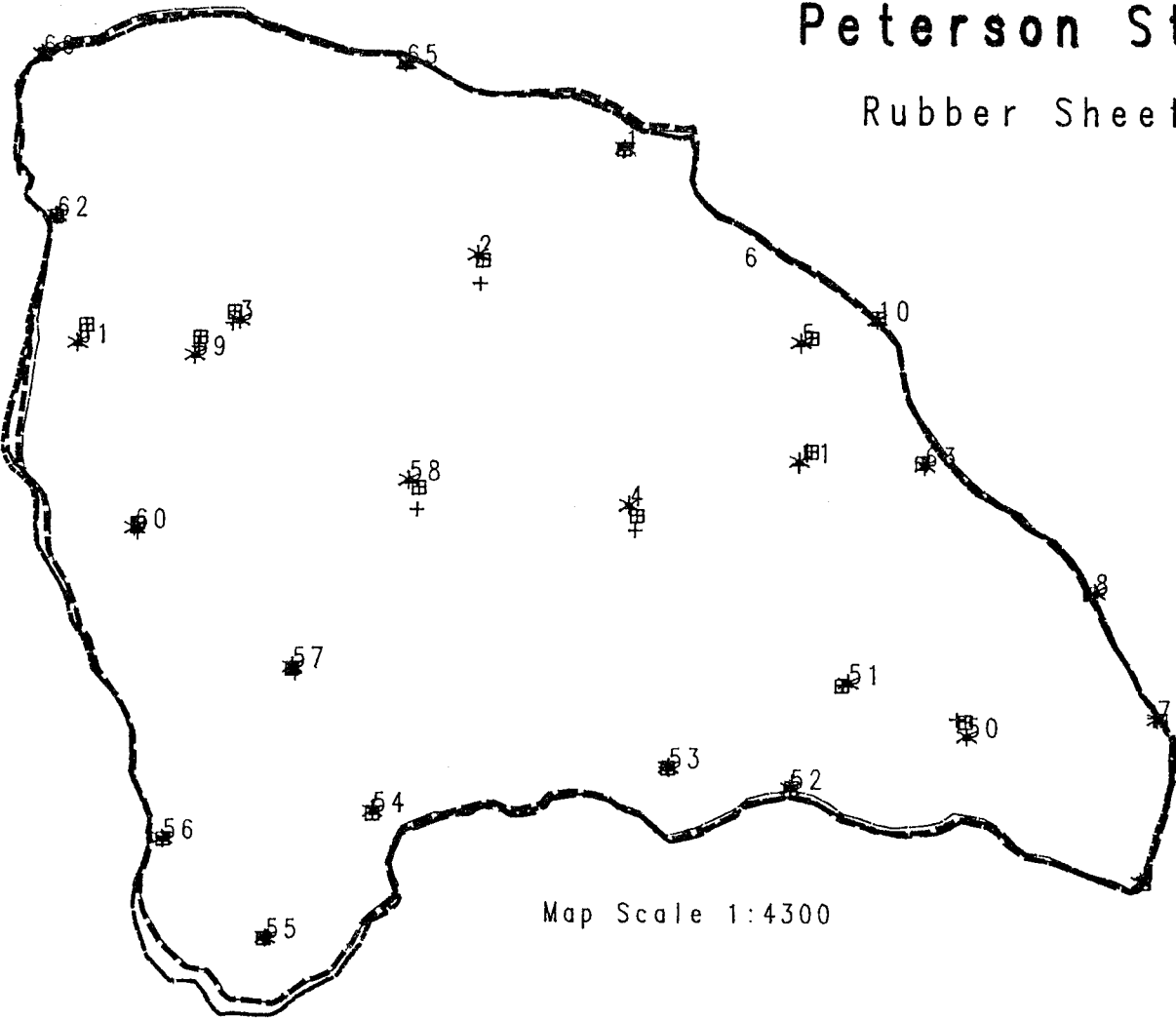


FIGURE 29

Peterson Study Area

Rubber Sheeting Methods



- Method 1
- Method 2
- · - Method 3
- - - Method 4

- Method 1
- + Method 2
- * Method 3
- 田 Method 4

Map Scale 1:4300



FIGURE 30

Randall Study Area

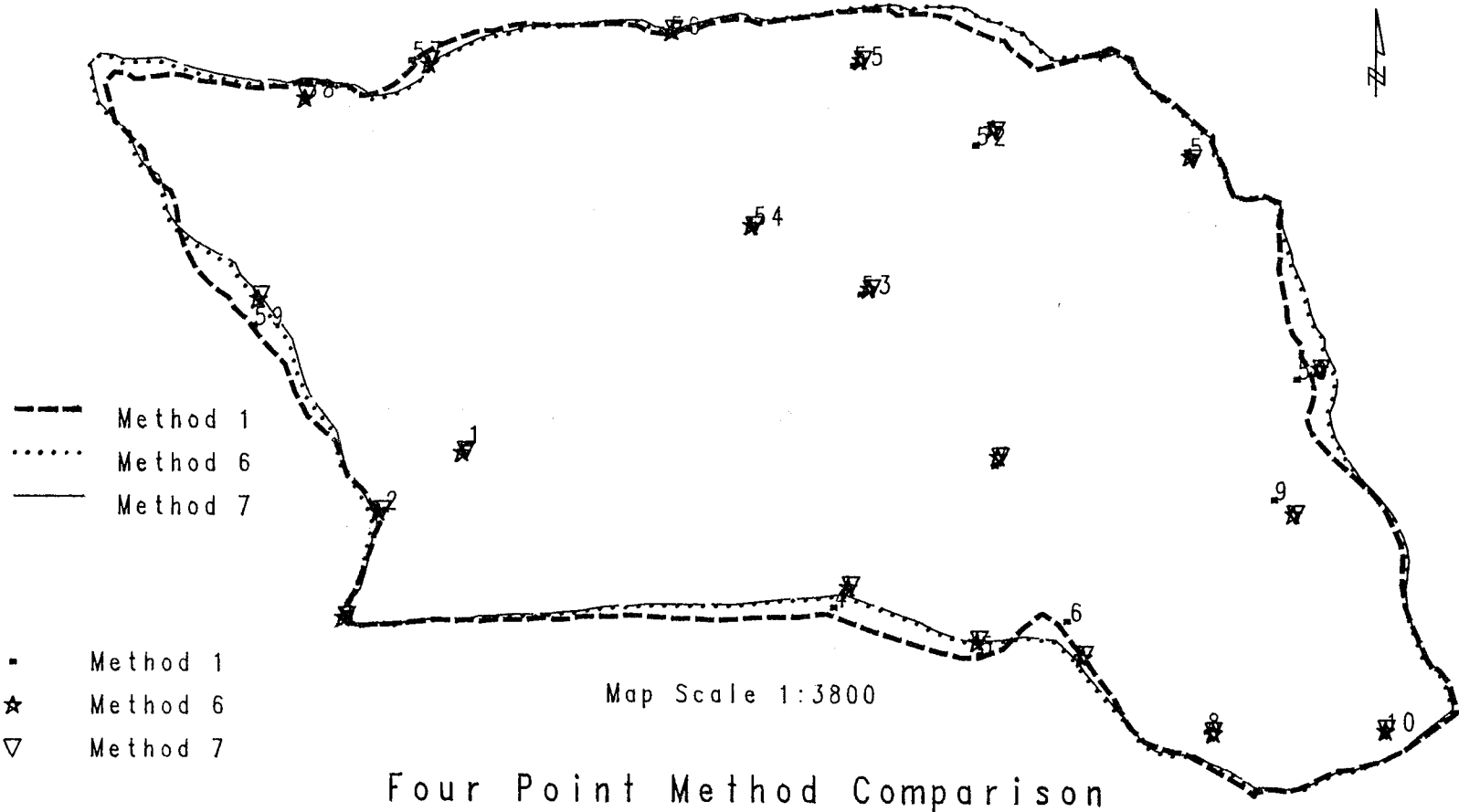


FIGURE 31

Gopher Flynn Study Area

Four Point Method Comparison

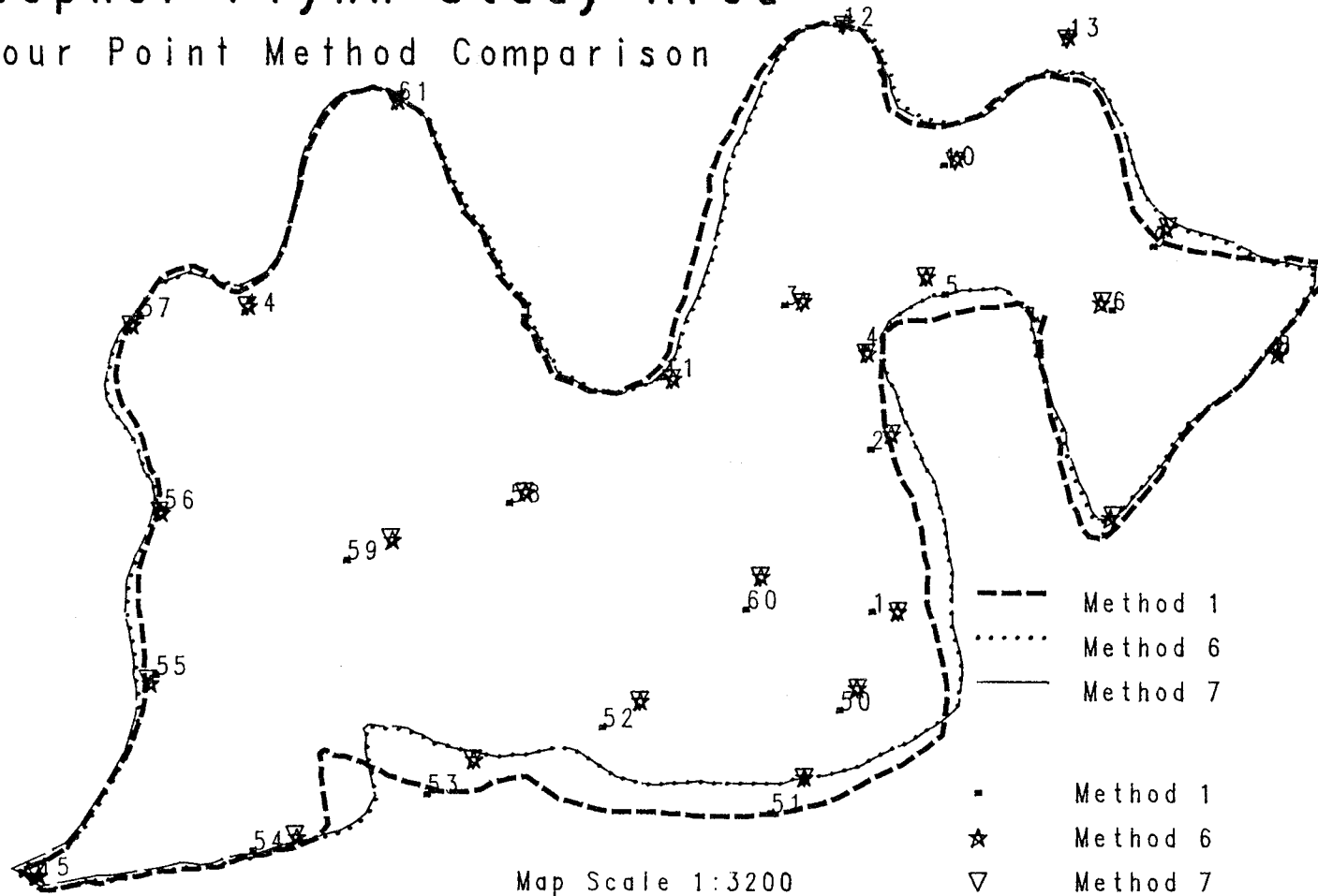
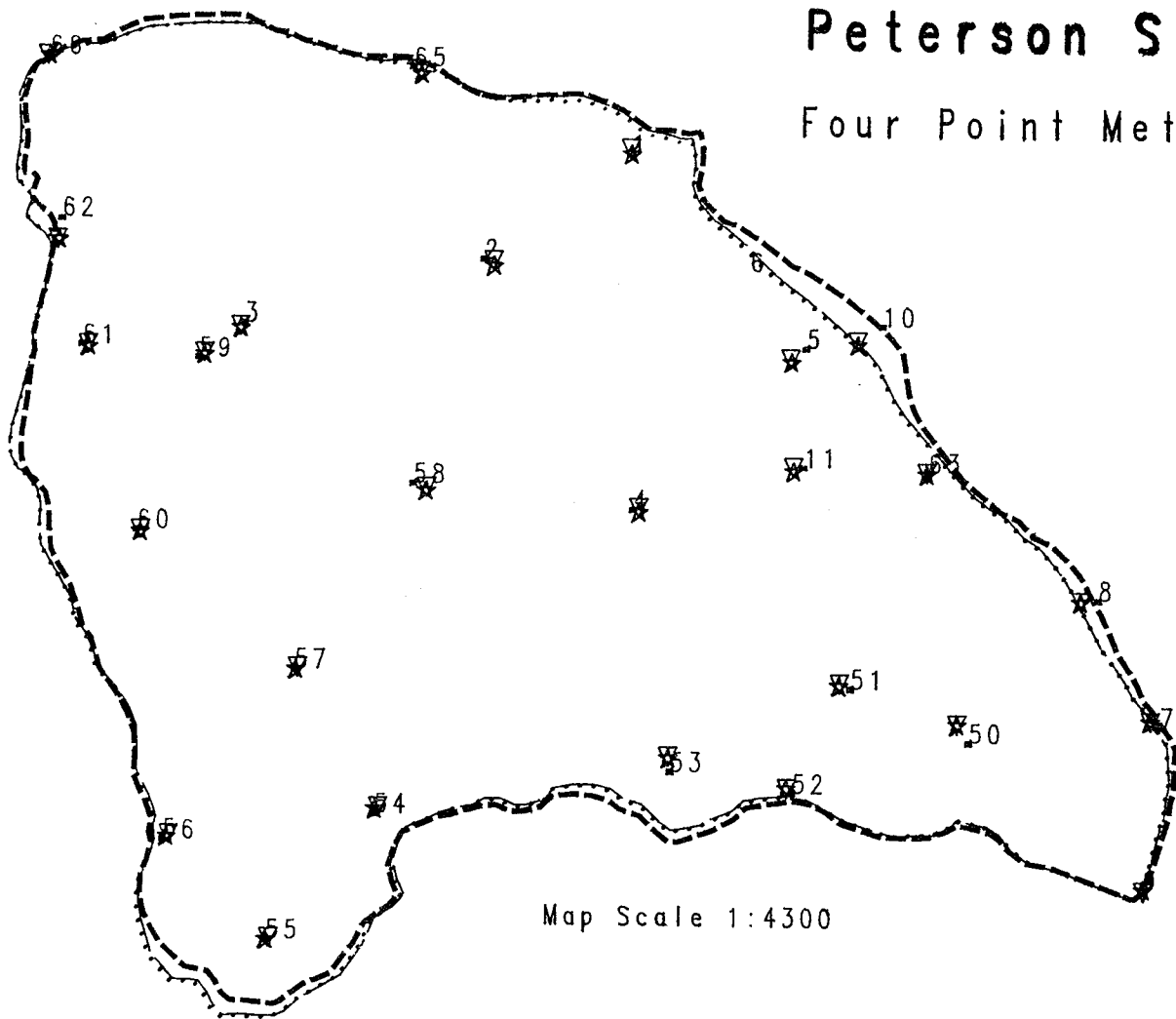


FIGURE 32

Peterson Study Area

Four Point Method Comparison



- Method 1
- Method 6
- Method 7

- Method 1
- ★ Method 6
- ▽ Method 7

Map Scale 1:4300



FIGURE 33

Randall Study Area

Buffered four point transformation

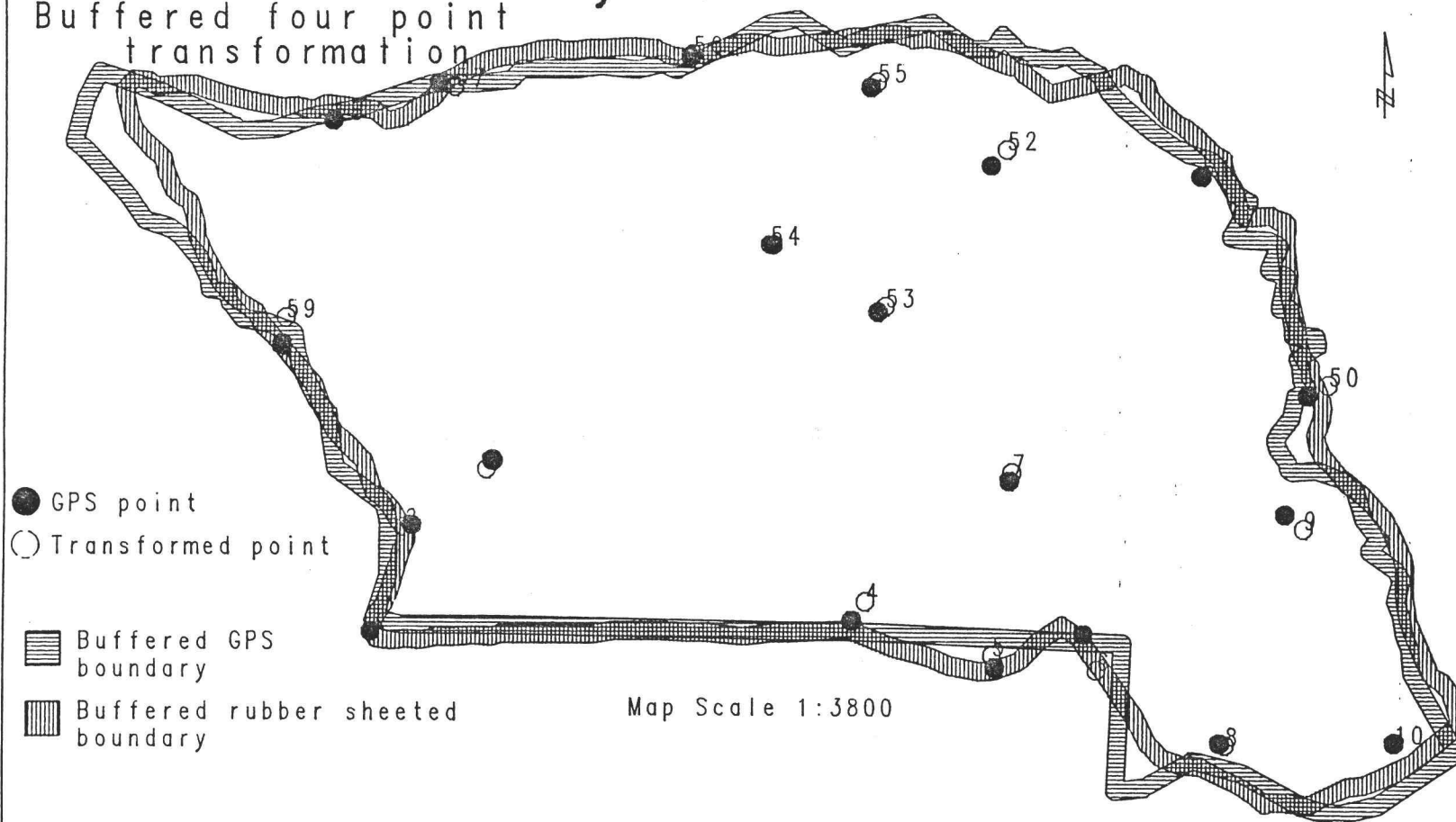


FIGURE 34

Gopher Flynn Study Area

Buffered four point transformation

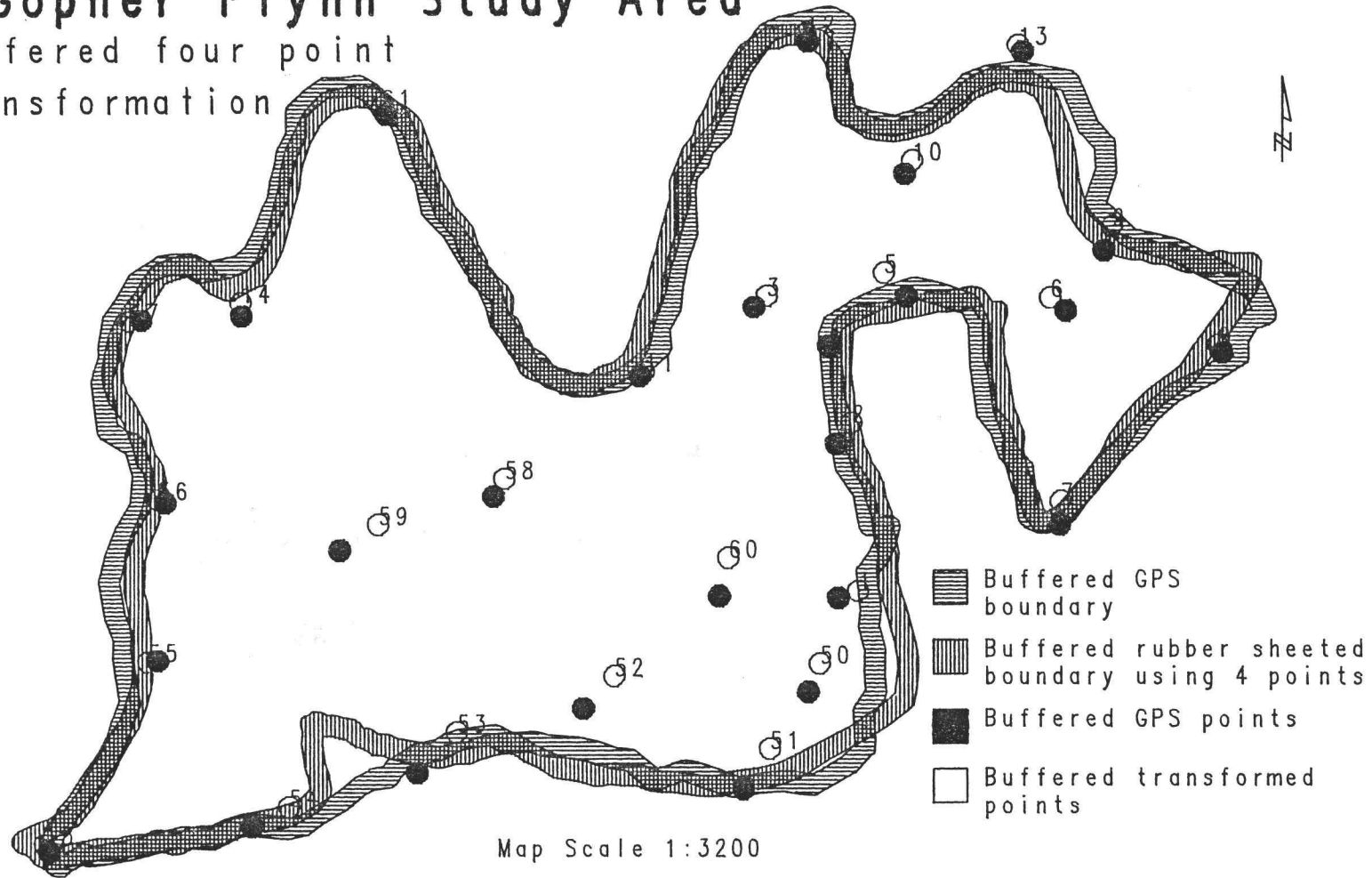


FIGURE 35

Randall Study Area

Buffered all point transformation

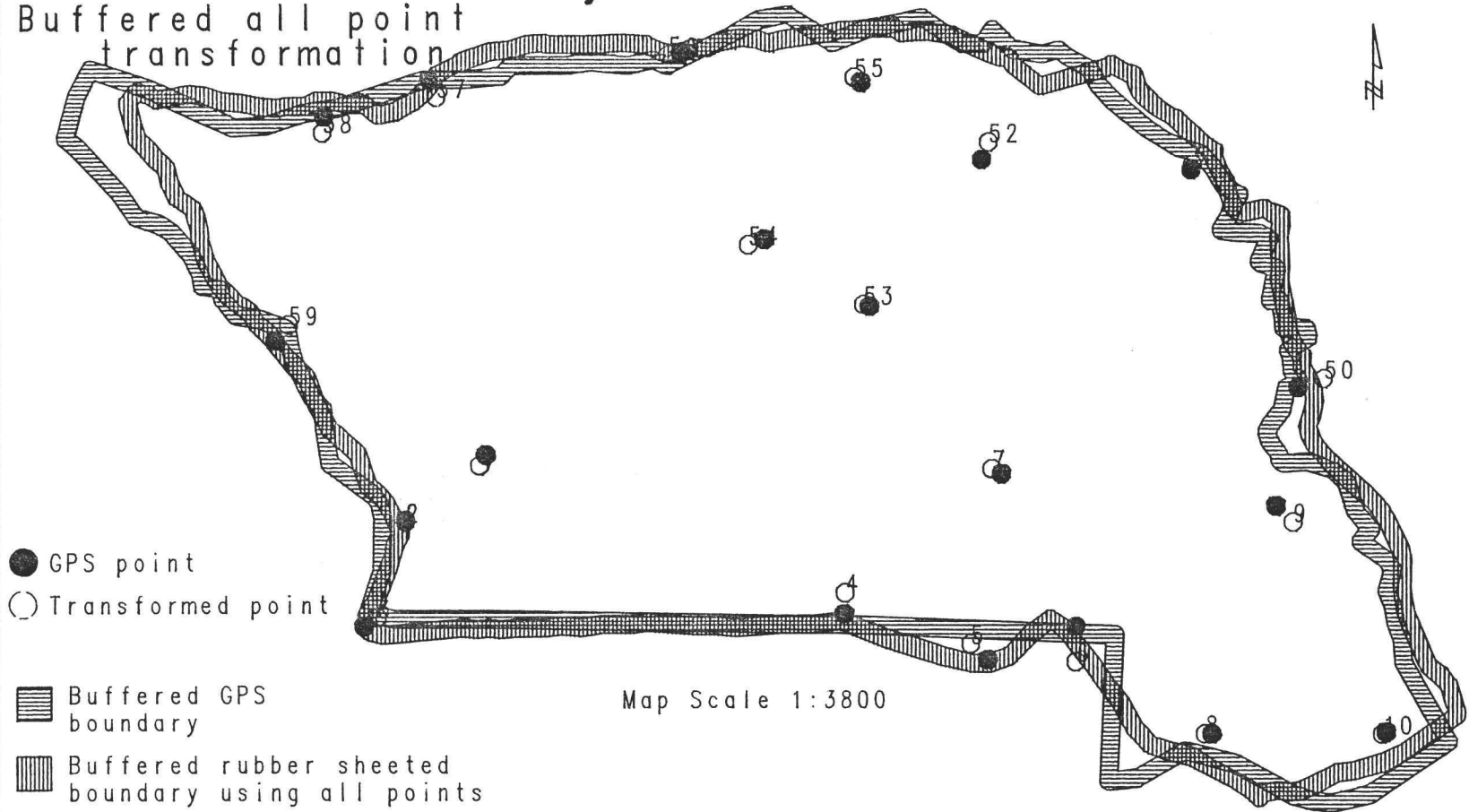


FIGURE 36

Gopher Flynn Study Area

Buffered all points
transformation

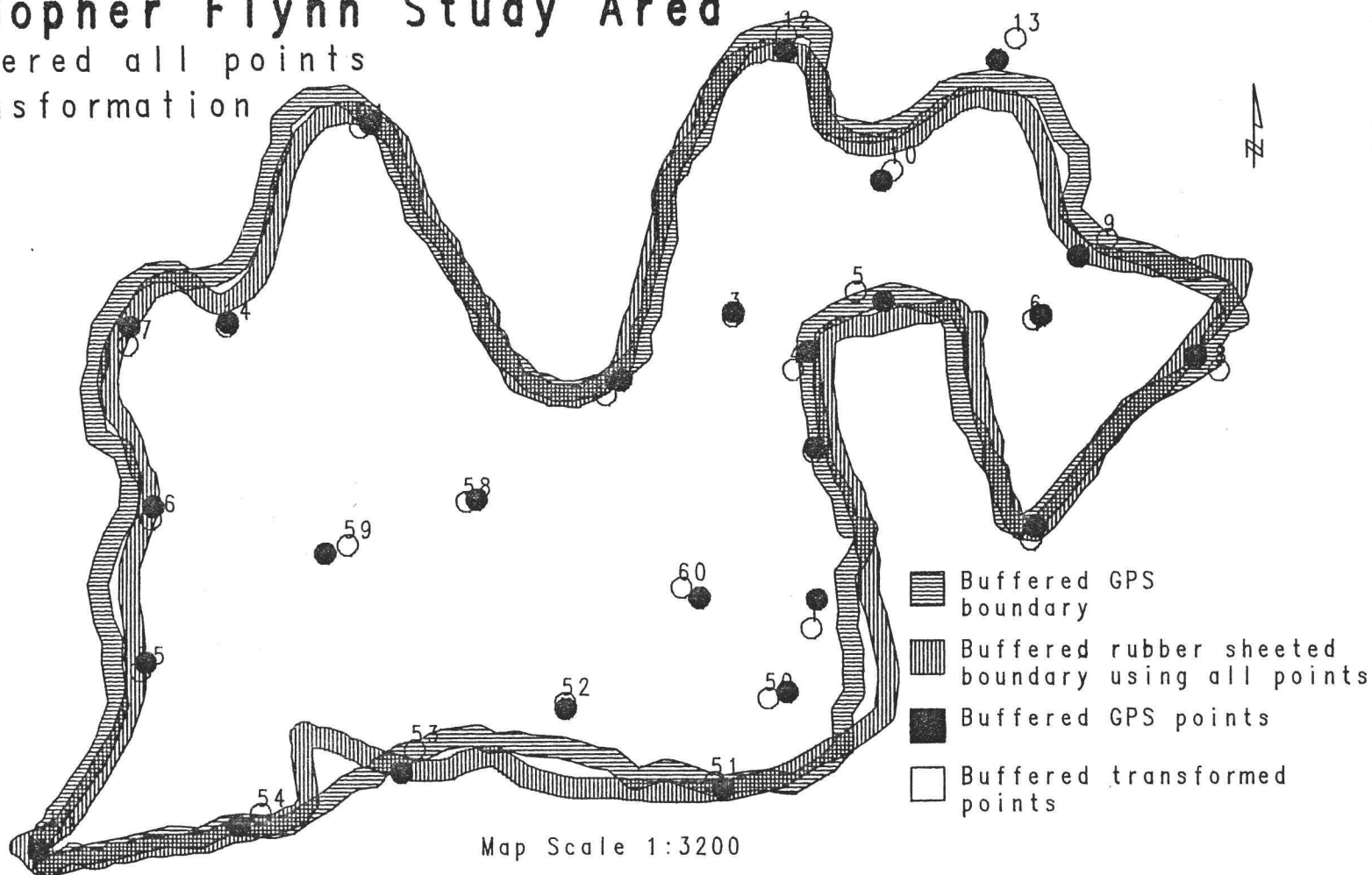
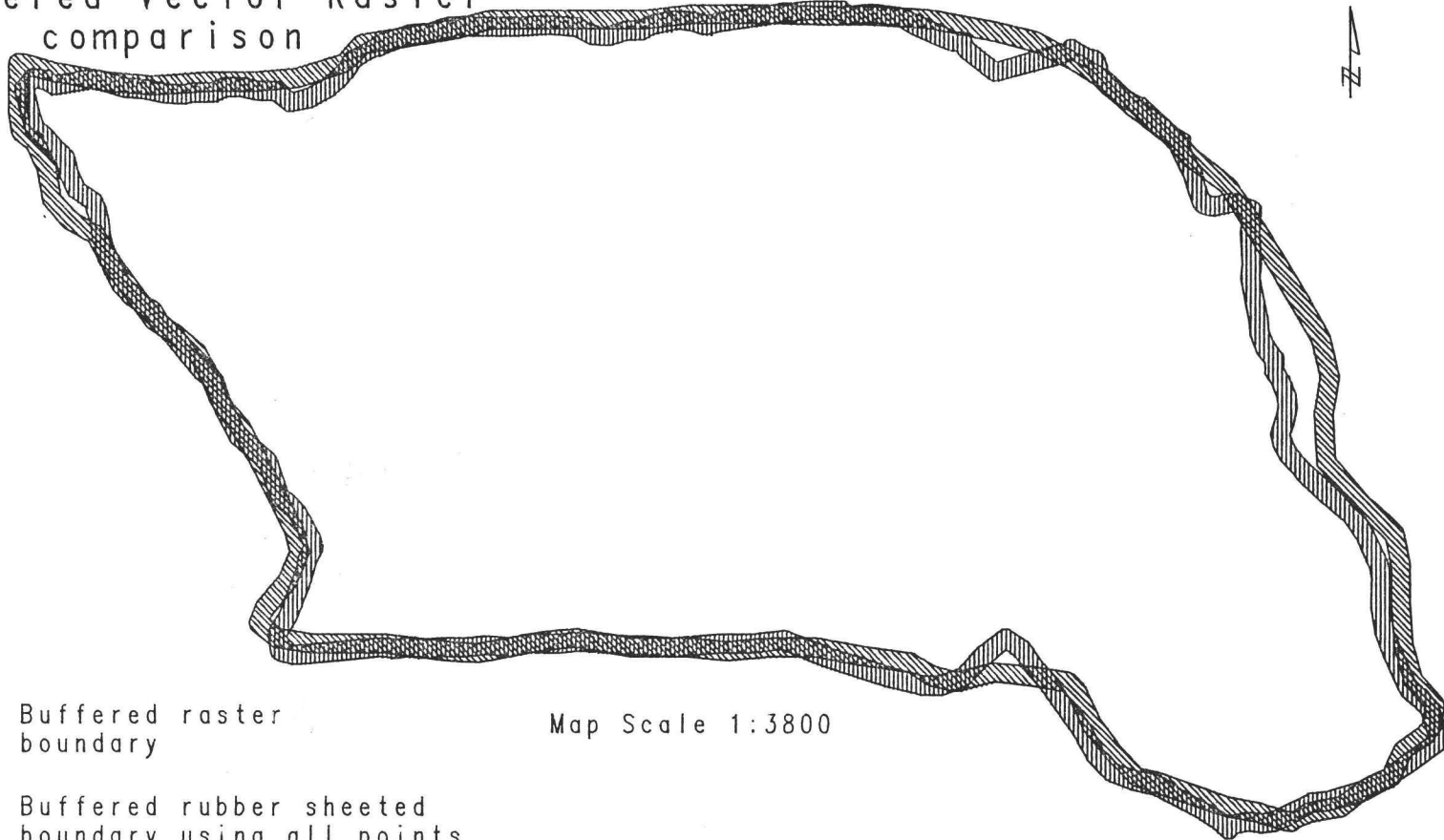


FIGURE 37

Randall Study Area

Buffered Vector-Raster
comparison



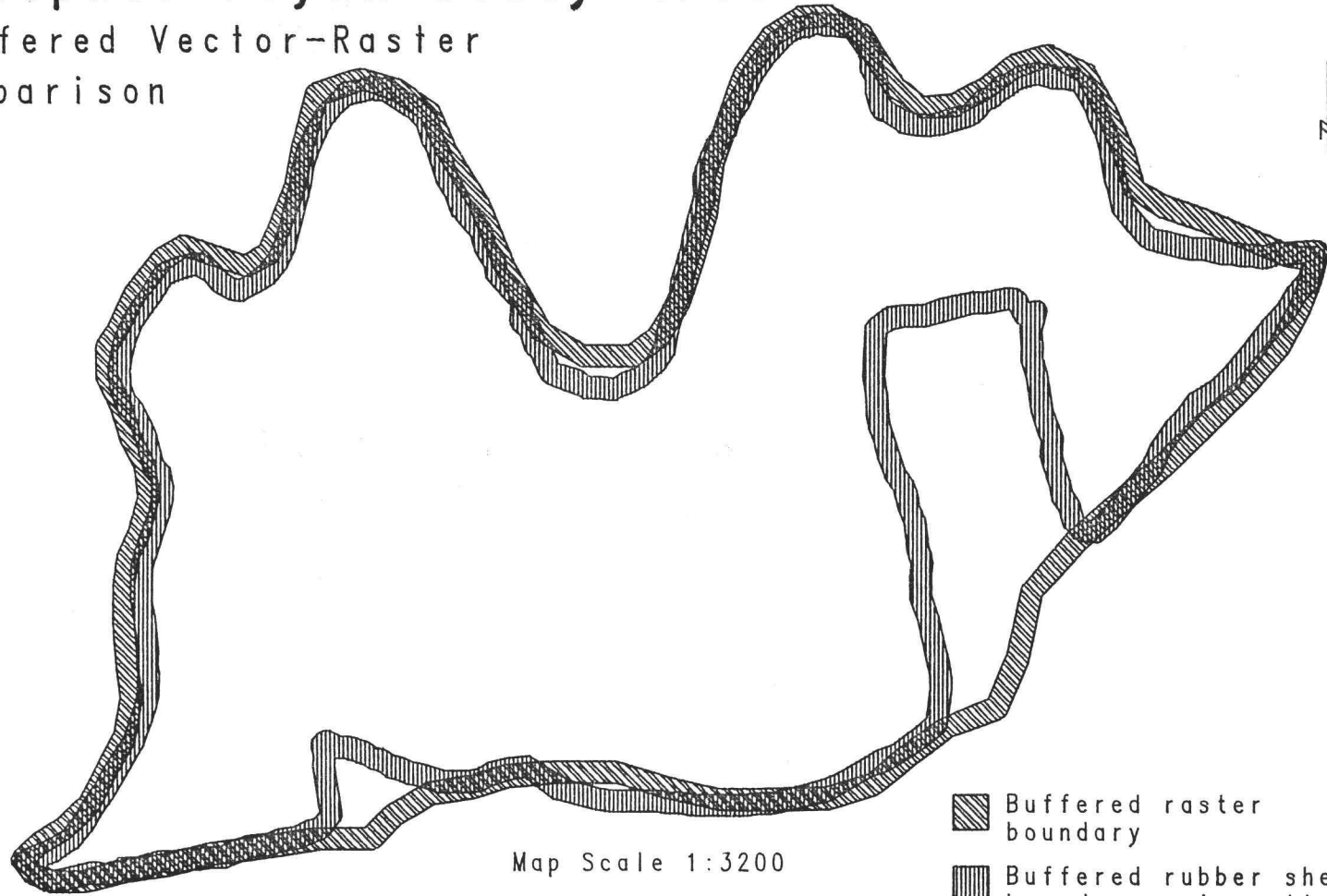
- Buffered raster boundary
- Buffered rubber sheeted boundary using all points

Map Scale 1:3800

FIGURE 38

Gopher Flynn Study Area

Buffered Vector-Raster
comparison



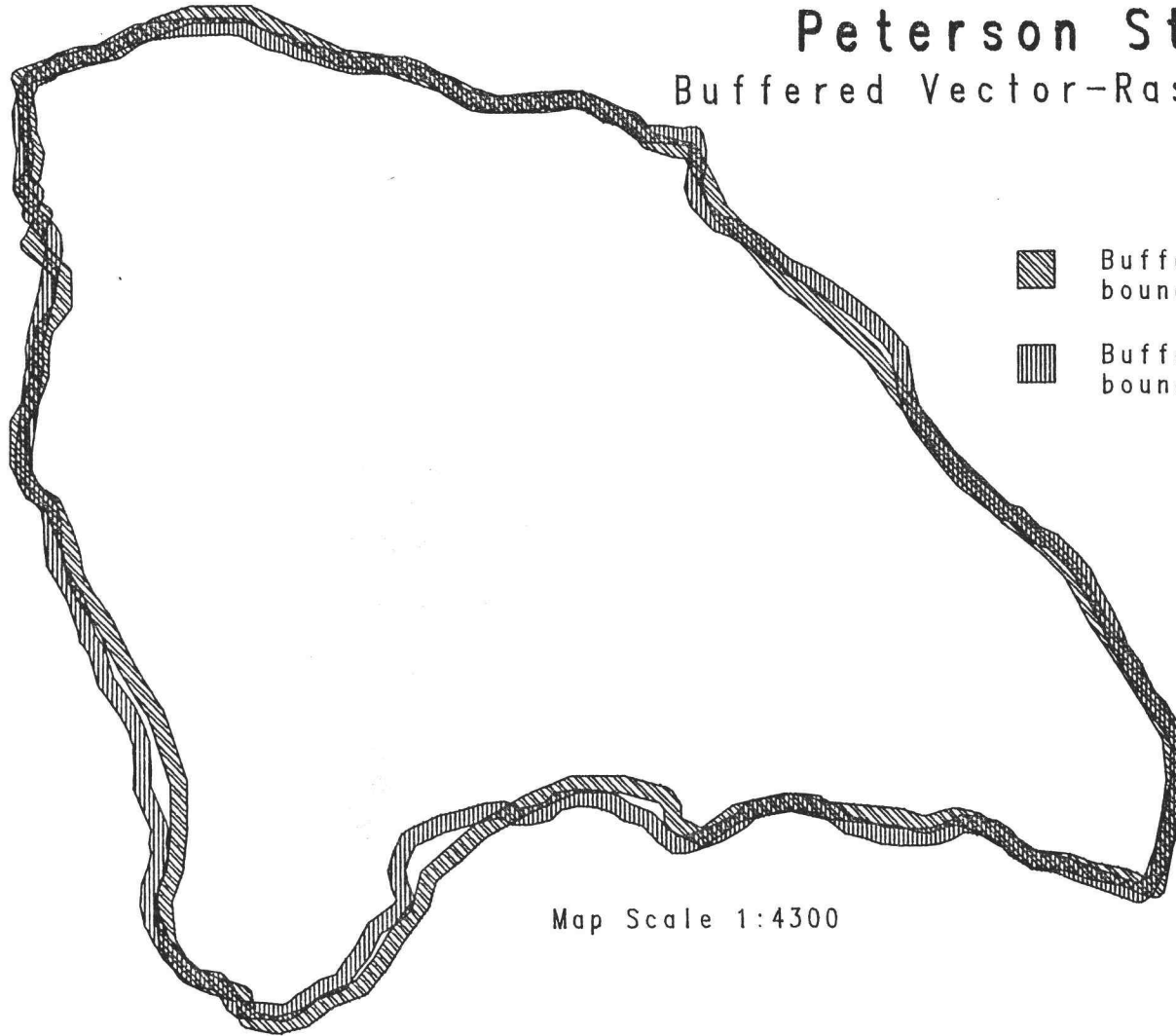
- Buffered raster boundary
- Buffered rubber sheeted boundary using all points



Map Scale 1:3200

FIGURE 39

Peterson Study Area

Buffered Vector-Raster comparison



-  Buffered raster boundary
-  Buffered rubber sheeted boundary using all points

Map Scale 1:4300



FIGURE 40

Randall Study Area

Vector-Raster comparison

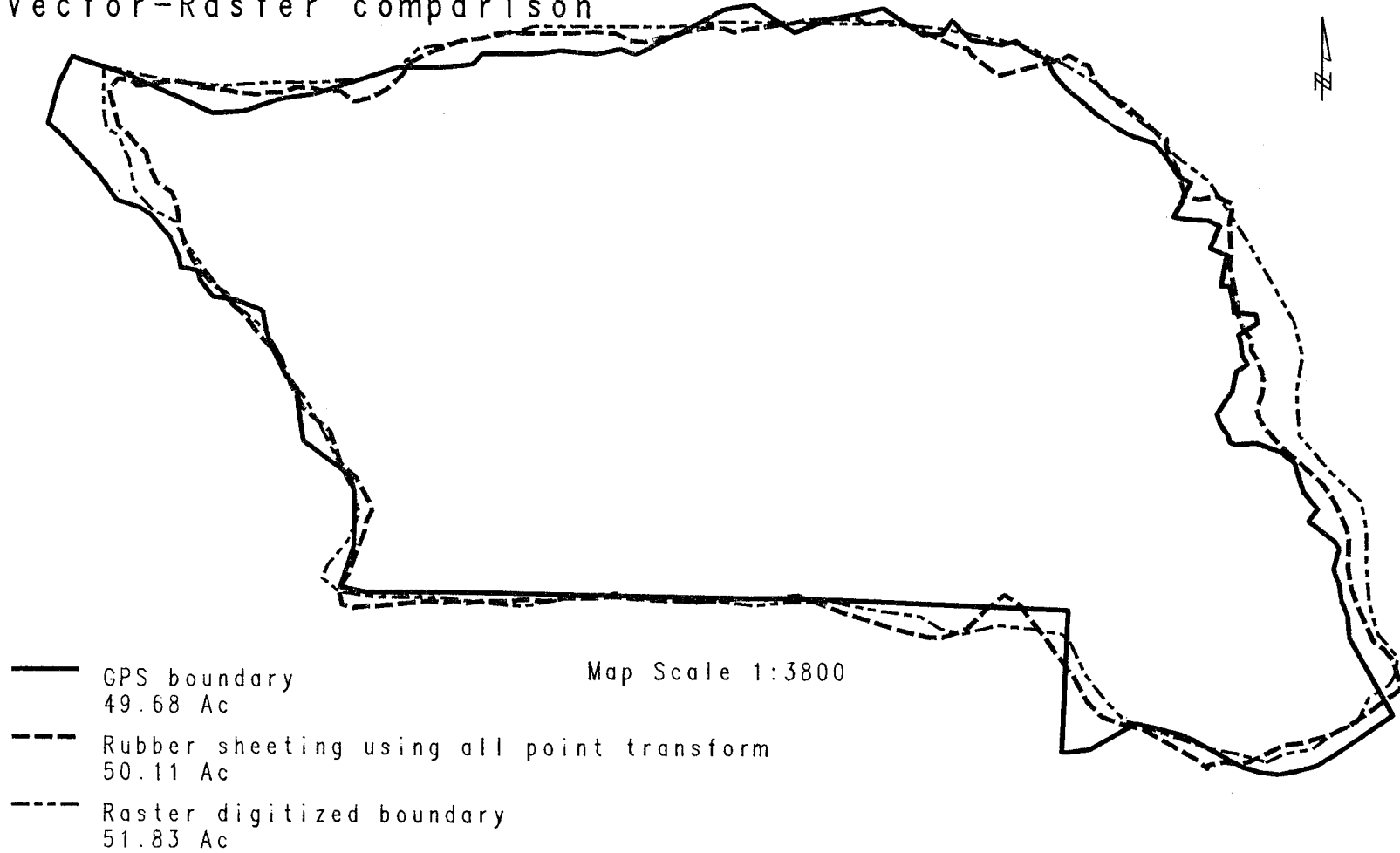


FIGURE 41
Gopher Flynn Study Area
Vector-Raster comparison

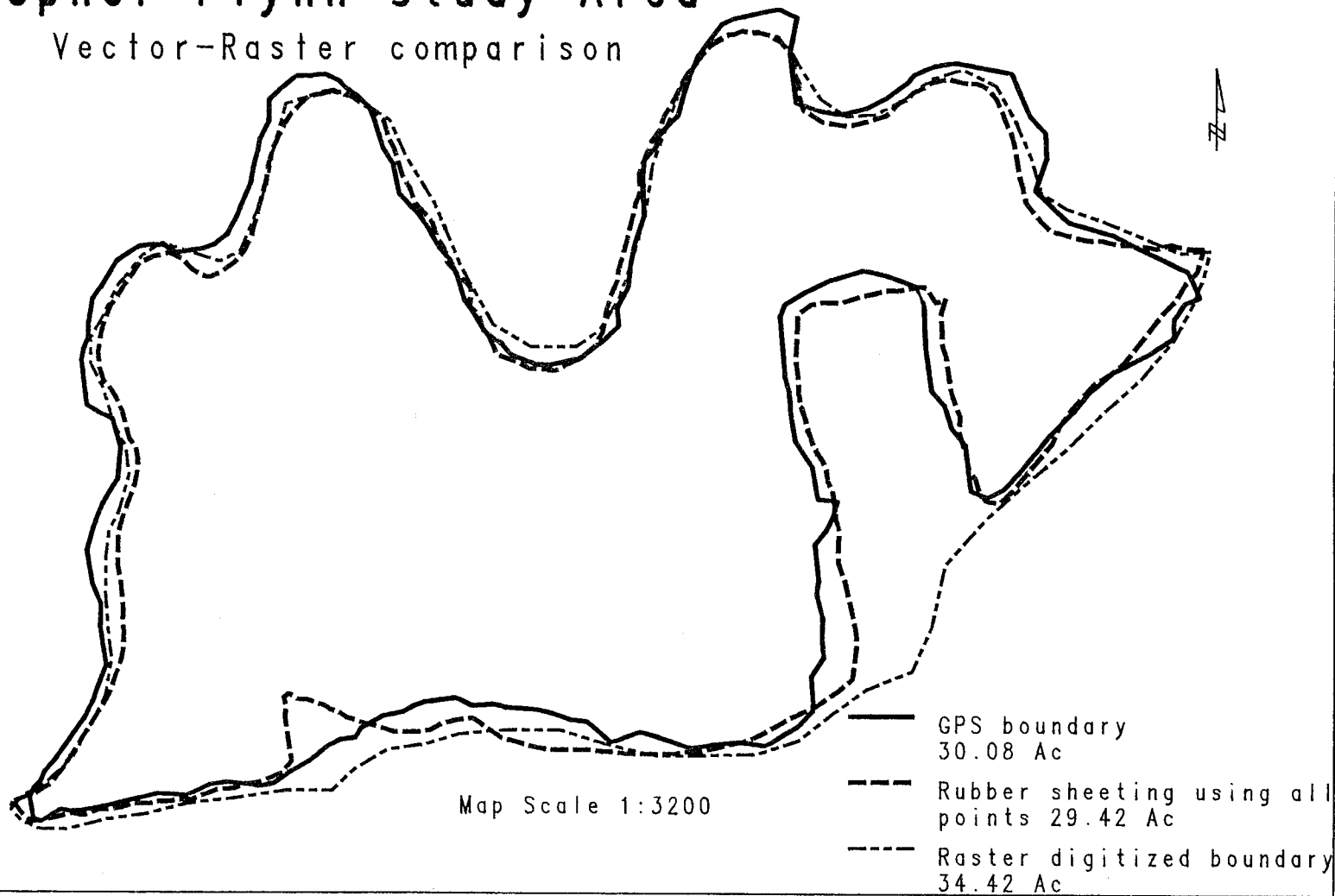
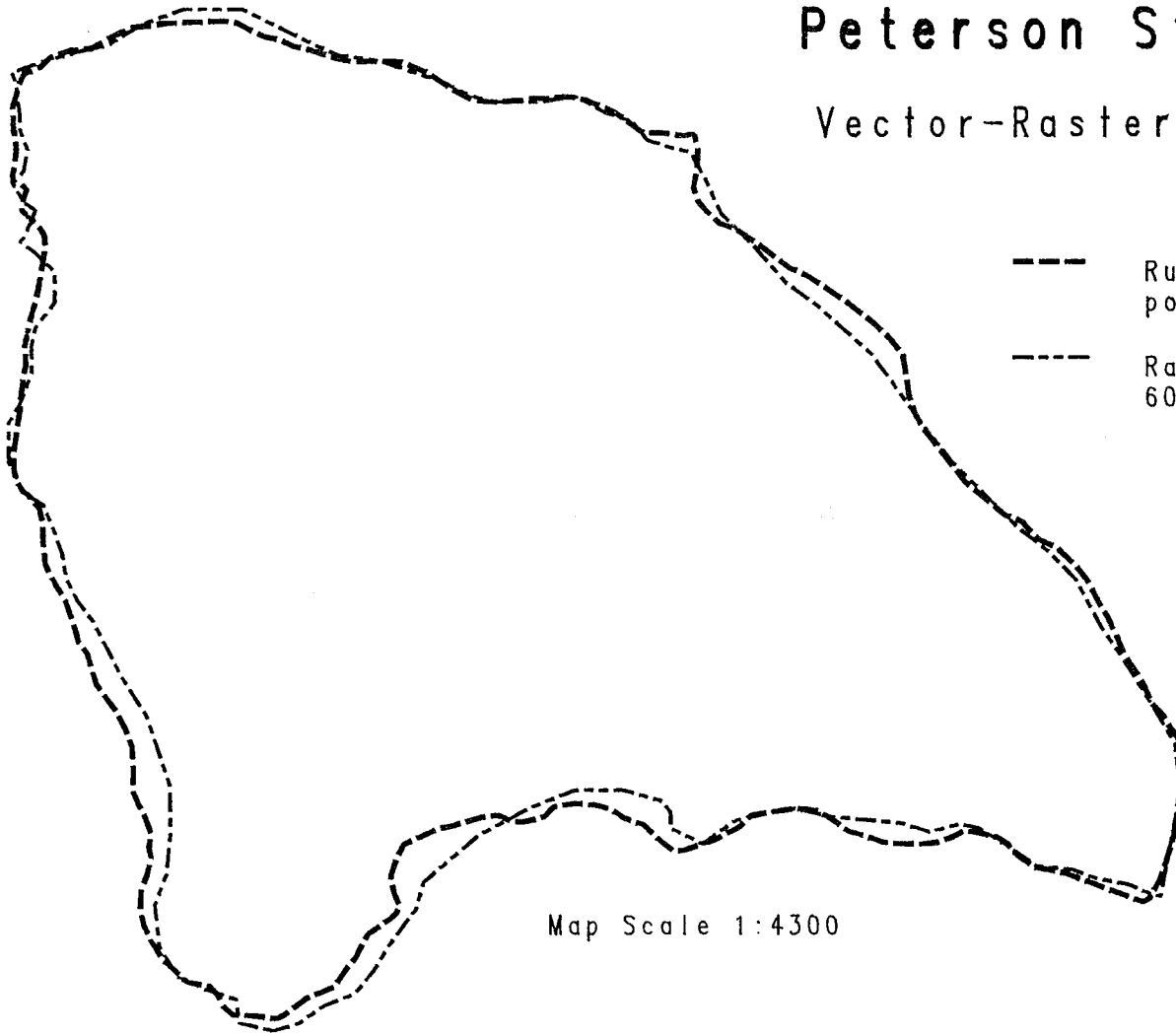


FIGURE 42

Peterson Study Area

Vector-Raster comparison



- Rubber sheeting using all points 61.79 Ac
- Raster digitized boundary 60.65 Ac

Map Scale 1:4300



APPENDIX 2
CARTESIAN COORDINATE TRANSFORMATIONS

A. Jon Kimerling
 Department of Geography
 Oregon State University

Cartesian coordinate transformations play an important role in digital cartographic data collection and manipulation. Transforming (X,Y) coordinates from a digitizing tablet to UTM or State Plane (E,N) grid coordinates and converting UTM to State Plane coordinates, or vice versa, are but two important applications of Cartesian transformations.

In the most general terms, the (E,N) coordinates desired are computed from two mathematical functions involving the (X,Y) or (E,N) coordinates in the original coordinate system. We can state this mathematically as:

$$\begin{array}{l} E=f_1 (X \text{ and/or } Y) \\ N=f_2 (X \text{ and/or } Y) \end{array} \quad \text{or} \quad \begin{array}{l} E_1=f_1 (E_0 \text{ and/or } N_0) \\ N_1=f_2 (E_0 \text{ and/or } N_0) \end{array}$$

where (E_0, N_0) and (E_1, N_1) are UTM and State Plane coordinates, or vice versa.

If the original and desired coordinate system axes are parallel (see Example 1), the coordinate transformation must account for what are called translational shifts and scaling differences. The equations that do this are of the form:

$$\begin{array}{l} E= mX + c_1 \\ N= mY + c_2 \end{array}$$

where c_1 and c_2 are the translational constants and m is the scaling coefficient. The scaling coefficient m is the number of feet or meters in the ground coordinate system per unit distance in the original coordinate system. For example, if UTM grid lines 10000m apart on the map have digitizer coordinates differing by 1 inch, the scaling factor would be 10000/1 or 10000. Example 1 illustrates the mathematics involved in transforming digitizer coordinates into UTM or State Plane when the latter systems' grid lines are made parallel with the digitizer coordinate axes.

The usual situation, however, is to have the desired coordinate system rotated by some angle θ with respect to the original system axes. If both coordinate systems were to have identically positioned origins (0,0) and were scaled identically ($m=1$), the well known Cartesian coordinate rotation equations can be used to transform coordinates as follows:

$$\begin{aligned} E &= X \cos \theta + Y \sin \theta \\ N &= Y \cos \theta - X \sin \theta. \end{aligned}$$

Since the two coordinate systems normally are scaled differently, the above equations must be rewritten to reflect the scaling constant m :

$$\begin{aligned} E &= m(X \cos \theta + Y \sin \theta) \\ N &= m(Y \cos \theta - X \sin \theta). \end{aligned}$$

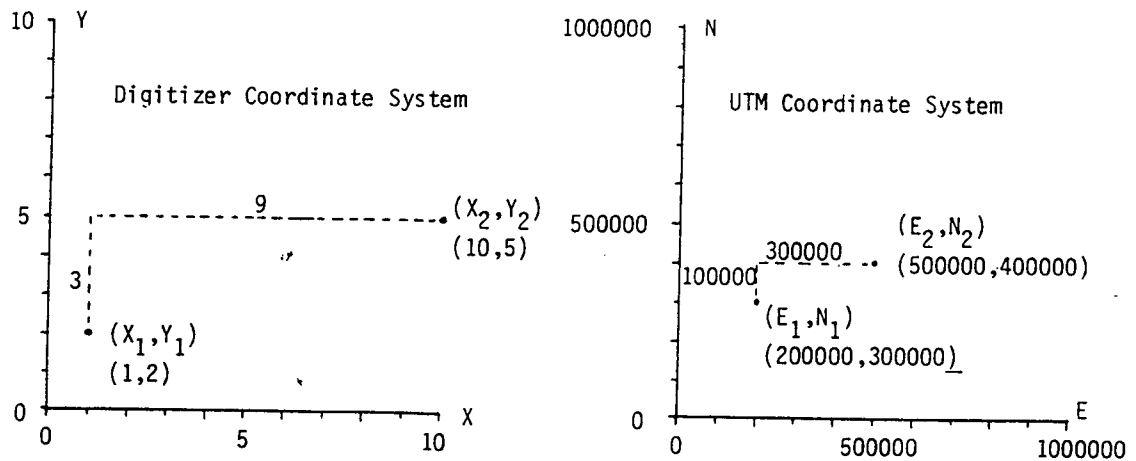
Of course, it is rare indeed that the digitizer origin corresponds with the false origin of a UTM or State Plane grid zone, and State Plane false origins never coincide with UTM false origins since the latter originate at the equator in the Northern hemisphere. Therefore, to make the above equations valid, they must be modified to:

$$\begin{aligned} E &= m(X \cos \theta + Y \sin \theta) + c_1 \\ N &= m(Y \cos \theta - X \sin \theta) + c_2 \end{aligned}$$

where c_1 and c_2 are translational constants needed to bring the two origins into coincidence, more specifically the position of the original system origin in terms of desired system coordinates (see Example 2). Note that subtracting c_1 from desired system Eastings and c_2 from Northings creates a common (0,0) for both systems.

The rotation angle between the digitizer axes and UTM grid lines must be measured accurately and the UTM coordinates of the digitizer origin must be measured carefully. The latter is a difficult measurement to make and instead we often compute C_1 and C_2 using the methods illustrated in Example 2. This method requires that the digitizer (X,Y) and UTM (E,N) coordinates of a point be determined accurately.

Example 1
Cartesian Coordinate Transformation On Parallel Axes



$$E = m X + c_1$$

$$N = m Y + c_2$$

$$m = \frac{(E_2 - E_1)}{(X_2 - X_1)} = \frac{300000}{9} = 33333.33 \quad \text{or} \quad m = \frac{(N_2 - N_1)}{(Y_2 - Y_1)} = \frac{100000}{3} = 33333.33$$

since $E_1 = m X_1 + c_1$,

$$c_1 = E_1 - m X_1 = 200000 - 33333.33 * 1 = 166666.67$$

therefore $E = 33333.33 X + 166666.67$.

Similarly $N_1 = m Y_1 + c_2$ and $c_2 = N_1 - m Y_1 = 300000 - 33333.33 * 2$

$$= 300000 - 66666.66$$

$$= 233333.33$$

Therefore $N = 33333.33 Y + 233333.33$

Cartographers rarely use the above equations; we employ the affine coordinate transformation instead mainly because the scaling coefficient, rotation angle, and translational constants do not have to be measured. To understand how the affine transformation is related to the above equations, notice that:

$$\begin{aligned} E &= m(X \cos \theta + Y \sin \theta) + c_1 \\ N &= m(Y \cos \theta - X \sin \theta) + c_2 \end{aligned}$$

can be rewritten as the affine transformations:

$$\begin{aligned} E &= a_1 X + b_1 Y + c_1 \\ N &= a_2 X + b_2 Y + c_2 \end{aligned}$$

where

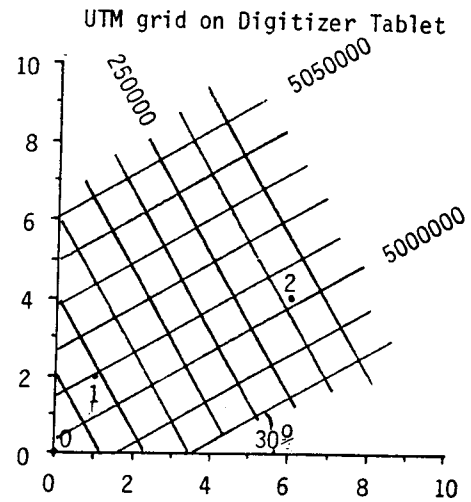
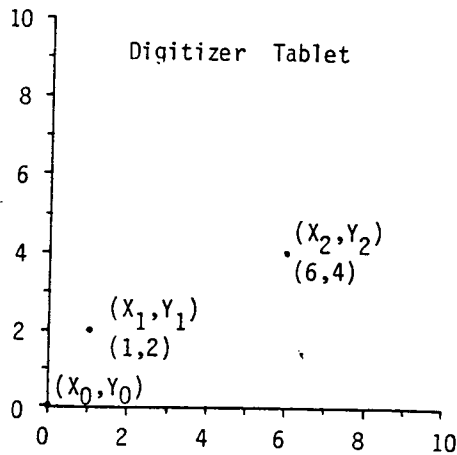
$$\begin{aligned} a_1 &= m \cos \theta, \quad b_1 = m \sin \theta \\ a_2 &= -m \sin \theta, \quad b_2 = m \cos \theta \end{aligned}$$

since m and θ are constants. These are first order polynomial equations that must be solved simultaneously for $a, b,$ and c . Three (or more) equations are needed to solve for the three unknowns, or:

$$\begin{aligned} E_1 &= a_1 X_1 + b_1 Y_1 + c_1 \\ E_2 &= a_1 X_2 + b_1 Y_2 + c_1 \\ E_3 &= a_1 X_3 + b_1 Y_3 + c_1 \\ \\ N_1 &= a_2 X_1 + b_2 Y_1 + c_2 \\ N_2 &= a_2 X_2 + b_2 Y_2 + c_2 \\ N_3 &= a_2 X_3 + b_2 Y_3 + c_2 \end{aligned}$$

This means that three points with known digitizer and UTM coordinates or known UTM and State Plane coordinates must be determined in order to solve the three equations simultaneously. In the first case, three UTM grid line intersections are digitized and recorded along with the UTM coordinates of the intersections.

Example 2
Cartesian Coordinate Transformation On A Rotated Grid



$$E = m(X \cos \theta + Y \sin \theta) + C_1$$

$$N = m(Y \cos \theta - X \sin \theta) + C_2$$

$$(E_0, N_0) = (C_1, C_2) = (189500, 4997000)$$

$$(E_1, N_1) = (208000, 5009500)$$

$$(E_2, N_2) = (262000, 5002000)$$

$$m = 20000/2 = 10000 \quad \theta = 30^\circ$$

interpolated
from map

$$\begin{aligned} E_1 &= 10000(1 \cdot 0.866 + 2 \cdot 0.5) + 189500 \\ &= 10000(1.866) + 189500 \\ &= 18660 + 189500 \\ &= 208160 \end{aligned}$$

$$\begin{aligned} N_1 &= 10000(2 \cdot 0.866 - 1 \cdot 0.5) + 4997000 \\ &= 10000(1.232) + 4997000 \\ &= 12320 + 4997000 \\ &= 5009300 \end{aligned}$$

APPENDIX 3

HANDBOOK ON WARPING VECTOR BOUNDARY WITH ARC/INFOGCP and area boundary coordinate files:

An ASCII file was made of the UTM coordinates for each control point in the study area. These files were called Rand.TIC, Goph.TIC, and Pete.TIC. The generic term <area> will be used to illustrate the sequence of procedures.

The ARC command CREATE was used to create an empty coverage.

The syntax for this is:



```
ARC>CREATE <out_cover>
```

```
CREATE <area>.Trans
```

This empty coverage has an unpopulated TIC and BND coverage.

To prevent typing errors in populating the empty TIC coverage for <area>.Trans.TIC with the GPS UTM coordinates of the <area>.TIC, the ADD command in INFO were used. This command brings in the files from the ASCII file called <area>.TIC to the <area>.Trans.TIC. The syntax is as follows:

```
INFO
```

```
ec>select <area>.Trans.TIC
```

```
ec>add from ^<area>.TIC
```

```
ec>list
```

```
ec>q stop
```

Next a copy is made of the <area>.Trans.TIC file. The syntax for this command is:

```
ARC>COPY <from_cover> <to_cover>
```

```
ARC>BUILD <coverage> {polygon, point, line}
```

```
BUILD <area>.DIG.PTS point
```

The projective transformation was used because the input coverage was taken from an aerial photograph. However, due to the high relief in the Siuslaw National Forest the projective transformation used alone would not correct the vector file. The syntax of the command is:

```
ARC>TRANSFORM <in_cover> <out_cover> {AFFINE|PROJECTIVE}
```

```
TRANSFORM <area>.DIG <area>.TRANS PROJECTIVE
```

<area>.DIG is the coverage of the digitized area boundary and GCPs. This coverage is in digitizer coordinates.

<area>.TRANS is a polygon coverage of the study area boundary in UTM Coordinates.

<area>.TRANS needs to have the ARC BUILD command performed to create the topology of the coverage. The syntax of the command is:

```
ARC>BUILD <coverage> {polygon, point, line}
```

```
BUILD <area>.TRANS polygon
```

Transformation of the ground control points in the study areas:

The next step is to TRANSFORM the coverage containing the (x, y) coordinates of the study area GCPs that were digitized from the uncontrolled photograph.

A copy of the <area>.Trans.BU file needs to be made. The syntax is as follows:

```
ARC>COPY <from_cover> <to_cover>
```

```
COPY <area>.Trans.BU <area>.PTS.TR
```

The PROJECTIVE TRANSFORM command was used next. The syntax is as follows:

```
ARC>TRANSFORM <in_cover> <out_cover> {AFFINE|PROJECTIVE}
```

```
TRANSFORM <area>.PTS <area>.PTS.TR PROJECTIVE
```

<area>.PTS.TR is a point cover of the study area GCPs in UTM Coordinates.

Vector Warping "Rubber Sheeting"

Point and polygon coverages now exist for the UTM coordinates for: a) the polygon coverage of the digitized boundary of the study areas <area>.DIG, b) the digitized point coverage of the GCPs of the study areas <area>.PTS, and c) the original GPS point coverage that was generated from the UTM GPS coordinates <area>.GPS. These transformed coverages are <area>.Trans (area boundary), and <area>.PTS.TR (GPS points).

Rubber Sheeting the Vector File:

The rubber sheeting transformation was used to adjust the boundary and GCPs of <area>.DIG and <area>.PTS to the points of the <area>.GPS coverage. The syntax of this procedure is as follows:

```
ARC>COPY <from_cover> <to_cover>
```

```
COPY <area>.PTS.TR <area>.RS
```

***The following commands sets the environment for the rubber sheeting:

```
ARC>ARCEDIT
```

```
>EDITCOVERAGE <area>.RS
```

```
>DRAWENVIRONMENT Links Arcs Labels
```

```
>DRAW
```


>EDITFEATURE Arc

***The next step brings the arcs over from <area>.TRANS

***and brings the points and polygons together

>GET <area>.TRANS

***The following commands set the display environment

>Backcover <area>.GPS 2

>Backenvironment Labels

>Draw

***The following commands sets the parameters for and does the rubber sheeting:

>SNAPCOVER <area>.GPS

>LINKFEATURE label label

>SNAPPING closest 20 (meters)

>EDITFEATURE link

>AUTOLINK

***when AUTOLINK does not set a link between all of the points, interactively set the links through EDITFEATURE link

>EDITFEATURE link

>ADD (or DELETE)

>ADJUST

>SAVE

***Topology must be built for <area>.RS

ARC>BUILD <cover>

>BUILD <area>.RS polygons